RESTRAINT OF THE WALLENDA/DLK MAP KINASE CASCADE BY THE KINESIN-3 MOTOR REGULATES THE ASSEMBLY OF SYNAPSES

by

Jiaxing Li

A dissertation submitted in partial fulfillment
of the requirements for the degree of
Doctor of Philosophy
(Molecular, Cellular and Developmental Biology)
in the University of Michigan
2017

Doctoral Committee:

Associate Professor Catherine A. Collins, chair
Arthur F. Thurnau Professor Richard Hume
Assistant Professor Brian Pierchala
Associate Professor Orie Shafer
Professor Haoxing Xu

To my family and friends

ACKNOWLEDGEMENTS

The thesis work I have completed has been supported by many people. First of all, I would like to thank my advisor, Dr. Catherine Collins for her relentless support during my PhD training. Her guidance, patience and advice has helped me along my thesis and her critical mind has inspired me to work with a high standard. Her hard work and kind heart easily sets a role model for me in future career. I also would like to thank Dr. Richard Hume, who has mentored me in electrophysiology, teaching and beyond. He has always been providing me advice in addressing challenges from research and career.

I would like to thank the nurturing environment of Collins lab. Galit Rudelson and Leni Truong have worked with me to carry out a genetics screen and Robert Doherty has helped me with live imaging. Pushpanjali Soppina has assisted me to find solutions for multiple technical tasks. Dr. Xin Xiong, Dr. Susan Klinedinst, Dr. Bibhudatta Mishra and Dr. Xin Wang have been truly helpful during my early PhD training. Dr. Ryan Insolera, Yan Hao and Elham Adib have been great resources and their interaction with me has always been intellectually stimulating. Dr. Laura Smithson, Eric Robertson, Lucas Junginger, Ross Carson, Dhwani Joshi, Ruohan Wang, Grace Kim, Nicolette Ognjanovski and Jennifer Diep have created a collaborative and enjoyable workplace for me. Outside the lab, several labs have provided help and support for my thesis work, including but not limited to Bing lab, Hume lab, Denver lab, Shafer lab, Aton lab and Kuwada lab. I would also like to thank Dr. Joeseph Knoedler, Samhitha Raj and Dr. Chen Zhang

for helpful discussions. It always feels heartwarming to receive care and help from Mary Carr, Diane Durfy and other MCDB staff members.

I appreciate all the help and advice from my thesis committee, Dr. Brian Pierchala, Dr. Orie Shafer and Dr. Haoxing Xu along my thesis project as well as career development. Their encouragement and accessibility are incredible and motivates me in science. I was very fortunate to have rotation advisors, Dr. John Schiefelbein and Dr. Lyle Simmons during the beginning of my PhD training.

I would like to thank my collaborators Yao Zhang and Tobias Rasse, who have provided insightful suggestions and have been consistently supportive all along. I would like to thank Dr. Dave Featherstone for providing support and tips in embryo dissection, and Dr. Heather Broihier and Dr. Crystal Miller for sharing their knowledges in embryonic development. Dr. Richard Daniels has made helpful suggestions on electrophysiology and Dr. Mostafa Ghannad-Rezaie helped me in live imaging. I am very grateful for the generous Drosophila community that have kindly shared reagents with me.

Last but not the least, I cannot be thankful enough to my parents, my sister and all my friends for their support and encouragement. While my thesis study has been to pursue a question in science, all of you have made this pursuit a splendid trip.

PREFACE

The content in Chapter II is adapted from a manuscript that is currently in review at *The Oxford handbook of Invertebrate Neurobiology.* The content in Chapter III is adapted from a prepared manuscript in submission. Data from Figure 3.1E, 3.2D&E and 3.5A&B were generated by Yao Zhang. Yao Zhang and I prepared Figure 3.1A&C&D, 3.9A&B and 3.12C&D. Doychin Stanchev contributed preliminary data to Figure 3.3. Elham Adib and I prepared Figure 3.14G.

TABLE OF CONTENTS

LIST OF FIGURES

Figure

LIST OF ABBREVIATIONS

AZ: active zone
CAMs: cell adhesion molecules
DCVs: dense core vesicles
DLK: Dual leucine zipper kinase
JIP1: JNK Interating Protein 1
JNK: Jun N-terminal Kinase
KLC: Kinesin light chain
LTP: long-term potentiation
LTD: long-term depression
LOF: loss of function
Mbp: myelin basic proteins
NMJ: neuromuscular junctions
PHR: Pam/Highwire/Rpm-1
PSDs: Postsynaptic densities
PTVs: Piccolo Bassoon transport vesicles
SNAREs: Soluble NSF Attachment protein REceptors
SVs: Synaptic Vesicles
t-SNAREs: target-SNAREs
VAChT: Vesicular Acetylcholine Transporter
VGAT: Vesicular GABA Transporter
VGlut: Vesicular Glutamate transporter
VGCC: voltage gated calcium channel
VMAT: Vesicular monoamine Transporter
Wnd: Wallenda

ABSTRACT

Synaptic connections are fundamental units of neuronal communication in the brain. They are composed of precisely opposed pre- and postsynaptic specializations, and these structures are dynamically regulated to adapt to changing needs of neuronal circuits. While mechanisms that regulate the postsynaptic composition of synapses are highly studied, less is known about presynaptic regulation. Within presynaptic terminals, synapse assembly requires the formation of active zones (AZs) and synaptic vesicle (SV) release machinery at synapses. An important role in presynaptic assembly has been assigned to a kinesin-3 family member, Unc-104/Imac/KIF1A. Unc-104/Imac/KIF1A is required for the delivery of synaptic components and SVs to nascent synapses. However, its distinct synaptic phenotype from other kinesins and the complexity of the phenotype is not well understood.

This thesis work describes how the synaptic defects of *Drosophila unc-104* mutants can be rescued by inhibiting the Wallenda (Wnd)/DLK MAP kinase signaling pathway. This pathway has been previously identified as a regulator of axonal damage signaling and presynaptic terminal morphology. The accessible genetic tools in Drosophila (reviewed in Chapter II) allow for characterization of the mechanistic relationship between Wnd/DLK and Unc-104. Wnd/DLK signaling becomes activated in *unc-104* mutants, and inhibits synapse formation independently of Unc-104's transport functions by controlling the levels and timing of the expression of AZ and SV components (Chapter III). In order to understand the activation

mechanism of Wnd signaling, multiple possibilities have been examined (Chapter IV). Cumulative findings lead to a model that accumulated presynaptic proteins in the cell body of *unc-104* mutants triggers the Wnd signaling pathway, which then down-regulates presynaptic protein levels. In this fashion Wnd signaling may function as a stress response pathway that regulates the expression level of synaptic proteins according to their ability to be transported in axons. This model also raises an interesting possibility that DLK activation may contribute to synapse malfunction and loss in the aged or diseased nervous system.

CHAPTER I. INTRODUCTION

1.1 Presynaptic development is regulated via highly orchestrated mechanisms including trafficking:

The nervous system enables an animal to control its body and respond to environmental stimuli. These functions rely on the brain's structural and functional units: neurons and the connections they make with each other. These connections, called synapses, are locations where two cells meet and are determined by the specific organization of molecules within each cell at the sites of contact. Machinery to promote release of a neurotransmitter signal must be organized on the presynaptic side, while machinery to detect the signal must be organized on the postsynaptic side. Synapses form during development, are dynamically regulated during developmental processes of circuit refinement and can also be modulated and reorganized in the adult nervous system. Synapse formation and its regulation are critical for the function and maintenance of neuronal circuits, and hence is important for nearly every function of brain, including sensory processing, motor output and memory formation. Mis-regulated assembly or disassembly of synapses has been implicated in autism, schizophrenia and mental retardation and in neurodegenerative diseases, including Alzheimer's disease and ALS (Henstridge et al., 2016; Volk et al., 2015).

1.1.1 The structure and dynamics of presynaptic and postsynaptic specializations are critical for synaptic release

At most synapses, chemical signals called neurotransmitters are packaged within synaptic vesicles (SVs), which can be released as individual units when the nerve fires an action potential. Neurotransmitters then cross the space between the pre and post-synaptic membranes, called the synaptic cleft. The receptors on the postsynaptic membrane bind neurotransmitters and gate a wide range of signals in the post-synaptic cell, depending on the receptor type. To enable this neurotransmission, the molecular composition is distinct across the synaptic cleft. On the presynaptic side, transmitter release requires SV fusion which is mediated by the SV release machinery, containing SNAp REceptors (SNAREs), which brings SVs close to the plasma membrane, and Synatotagmin1, which senses the calcium influx from an action potential and promotes membrane fusion. Prior to SV fusion, SV docking and priming is required to locate SVs in close proximity to sites of release and is mediated by SNAREs and a specialized structure, known as the active zone (AZ) (Rizo and Xu, 2015; Südhof, 2012). On the postsynaptic side neurotransmitter receptors cluster at electron dense Postsynaptic densities (PSDs). PSDs also contains a number of cytoplasmic signaling molecules that act downstream to receptors and scaffolding proteins that stabilize and organize receptors and signaling molecules (Sheng and Kim, 2011). Consistent with functional coupling, AZs and PSDs are always closely opposed to each other in mature and healthy synapses.

The composition and structure of PSDs is dynamically regulated during development and activity-dependent synaptic changes. During synaptogenesis in mammalian organisms, the expression of many PSD proteins increase (Petralia et al., 2005; Sans et al., 2000) and GluN2B glutamate receptors are replaced with GluN2A glutamate receptors in a controlled manner in many different types of synapse (Matta et al., 2011; Sans et al., 2000; Yoshii et al., 2003). In adult nervous system, PSDs undergo constant molecular remodeling through regulated AMPA

glutamate receptor trafficking, scaffolding protein modification and degradation, and cytoskeleton reorganization (Sheng and Kim, 2011; Shepherd and Huganir, 2007). This remodeling is more dramatic upon activity and underlies activity-dependent change of synaptic strength, found in long-term potentiation (LTP) or long-term depression (LTD) (Inoue and Okabe, 2003). While the composition and regulation of PSDs have been highly studied, the mechanisms that regulate the assembly and disassembly of presynaptic structure are still poorly understood.

The AZ localize in close proximity to the SV release machinery and facilitates SV docking and priming, recruitment of voltage gated calcium channel (VGCC) and specifies locations for precisely opposed pre- and postsynaptic specializations. Under Electron Microscopy (EM), an AZ appears as electron-dense structure and is surrounded by numerous SVs. AZs in different synapse types have different morphologies, ranging from a 'disc' in the vertebrate central nervous system, a 'string' in the vertebrate neuromuscular junction (NMJ), to a 'ribbon' in the vertebrate retina and cochlear hair cells. At the *Drosophila* NMJ it appears universally as a 'T' bar. The AZ contains multiple molecules and its core components are conserved across animal kingdom. These include Rim, Rim-binding protein, ELKS, Liprin-a and Unc-13 (Südhof, 2012). These core components interact with additional components at synapses, including SNAREs (SV fusion machinery), VGCC (calcium influx upon action potential), Syd-1 (regulating synapse assembly) and Piccolo and Bassoon (SV recruitment).

The precise structure and mechanism of assembly for AZs is still poorly understood and is the subject of current investigation (Petzoldt and Sigrist, 2014). The current model is that cell adhesion molecules (CAMs) from both pre- and post-synaptic compartments arrive first and define the location of the synapse through their transynaptic interaction. This is followed by the

arrival of postsynaptic receptors and AZ organizers, Liprin-α and SYD-1. Brp/ELKS, a major structural component of the AZ is recruited later (Figure 1.1). This model is based on evidence from super resolution imaging and functional analysis carried mostly at the *Drosophila* NMJ (Fouquet et al., 2009; Kaufmann et al., 2002; Zhen and Jin, 1999). Rim, Rim binding protein and Unc-13 are important for synaptic transmission and AZ function, but AZs can nevertheless form in their absence (Aravamudan et al., 1999; Graf et al., 2012; Jung et al., 2015; Koushika et al., 2001; Liu et al., 2011; Richmond et al., 1999). Two isoforms of Unc-13 were found in *Drosophila* and are recruited by Liprin-α and Brp separately (Böhme et al., 2016). The assembly steps for Rim and Rim-binding protein are not clear, except Rim-binding protein tightly associates with Brp (Siebert et al., 2015).

After the core of AZs is in place, the release machinery components, including VGCC and target-SNAREs (t-SNAREs), need to localize to AZs (Gasparini et al., 2001; Kasai et al., 2012; Li et al., 2007). While the VGCC is likely recruited by Brp/ELKS and Rim binding protein, t-SNAREs distribute broadly on the axon membrane (Südhof and Rothman, 2009) and whether an AZ recruitment mechanism exists for t-SNAREs is not clear. As the synapse maturates, it is not clear whether presynaptic structure and composition undergoes changes, comparable to postsynaptic remodeling (McMahon and Díaz, 2011). The presynaptic compartment forms a button-like bouton, which enlarges in size and become filled with SVs. While presynaptic boutons at CNS synapses are thought to contain one site of release and one AZ, the boutons at the larval NMJ grow to contain multiple AZs and form multiple synaptic contacts. This structure of the bouton is likely coupled to the process of synapse formation since mutations that disrupt the normal morphology of boutons commonly cause significant impairments to synaptic transmission (Menon et al., 2013).

1.1.2 Control of presynaptic assembly

To tune its function within a circuit, a neuron tightly controls the number and structure of synapses. On the presynaptic side, there are three main features that a neuron can modulate to regulate the number and structure of its presynaptic contacts. It can modulate (1) the assembly of the AZs and SV release machinery from individual components; (2) the expression of components that are needed for AZs and SV release machinery; and (3) the transport and localization of these components to presumptive or existing synapses. Notably, compared to the long-lasting neuron, the presynaptic proteins are ultimately degraded. The half-life of most presynaptic proteins examined thus far (including ELKS, Synaptotagmin1 and SNAREs) is at the range of days or weeks (Rosenberg et al., 2014). Thus a continuous replenishment of the presynaptic proteins to the AZs and SV release machinery through (1) to (3) are also critical for the maintenance of synaptic structure and function in the course of a neuron's life.

Though little is known on (1-3), some recent studies are beginning to reveal new information. Much of these recent development comes from studies using the *Drosophila* NMJ. The accessible genetic and molecular tools in *Drosophila* (see Chapter II) and the amenability of the larval NMJ to visualization are great advantages that allow this synapse to serve as a 'model synapse'. In addition, the *Drosophila* genome contains only a single copy of most AZ genes, compared to 3 to 4 paralogs for each AZ core component in mice (Südhof, 2012). Here I summarize our current understanding of the three processes (1-3) in synapse regulation.

In regulating the assembly of AZs and synapses, Liprin-α, SYD-1 and Rab3 play important roles. Liprin-α and SYD-1 interact with each other and function closely in organizing AZ morphology (Dai et al., 2006; Kaufmann et al., 2002; Owald et al., 2010, 2012; Spangler et

al., 2013; Zhen and Jin, 1999). They appear at nascent synapses before the arrival of other AZ components and hence initiate important steps in AZ assembly (Fouquet et al., 2009; Owald et al., 2010). Interestingly, the loss of Syd-1 or Liprin-α leads to aberrant localization of synaptic material in axons or presynaptic specializations in dendrites (Hallam et al., 2002; Li et al., 2014), reflecting their roles in determining AZ localization. Rab3 was originally identified as a SV protein, and interacts with Rim (Rab3-interacting molecule) to prime SVs for release (Fischer von Mollard et al., 1990; Wang et al., 1997). Later, an additional role was identified for *Drosophila* Rab3 in regulating the initiation step of AZ assembly: mutations in rab3 and its regulators have reduced numbers of AZs and these AZs grow to an abnormal size (Bae et al., 2016; Graf et al., 2009).

Whether and how the expression of presynaptic proteins is regulated in synapse formation is not clear. But an increasing amount of evidence suggests the existence of expression regulation. Work from *Drosophila* has revealed dynamic expression profiles of many presynaptic genes during development, with their peak expression coinciding with the timing of synapse formation during embryo and pupal stages (Graveley et al., 2011). In a ribosomal profiling study in *Drosophila* photoreceptor neurons, the translation of many presynaptic protein is regulated specifically at the onset of synaptogenesis (Zhang et al., 2016). Studies using *Drosophila* visual system also suggest a dynamic change of presynaptic proteins in adults: the expression of Brp displays circadian changes at the neuropils of *Drosophila* lamina (Górska-Andrzejak et al., 2013) and the expression of Brp, Liprin-α and Rim binding protein, but not SYD-1 and VGCC, is reduced upon increased synaptic activity (Sugie et al., 2015). This reduction of presynaptic expression may be mediated by targeted degradation at synapses, which has been shown as an effective pathway to regulate synapse function (Speese et al., 2003; Waites et al., 2013; Yao et

al., 2007). Though the importance of these expression change is unclear, it is interesting to note that the expression of Dscam, a cell adhesion molecule, regulates the morphology of presynaptic terminals in *Drosophila* larval sensory neurons (Kim et al., 2013). Aberrant expression of presynaptic proteins are also implicated in neuronal pathology (Beneyto et al., 2007; Jang et al., 2014; Moechars et al., 2006).

Another important, but poorly understood process that is crucial for synapse formation is the trafficking of presynaptic components. Presynaptic proteins are generally thought to be synthesized in the cell body and trafficked to synapses via the fast axonal transport machinery. The transport of vesicle-associated proteins are the best studied. SVs carry vSNARE proteins (such as Synaptotagmin and Synapsin) and transporters of neurotransmitter (such as the Vesicular Glutamate transporter (VGlut)). Dense core vesicles (DCVs), which are named based on their distinct electron-dense appearance by EM, are known to contain neuropeptides and likely heterogeneous and diverse according to content. One type of DCVs carries the AZ components Piccolo and Bassoon and thus are named Piccolo Bassoon transport vesicles (PTVs). PTVs (as characterized in culture hippocampal neurons) are found to have a uniform size of 80 nm and associate with other AZ regulators or components including Unc-18, Rab3, SNAREs (Syntaxin and Snap25) (Shapira et al., 2003; Zhai et al., 2001). Based on quantitative comparisons of immunostaining for Rim, Piccolo and Bassoon associated with PTVs versus AZs, a 'unitary' model was proposed that two or three PTVs could fuse to form a complete AZ. Other studies suggest 'co-transport' of PTVs and SVs, based on nearby localization of their associated proteins under light microscopy and EM in cultured hippocampal neurons (Ahmari et al., 2000; Tao-Cheng, 2007). These studies propose that AZ components are pre-assembled on vesicles before they arrive at synapses. This 'preassembling' theory likely requires a selective

mechanism by which AZ components are sorted and enriched on PTVs. Where and how this occurs is currently unknown. It is also worth noting that no PTV has been found in invertebrates and there is no direct invertebrate homologue of Piccolo and Bassoon, even though AZ components and SVs are found co-transported frequently in *C. elegans* (Wu et al., 2013). In *Drosophila*, the AZ component Fife has been identified as a hybrid molecule of Piccolo and Rim-like protein, though the sequence similarity is not high (Bruckner et al., 2012). Whether a Fife-associated vesicle or a PTV-equivalent vesicle exists in invertebrates remains unidentified.

The trafficking of synaptic components to synapses requires exiting the cell body into axons, anterograde transport through axons and cessation of transport at an appropriate synaptic destination. Very little is known for how each of these events is regulated for different synaptic cargos. Despite emerging evidence of a cargo sorting mechanism (Kuijpers et al., 2016; Maeder et al., 2014), it is not clear how synaptic proteins are packaged into or with vesicles especially considering many presynaptic proteins including AZ components are not transmembrane proteins. Presumably, proteins and vesicle precursor cargos are then guided into axon and shipped along axon via kinesin-driven transport on microtubules. However which of the many kinesin family members are involved in different stages of transport is unclear and a basic assignment of roles for individual kinesins to cargos has yet to be clearly laid out. Finally, the presynaptic proteins needs to disassociate from kinesins at the proper synaptic location and a small G protein, ARL-8 is proposed to promote this process by inhibiting the binding between cargos and the kinesin (Wu et al., 2013). How ARL-8 is regulated and whether other regulators are involved remains unclear.

1.1.3 Unc-104/Imac/KIF1A is essential to synapse formation

An important role in transporting many presynaptic components has been assigned to a kinesin-3 family member, Unc-104/Imac/KIF1A. Mutations in this gene leads to severe synaptic defects in C. elegans, D. melanogaster and mice. These defects include a profound depletion of AZs, SVs and DCVs from synapses and severely impaired synaptic transmission (Barkus et al., 2008; Gong et al., 1999; Otsuka et al., 1991; Pack-Chung et al., 2007; Yonekawa, 1998). These defects are also accompanied by a substantial accumulation of vesicles and synaptic proteins in the cell body. Thus, despite limited biochemical evidence, it has been interpreted that Unc-104 directly transports presynaptic components in axons. Studies in both *Drosophila* and *C. elegans* suggest that Unc-104 is not required for the initial localization of AZs to presynaptic terminals (Hall and Hedgecock, 1991; Pack-Chung et al., 2007), however *unc-104-null* mutants fail to add additional AZs during the expansion of the developing Neuromuscular Junction (NMJ) terminal. It is therefore possible that Unc-104 regulates AZ localization and assembly through an indirect mechanism. Besides its role in early development, Unc-104 has been recently shown to be important for synaptogenesis in learning progress and synapse integrity in aging (Kondo et al., 2012; Li et al., 2016).

A separate kinesin family member, Kinesin-1, is also functionally implicated in the transport of SVs and AZ components. However, mutations that disrupt kinesin-1 function, exhibit distinct phenotypes from *unc-104* mutants: SV associated proteins and AZ components accumulate aberrantly in axons (Gindhart et al., 1998; Kurd and Saxton, 1996; Siebert et al., 2015). In contrast, the accumulation in *unc-104* mutants are restricted to cell bodies and not axons (Otsuka et al., 1991; Pack-Chung et al., 2007; Yonekawa, 1998). Whether and how kinesin-1 and Unc-104/Imac/KIF1A coordinate with each other is unclear. Studies of motor

modification and adaptor choice would likely shed lights on these questions (Hirokawa et al., 2009).

The origin of my thesis work began with a surprising observation that many of the synaptic defects observed in *unc-104* mutants could be rescued by mutations that disrupt signaling by the Wallenda/DLK MAP kinase. The initial observation was first made by Yao Zhang in Tobias Rasse's at the University of Tubingin. After confirming the rescue with further characterization, my goal was to understand the relationship between Unc-104 and Wallenda. This work results in a better understanding of Unc-104's function and reveals a role for Wallenda pathway in regulating synaptic structure and function.

1.2 Wallenda/DLK regulates responses to axonal injury response and morphology of the presynaptic terminal

Wallenda (Wnd)/DLK is a MAPK kinase kinase kinase, hence an upstream regulator of MAP kinase signaling. A kinase signaling cascade, comprised of Wnd, Mek4 (MAPKK) and JNK or p38 (MAPK) has been characterized in both vertebrates and invertebrates to regulate nuclear events in response to axonal injury. Conserved across species, Wnd/DLK function is critical for the ability of injured axons to initiate new axon growth (axon regeneration) (Hammarlund et al., 2009; Shin et al., 2012; Watkins et al., 2013; Xiong et al., 2010). Besides its critical role in axon regeneration, Wnd/DLK promotes axon degeneration and cell death in mammals (Miller et al., 2009; Pozniak et al., 2013; Watkins et al., 2013; Xiong and Collins, 2012; Xiong et al., 2012). (For more details, see Chapter II)

Prior to its discovery as a regulator of axonal injury responses, Wnd/DLK was previously known to play a role in restraining synapse development. In *Drosophila* larval

motoneurons, Wnd levels are normally restrained by an E3 ubiquitin ligase (Hiw), and loss of this regulation activates Wnd signaling, which leads to a dramatic overgrowth of presynaptic terminals, featured by a >5 fold increase in the number of boutons and synaptic branches at every NMJ terminal. This overgrowth occurs with a decrease of bouton size and SV markers per NMJ (Collins et al., 2006). Similar overgrowth of presynaptic terminals was also observed in sensory neurons (Kim et al., 2013). Consistently, the loss of function (LOF) Wnd mutations cause bigger boutons at the NMJ (Klinedinst et al., 2013). Downstream signaling components including Jun N-terminal Kinase (JNK) and transcription factor Fos, are important mediators of these presynaptic terminal phenotypes. However the mechanism(s) that Wnd pathway employs to regulate bouton/NMJ morphology are not clear. It was also not addressed in *Drosophila* whether presynaptic assembly of AZs is affected by Wnd signaling.

In *C. elegans*, misregulation of Wnd's homologue Dlk-1 also leads to defects in synapse morphology, however the manifestation of the defect is slightly different from *Drosophila*. In GABAergic motoneurons, overexpression of DLK-1 or mutation in the ubiquitin ligase *rpm-1* leads to a reduced number of SVs at individual synapse and an abnormal distribution of AZs at individual synapses: some synapses contain 2-3 AZs instead of a single AZ (Nakata et al., 2005; Yan et al., 2009). Distinct from bouton-localized synapses in vertebrates and *Drosophila*, *C. elegans* form most synapses uniformly along axons (White et al., 1986). This uniformity is disrupted when DLK-1 is activated (Nakata et al., 2005), suggesting Dlk-1's role in organizing synapses. Over-expression of Dlk-1is proposed to activate the downstream MAPK p38, which in turn enhances the mRNA stability of a transcriptional factor (cebp-1) (Yan et al., 2009). Thus far it is not clear how cebp-1 regulates the synapse distribution and SV level. Interestingly, some evidence suggests that activated Dlk-1 causes aberrant accumulation of postsynaptic glutamate

receptors (Park et al., 2009), however it is not known whether these postsynaptic defects have anything to do with the presynaptic defects.

Given the importance of DLK at presynaptic terminal, it is tightly controlled in neurons. Pam/Highwire/Rpm-1 (PHR) is proposed to regulate Wnd/DLK through protein turnover. In *phr* mutants Wnd/DLK signaling is highly activated and accounts for most rpm-1-induced synaptic defects (except for a reduction of quantal content) (Collins et al., 2006; Nakata et al., 2005). In *hiw* mutants Wnd protein becomes enriched at the presynaptic axon terminals. This suggest that PHR may down-regulate Wnd at synapses, and this is consistent with localization of Rpm-1 and Dlk-1 at *C. elegans* synapses (Nakata et al., 2005; Zhen et al., 2000). PHR functions within an SCF complex with other components of ubiquitin ligase machinery, including FSN-1 (Liao et al., 2004; Saiga et al., 2009; Wu et al., 2007). However it is still not entirely clear whether it regulates Wnd/DLK via direct ubiquitination. One study provided some biochemical evidence that the RING domain within Rpm-1 could stimulate ubiquitination of Dlk-1 in HEK cells, but important controls are missing from the experiment (Nakata et al., 2005). Interestingly, a recent study found that cAMP effector kinase increases the stability of Wnd/DLK (Hao et al., 2016). Given that PHR contains a domain that can function as an inhibitor of adenylate cyclase in vitro (Pierre et al., 2004; Scholich et al., 2001), an indirect mechanism via cAMP is possible (Hao et al., 2016). In addition, another study found that rpm-1 interacts with a phosphatase to dephosphorylate dlk-1 (Baker et al., 2014).

My early observations that mutations that disrupt axonal transport (including *unc-104* mutants) activates a reporter of Wnd signaling drew my desire to understand the potential mechanism. My work has led me to a model for Wnd signaling that explains the synaptic defects in *unc-104* mutants and the genetic interactions between Unc-104 and Wnd. In this model, Wnd

signaling is activated by the accumulation of presynaptic proteins due to defective transport caused by the loss of *unc-104* and in turn downregulates synapse formation by inhibiting the expression of presynaptic proteins. Thus, I propose that Wnd regulates a negative feedback mechanism to match the expression of presynaptic proteins to their transport capacity.

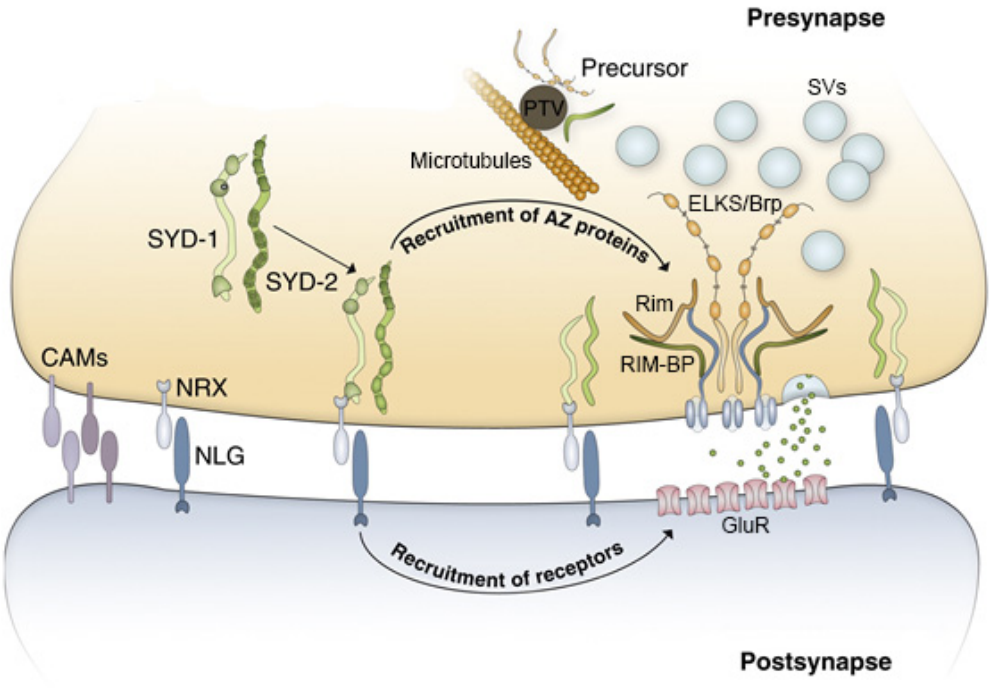

Figure 1.1: Overview of synaptic assembly, adapted from (Petzoldt and Sigrist, 2014)
Cell adhesion molecules (CAMs) define the location of synapses through interaction between pre- and postsynaptic counterparts. NRX/NLG are Synaptic-specific CAMs and are identified critical for synapse assembly. SYD-2 (Liprin-α)/SYD-1 complex is recruited by NRX/NLG and then initiate the assembly of AZs by recruiting AZ components including Brp/ELKS, VGCCs and RIM. AZs dock and prime SVs and SV release machinery mediates calcium-dependent SV fusion during synaptic transmission.

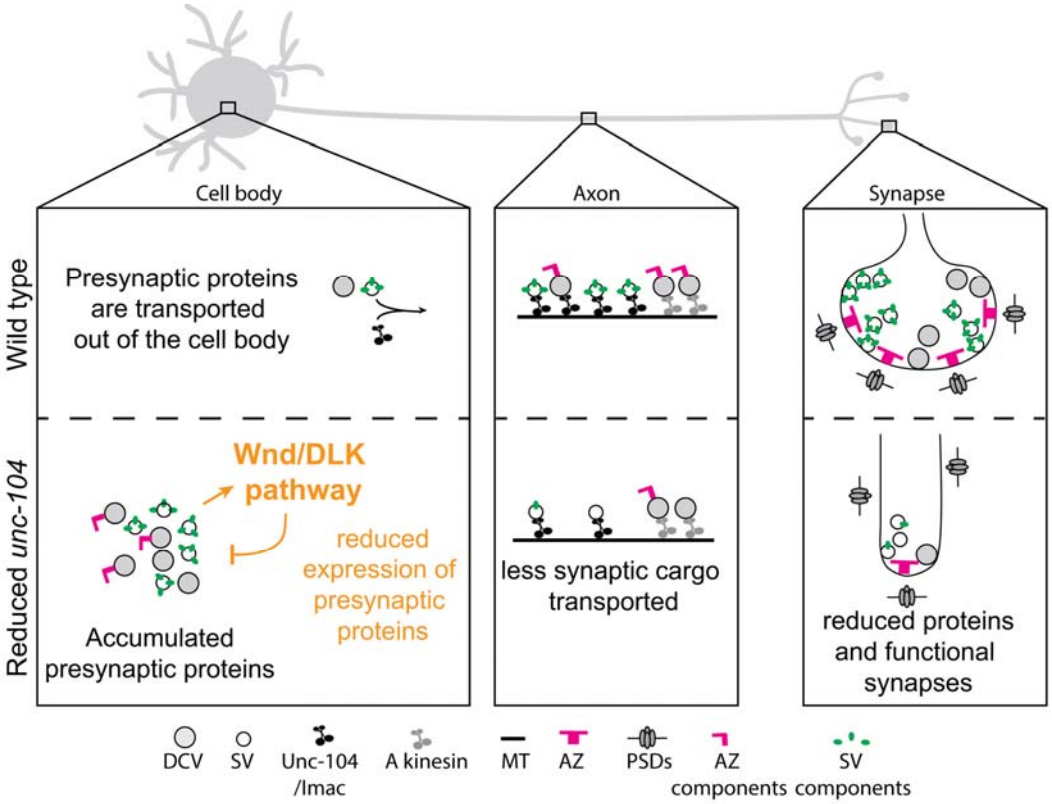

Figure 1.2: Model for the molecular mechanisms underlying synaptic defects when Unc-104's function is reduced.
The formation of synapses require the synthesis of presynaptic components (including AZ components (purple) and SV components (green)) and the delivery of them through axonal transport to proper locations in synaptic terminals. While the delivery of SV components solely relies on Unc-104 (black), the delivery of AZ components likely involves another kinesin (grey). When Unc-104's function is impaired/reduced, its capacity to transport SV components decreases, resulting in accumulation of presynaptic components in cell bodies. The increase of presynaptic proteins in cell bodies activates Wnd pathway, which initiates a signaling cascade to turn down the expression of presynaptic components. This directly reduces the amount of presynaptic components that are recruited by SVs (empty circle) and DCVs (grey circle) for transport. The defective transport and reduced presynaptic components together lead to insufficient material for synapse development and maintenance, and eventually manifests reduced number of synapses and mismatched pre- and postsynaptic structures.

CHAPTER II

MECHANISMS OF AXONAL DEGENERATION AND REGENERATION: LESSONS LEARNED FROM INVERTEBRATES

2.1 Introduction:

Neurons and the connections that they make with each other typically need to persist for an animal's entire life, even in the face of injury. How do nervous systems, including our own, cope with and respond to damage? It would be ideal if we simply could regenerate the damaged part, like a planarian which can regenerate an entire head de novo (Owlarn & Bartscherer, 2016). However most nervous systems across the animal kingdom lack such capacity. Instead, many nervous systems do their best to repair damaged axons and synapses. And in many cases of adult nervous systems, damaged axons and synapses are simply lost.

Axons are thought to be particularly vulnerable components of neuronal circuitry. They are often exceptionally long: human motoneuron axons can reach lengths over 10,000 times the diameter of their cell body and even in small invertebrates such as *Drosophila* an axon can be 200 times the cell body diameter. Such length can be a vulnerability: a problem occurring anywhere along the axon's length could result in lost ability to communicate with downstream cells. Furthermore, because axons connect to distant sites, it can be difficult to re-establish lost connections, especially in the adult nervous system. During development, axonal growth to specific targets is directed via a series of growth promoting and guidance cues (Tessier-Lavigne

& Goodman, 1996). Many of these cues are only transiently present during nervous system development, and are largely absent in the adult system.

In this chapter we review some important factors that mediate neuronal responses to axonal damage. We will emphasize here what has been learned from research using invertebrate model organisms (especially *Drosophila* and *C. elegans*), which has directed exciting discoveries of mechanisms that are conserved across the animal kingdom.

2.2. Overview of Acute and Chronic models of axonal damage

The response(s) that neurons make to axonal damage or stress can vary according to the types of damage and neuron type (Figure 2.1, and Table 2.1). However a simple determinant for classification is the duration of the harmful stimulus: acute (short term, cartooned in Figure 2.1A-C) verses chronic (long term, cartooned in Figure 2.1D-E).

Acute axon injuries can be induced experimentally by directly transecting or crushing nerves, or by micro-surgical cutting of individual axons using a high-energy laser. After such an injury, repair may be possible if the part of the axon that remains attached to cell body (the proximal 'stump') can grow again. The ability of an injured axon to re-initiate new axonal growth and eventually reconnect to its target (Figure 2.1Bi and Ci) is commonly termed axon 'regeneration'. Axon regeneration has been documented and studied in many invertebrate models, including cockroach, crickets, crayfish, squid, Aplysia, Great pond snail, earthworm, leech and more recently *C. elegans* and fruit flies (**Table 2.1**). Is the ability to regenerate axons universal for invertebrate neurons? Probably not, since failures have also been documented (Ayaz et al., 2008; Song et al., 2012; Z. Wu et al., 2007). It is interesting that some of these failures occur after injuries in the Central Nervous System (CNS) (Ayaz et al., 2008; Song et al., 2012), where stalled regeneration (Figure 2.1Bii), followed by degeneration of the proximal

stump (Figure 2.1Ciii) have been described. In the mammalian CNS, the failure to regenerate damaged axons is a major clinical impediment to recovery after brain and spinal cord injuries, hence the possibility that some aspects of this failure is shared with invertebrates, where it can be studied in a simple model system, is interesting and potentially exciting.

While the proximal stump can either regenerate or fail to regenerate, the common fate of the 'distal stump', which is no longer connected to the cell body, is to degenerate (Figure 2.1Biii). Most *Drosophila* neurons behave similarly to mammalian neurons by initiating axonal degeneration quite rapidly (within a day) after injury. This fast process, in theory, may allow for a 'replacement' by new growth from a regenerating 'proximal stump' (Figure 2.1Ci). However an injured 'distal stump' has been observed in some invertebrate animals (crayfish and leech) to persist for months after injury with no signs of degeneration (Frank, Jansen, & Rinvik, 1975; Hoy, Bittner, & Kennedy, 1967). In these cases, as well as in *C. elegans*, a process of re-fusion between the two separated stumps (Figure 2.1Cii) has been observed (Birse & Bittner, 1976; Hall, 1921; Hoy et al., 1967; Muller & Carbonetto, 1979; Neumann, Nguyen, Hall, Ben-Yakar, & Hilliard, 2011). Whether the repair is achieved by replacement (in Figure 2.1Ci) or fusion (Figure 2.1Cii), the two processes of axonal degeneration and regeneration need to be coordinated.

Axonal damage can also occur in other scenarios of injury and stress which we define here as 'chronic injuries'. These scenarios include prolonged presence of a neurotoxin (such as taxol and colchicine, which induce axonal loss), or the presence of a mutation which induces a persistent 'stress' to the integrity and function of the axon (Figure 2.1D). Mutations that are known to cause axonal and/or synaptic loss are often associated with inherited neurodegenerative disorders in humans (Saxena & Caroni, 2007). One such example are mutations in *SOD1* gene

that cause degeneration of human motoneuron axons in patients affiliated with familial ALS (Fischer et al., 2004). In these cases, loss of synapses (Figure 2.1Ei) and/or axons (Figure 2.1Eii) is thought to precede the death of the neurons.

A unifying feature of both acute and chronic models of axonal damage is the impairment of intracellular transport processes within axons. The transport of organelles and proteins in axons relies upon the action of motor proteins, which physically carry their cargo by walking upon microtubule tracts. In acute axonal injuries, the delivery of molecules from the cell body to the distal axon is irreversibly blocked due to the fact that they are no longer physically connected. In chronic models, although the connection remains, the process of axonal transport is also thought to be persistently impaired (Figure 2.1D). This has been shown by altered movement of fluorescently tagged organelles such as mitochondria or synaptic vesicle precursors, or by accumulations of organelles in axons or cell bodies (Millecamps & Julien, 2013). Mutations that disrupt the cytoskeleton, comprised of the microtubule tracts and associated molecules, often lead to degeneration of axons and/or synapses (Bounoutas et al., 2011; Pielage, Fetter, & Davis, 2005; M. K. E. Schaefer et al., 2007).

In contrast to acute injuries that completely disconnect cell bodies with their synaptic targets, neurons in a chronic injury condition have the chance to try to adapt to the stress and make their axons more resilient to degeneration (Figure 2.1Eiii). While adaptive changes and mechanisms are still very poorly characterized, they may potentially entail an induced expression of chaperones and transport of additional cytoskeletal components into axons. Depending upon the severity and duration of the stress, this response may or may not be enough to maintain the axon and/or to prevent cell death.

The processes of degeneration, regeneration, and adaptation are all interesting from the perspective of human health. The mechanisms that neurons engage to either delay or accelerate axonal and synaptic loss and repair after injury could be valuable therapeutic targets for treatment of traumatic injuries as well as neuropathies and even potentially neurodegenerative diseases in which axonal loss occurs.

2.3. Axon and Synapse loss

The process of axonal degeneration after acute injury (Figure 2.1Biii) is highly stereotyped and is termed Wallerian Degeneration (WD), based on its first description by Augustus Waller in 1851. For a period of time after injury (termed the 'lag phase') the distal stump of the axon remains intact and is able to propagate action potentials (Beirowski et al., 2005; Lubińska, 1977). In most cases, the lag phase is then followed by a rapid fragmentation phase, in which the axon breaks into many individual pieces, which are then phagocytosed by glia and immune cells (Bhatheja & Field, 2006). WD likely entails a cell autonomous chain of events that occur within the distal axon itself, hence can be considered as a 'self-destruction' pathway, akin to apoptosis. However WD appears to involve a molecular pathway that is quite distinct from apoptosis (Deckwerth & Johnson, 1994; Finn et al., 2000). The pathway itself and its molecular players are still at the early phases of being described, and studies in the invertebrate model organism *Drosophila* have led the way in this exciting area of study.

In *Drosophila*, multiple approaches for inducing axonal injury and studying WD have now been described (**Table 2.1;** also see (Fang & Bonini, 2012)). Combined with the powerful genetics of this model organism, such approaches provide an ideal vehicle to uncover vital molecular mediators of the WD pathway. Many of the injury approaches (such as cutting an antenna or a wing) are simple to carry out, enabling genetic screens to identify molecules whose

function is required for degeneration to occur. For some of the approaches (including laser-directed transection and nerve crush injuries in peripheral neurons of larvae which are semitransparent) the process of WD is amenable to detailed study of the cellular changes during the course of WD, including changes in intracellular calcium, mitochondria and cytoskeleton. Here we briefly highlight some of the discoveries made in *Drosophila* that have strongly influenced our understanding of WD.

2.3.1 Central molecular regulators of WD

(a) Sarm

A heroic large-scale genetic mosaic screen in *Drosophila* led to the discovery of dSarm (*Drosophila* Sterile alpha and HEAT/Armadillo motif containing), as a critical molecular player in WD (Osterloh et al., 2012). Neurons that are mutant in *Sarm* fail to degenerate distal axons after axonal injury. This role for Sarm role in promoting degeneration was then shown to be conserved in mammals and in *C. elegans* (Osterloh et al., 2012; Vérièpe, Fossouo, & Parker, 2015). Although dSarm has been previously implicated in innate immunity and neuronal development (C.-Y. Chen, Lin, Chang, Jiang, & Hsueh, 2011; Chuang & Bargmann, 2005; Couillault et al., 2004; Liberati et al., 2004), a role in axonal degeneration would have never been guessed, highlighting the importance of forward genetic approaches. With Sarm's central role in degeneration revealed, current work is now focused upon its mechanism. Domain analysis suggests that dimerization of Sarm's TIR domains is sufficient to activate WD in uninjured axons and this activation leads to a rapid rundown of intracellular metabolites NAD+ and ATP (Gerdts, Brace, Sasaki, DiAntonio, & Milbrandt, 2015; Summers, Gibson, DiAntonio, & Milbrandt, 2016). Much work remains to be done to understand the molecular events that lead to the activation of Sarm and its downstream actions.

(b) Nmnat

In contrast to the unanticipated discovery of Sarm, a potential role for Nicotinamide mononucleotide adenylyl transferase enzyme (Nmnat) had been suspected for years, ever since a *gain-of-function* mutation in the Nmnat1 enzyme was fortuitously discovered in the background of a mouse strain. WD fails to occur in these mutant mice, and this effect can be recapitulated in *Drosophila* neurons, by over-expressing the Nmnat enzyme (MacDonald et al., 2006).

Loss-of-function studies in both *Drosophila* and mice suggest that endogenous versions of Nmnat enzymes in healthy neurons play a protective role to inhibit degeneration (Fang & Bonini, 2012; Gilley & Coleman, 2010; Hicks et al., 2012; Rallis, Lu, & Ng, 2013; Sasaki, Margolin, Borgo, Havranek, & Milbrandt, 2015; Wen, Parrish, He, Zhai, & Kim, 2011; Zhai et al., 2006). In many of these studies, depletion of Nmnat function leads to spontaneous axonal degeneration even in the absence of injury. To explain these observations, it has been proposed that Nmnat is an axonal 'survival' factor. *Drosophila* Nmnat and mammalian Nmnat2 are continuously transported into distal axons, where the protein is then rapidly turned over (Gilley and Coleman, 2010; Milde et al., 2013; Xiong et al., 2012; Figure 2.2). Once disconnected from the cell body, the distal stump loses the supply of Nmnat from the cell body and its essential but still poorly understood survival function, which leads to the initiation of degeneration.

What exactly the Nmnat enzymes do to maintain axon integrity is still not clear, and this is the subject of much investigation and discussion (Ali, Li-Kroeger, Bellen, Zhai, & Lu, 2013). It is clear that Nmnat enzymes need to localize in the cytosol (Figure 2.2A) and they become more potent at protecting axons from degeneration when they are targeted to axons (Avery, Sheehan, Kerr, Wang, & Freeman, 2009; Beirowski et al., 2009; Sasaki, Vohra, Baloh, & Milbrandt, 2009). The enzymatic activity for NAD+ synthesis also appears to be important

(Araki, Sasaki, & Milbrandt, 2004; Jia et al., 2007; Sasaki, Vohra, Lund, & Milbrandt, 2009). In line with this, a recent study has linked Sarm's role in degeneration to a rapid rundown in NAD+ (Gerdts et al., 2015). However whether inhibiting NAD rundown is a direct action of the Nmnat enzymes has been difficult to address, and some studies have linked other metabolites on the NAD biosynthesis pathway with axonal degeneration (Conforti, Gilley, & Coleman, 2014).

A quite different idea is that Nmnat performs an additional function that is separate from NAD+ synthesis, by acting as a molecular chaperone, akin to the function of heat shock proteins (Ali et al., 2013). This idea builds upon observations that Nmnat transgenes that are non-functional for NAD synthesis activity can still have protective effects when over-expressed in *Drosophila* neurons (Zhai et al., 2006, 2008). Further, endogenous Nmnat isoforms become upregulated in several models of protein-folding disorders, and in these cases Nmnat protein is observed to co-localize with protein aggregates. In addition, Nmnat can facilitate the folding of denatured luciferase *in vitro*, possibly via its ATPase domain (Ali et al., 2016; Ali, McCormack, Darrand, & Zhai, 2011; Ali, Ruan, & Zhai, 2012; Zhai et al., 2008). While it is challenging to nail down a chaperone function in vivo, the idea remains attractive since other known chaperones (such as TBCE, CSP and Hsp70) are required for continued axon and synapse integrity (Fernández-Chacón et al., 2004; Rallis et al., 2013; M. K. E. Schaefer et al., 2007).

(c) Potential Sarm and Nmnat independent pathways

While axonal degeneration usually initiates within hours of injury in *Drosophila* and mammalian neurons, crayfish and leech axons have been observed to persist for months after injury (Ballinger & Bittner, 1980; Frank et al., 1975; Hoy et al., 1967). This implies the existence of mechanisms that has been adopted by some animals to maintain the integrity of distal 'stump' and/or inhibit degeneration. Do these axons fail to activate Sarm? If so, how and why is this

change achieved in these neurons? Or are there additional pathways involved. Interestingly, a recent study has documented WD in *C. elegans* which occurs independently of any manipulation to TIR-1, the *C. elegans* homologue of Sarm, or Nmnat (Nichols et al., 2016). This suggests that Sarm/TIR-1 may not universally promote degeneration in all neuron types, or may be utilized to different degrees in different contexts. A revisit to old observations of axonal degeneration in non-model organisms with contemporary techniques may help to reveal the origin and evolution of the degeneration program.

2.3.2 Adaptive mechanisms to chronic stress

Similarly to WD after injury, chronic stressors (such as cytoskeletal toxins and/or mutations) can also cause axonal degeneration (Figure 2.1D and Eii). Since in most cases degeneration is inhibited by manipulations that increase Nmnat activity, it is thought that degeneration in these models shares a common underlying mechanism with WD (Coleman & Freeman, 2010). However neurons in different injury models exhibit various tolerances to chronic stressors (Conforti et al., 2014). We posit that some of these differences are determined by whether the cell is able to make an adaptive response to delay the degeneration process (Figure 2.1Eiii).

Some recent studies in *Drosophila* suggest that nuclear signaling pathways may become engaged in response to chronic stress and damage with an output that serves to enhance and/or maintain axon integrity. An important example is the upregulation of Nmnat expression and alternative splicing of Nmnat isoforms, which has been observed in response to proteotoxic stress, heat shock stress and hypoxia (Ali et al., 2011; Ruan, Zhu, Li, Brazill, & Zhai, 2015; Zhai et al., 2008). An additional pathway, discussed further in part III, is the DLK signaling pathway, which becomes activated in injured axons. In *Drosophila* motoneuron axons, this pathway

induces cellular changes that delay the process of WD, such that an axon that has been injured once becomes more resilient to degeneration after a second injury (Xiong & Collins, 2012). The manifestation of this protective response only occurs for the proximal stump but not the distal stump, likely because the process involves the expression and transport of new molecules into axons.

It is interesting that both Nmnat and the DLK kinase share commonalities in their regulatory mechanisms. First, both are transported in axons and associated with Golgi-derived vesicles (Figure 2.2A). Palmitoylation allows for this localization and is required for the rapid turnover of Nmnat (Milde, Gilley, & Coleman, 2013) and the function of DLK (Holland et al., 2015) in mammalian neurons. While this has yet to be tested in invertebrate neurons, *Drosophila* Nmnat and DLK proteins contain palmitoylation consensus sequences. Second, the protein turnover of both Nmnat and DLK are regulated by a conserved ubiquitin ligase complex, whose signature component is a highly conserved PHR protein, named Highwire (Hiw) in *Drosophila*, RPM-1 in *C. elegans* and PAM in mice (Babetto, Beirowski, Russler, Milbrandt, & DiAntonio, 2013; Brace, Wu, Valakh, & DiAntonio, 2014; Collins, Wairkar, Johnson, & DiAntonio, 2006; Nakata et al., 2005; C. Wu, Daniels, & DiAntonio, 2007; Xiong et al., 2010, 2012). Hiw therefore becomes an intriguing regulator (and is perhaps a coordinator) of adaptive responses to axonal damage (Figure 2.2).

Finally, it is interesting to consider that many chronic paradigms of axonal injury can originate or manifest at presynaptic terminals. Several mutations that disrupt synaptic structure lead to axon and/or synapse degeneration (Burgoyne & Morgan, 2011; Fernández-Chacón et al., 2004; Pielage et al., 2005; Wishart et al., 2012). Also, in many neuropathies, the most terminal connections of the axon are lost first, suggesting a ‘dying back’ mechanism, which may be

initiated by a toxic stimulus at the synapse (Yaron & Schuldiner, 2016). Since it has been suggested that a degeneration program may be initiated and/or restrained at synapses (Figure 2.1Ei), the Hiw ubiquitin ligase complex gains even further cache, since Hiw and its homologues are known to localize to presynaptic terminals (A. M. Schaefer, Hadwiger, & Nonet, 2000; Wan et al., 2000; Zhen, Huang, Bamber, & Jin, 2000), and can inhibit synaptic degeneration in at least one chronic paradigm (Massaro, Pielage, & Davis, 2009).

2.4. Axon and synapse repair

For a damaged axon to grow (or re-grow) it needs to have a growth cone (Ertürk, Hellal, Enes, & Bradke, 2007; Tom, Steinmetz, Miller, Doller, & Silver, 2004). Many early studies in cultured neurons from Aplysia and cockroach (whose giant axons are very amenable to imaging and recording after injury in culture) have helped to describe cellular events that direct a transformation of a severed axonal stump into a growth cone: calcium influx triggered by the injury itself directs axon membrane resealing at the injury site (Davenport & Kater, 1992; M E Spira, Benbassat, & Dormann, 1993; Strautman, Cork, & Robinson, 1990; Yawo & Kuno, 1985; Ziv & Spira, 1995) and activation of local calcium-regulated proteases, which promote reconstructuring of neurofilaments and microtubules close to the stump ending (Gitler & Spira, 1998, 2002; Micha E. Spira, Oren, Dormann, & Gitler, 2003). These events ultimately lead to the formation of a growth cone that has dynamic lamelopodia and filopodia (Baas & Heidemann, 1986; Ertürk et al., 2007; Hellal et al., 2011; A. W. Schaefer et al., 2008).

The ability of the growth cone to direct new axonal growth is associated with transcriptional and translational changes in the cell body. These changes are induced by signaling pathways that become activated in injured axons, and this 'injury signaling' appears to be mediated, at least in part, by molecules which are physically transported in axons (Hanz &

Fainzilber, 2006). Early studies in Aplysia led to the identification of several proteins that are retrogradely transported specifically in injured neurons (Ambron, Schmied, Huang, & Smedman, 1992; R Schmied, Huang, Zhang, Ambron, & Ambron, 1993; Robert Schmied & Ambron, 1997; Y. J. Sung, Povelones, & Ambron, 2001; Y.-J. Sung, Walters, & Ambron, 2004; Zhang, Ambron, Mason, & Erskine, 2000). These findings inspired later studies in mammalian peripheral sciatic nerves, which have revealed critical components of "retrograde signaling" (Ben-Yaakov et al., 2012; Lindwall & Kanje, 2005; Perlson et al., 2005).

Upon this foundation of knowledge from *Aplysia* and other invertebrate studies (**Table 2.1**), our understanding of molecular pathways underlying regeneration was brought to an exciting new level in studies using *C. elegans* and *Drosophila*, which have enabled genetic screens and genetic dissection of pathways required for axonal growth after injury. (Detailed review can be found in (Byrne & Hammarlund, 2016; Hammarlund & Jin, 2014)). We'll focus our discussion on what is perhaps the most important discovery, the elucidation of the DLK/Wallenda signaling pathway which detects and initiates responses to axonal damage.

2.4.1 DLK/Wallenda is essential for axonal regeneration

A role for the DLK kinase in axonal regeneration was first identified in a cleverly-designed genetic screen in *C. elegans* (Hammarlund, Jorgensen, & Bastiani, 2007). The screen was built upon the observation that axons in *β-spectrin* mutant break spontaneously, however in response form new growth cones. Hammarlund and colleagues screened for mutants that failed to do so, and identified a signaling cascade governed by DLK kinase, which is essential for the transformation of axonal breaks into new growth cones. Importantly, *dlk* mutants have no obvious phenotype in axonal outgrowth during development (Collins et al., 2006; Miller et al.,

2009; Nakata et al., 2005). These findings suggest that DLK carries out a specific post-developmental role in regulating responses to axonal injury.

Several points emphasize the importance of DLK as a central player in regulating the ability of injured axons to regenerate. First, the requirement for DLK in axonal regeneration appears conserved across multiple neuron types in *C. elegans, Drosophila*, and also in mammalian PNS neurons which regenerate (Pinan-Lucarre et al., 2012; Shin et al., 2012; Xiong et al., 2010; Yan, Wu, Chisholm, & Jin, 2009). Second, DLK functions as an upstream regulator of a MAP Kinase signaling cascade. A number of observations suggest that it is transported in axons and becomes acutely activated after axonal damage. Activated DLK or its downstream targets give rise to retrograde signaling to initiate a nuclear response , hence DLK appears to function as a regulator of signaling molecules that are retrogradely transported in axons (Bounoutas et al., 2011; Shin et al., 2012; Watkins et al., 2013; Xiong et al., 2010; Yan et al., 2009). In mammalian neurons DLK has also been implicated in other processes that seem to be quite distinct from axonal regeneration: DLK promotes neuronal death after nerve growth factor withdrawal (Ghosh et al., 2011), and death after axonal injury in the CNS (Retinal ganglion cell) (Fernandes, Harder, John, Shrager, & Libby, 2014; Watkins et al., 2013; Welsbie et al., 2013), and in models for excitotoxicity (Pozniak et al., 2013). A shared component of all of these processes that activate DLK is the presence of stress and/or damage to the axon/synapse. The current unified view in the field is that DLK functions as a 'sensor' of axonal damage, with the downstream consequences of its activation varying depending upon context.

The amenability of *Drosophila* and *C. elegans* to combining mutagenesis and genetic interaction analysis has provided insight into the cellular pathways and processes that appear to regulate DLK's signaling functions in neurons. In *C. elegans*, a mechanism for direct regulation

by intracellular calcium has been described (Yan & Jin, 2012): an isoform of DLK binds to and inhibits the full-length form of DLK, and this inhibitory binding is released in conditions that elevate intracellular calcium. However, the sequences that mediate these interactions are not conserved in mammalian or *Drosophila* DLK, so there are likely additional important mechanisms for its regulation. Indeed a recent study has identified the cAMP effector kinase PKA as an important upstream activator of DLK in *Drosophila* and mammalian neurons (Hao et al., 2016).

Interestingly, studies in all model organisms have noted DLK's relationship with microtubules and the actin cytoskeleton. Induced cytoskeletal stresses, such as treatment with taxol or cholchicine, or mutations in cytoskeletal components (tubulin) or regulators (microtubule associated protein), lead to changes of structure and expression in neurons. Interestingly, many of these changes are suppressed when DLK is mutated (Bounoutas et al., 2011; C.-H. Chen, Lee, Liao, Liu, & Pan, 2014; Marcette, Chen, & Nonet, 2014; Richardson et al., 2014; Valakh, Walker, Skeath, & DiAntonio, 2013). These findings imply that DLK acts downstream to these manipulations to the cytoskeleton, and indeed, DLK signaling becomes activated in mammalian neurons that are treated with cytoskeletal destabilizing agents (Valakh, Frey, Babetto, Walker, & DiAntonio, 2015; Valakh et al., 2013). Complementary to this point, it appears that a downstream effect of DLK signaling is the induction of alterations in cytoskeleton organization (Eto, Kawauchi, Osawa, Tabata, & Nakajima, 2010; Feltrin et al., 2012; Hendricks & Jesuthasan, 2009; Klinedinst, Wang, Xiong, Haenfler, & Collins, 2013; Lewcock, Genoud, Lettieri, & Pfaff, 2007) and tubulin expression (Nadeau, Hein, Fernandes, Peterson, & Miller, 2005). These findings place DLK as both a sensor and effector to regulate cytoskeleton dynamics.

2.4.2 Is regeneration 'programmed'?

During development axons respond to specifically placed cues to direct their growth correctly, often over a long path that involves many intermediate targets, to find their appropriate synaptic targets. Is the same developmental process re-engaged for regeneration? The answer is likely both Yes and No. Extracellular factors are important for both development and regeneration. However, in mammalian PNS regeneration, where motor neurons can reinnervate their targets accurately after crush (Nguyen, Sanes, & Lichtman, 2002), nerve growth factors are released by Schwann cells and microphages rather than targets which are the main source during development. Schwann cell 'tubes' can physically confines axon outgrowth during regeneration, but not during development (Bhatheja & Field, 2006; Scheib & Höke, 2013). In invertebrates, little is known on the mechanism governing path-finding and reinnervation, though reconnection to original targets after axon injury has been observed in many species including cockroaches, crickets, leech, crayfish, Aplysia and snails (Allison & Benjamin, 1985; Benjamin & Allison, 1985; Bodenstein, 1957; Case, 1957; Edwards & Sahota, 1967; Hoy et al., 1967; Muller & Carbonetto, 1979). However in instances where regeneration has been studied on a molecular level (in *C. elegans* and *Drosophila*) pathways that are distinctly required for regeneration and not for development have been most notable and well characterized. These include the DLK/Wallenda and PTEN/PI3K signaling pathways. In *C. elegans*, DLK is dispensable for axon outgrowth during development (Hammarlund, Nix, Hauth, Jorgensen, & Bastiani, 2009). Likewise, in the *Drosophila* mushroom body, neither PI3K nor DLK are required for axon outgrowth during development (Marmor-Kollet & Schuldiner, 2016). On the other hand, unc-40/DCC is required for axon initial outgrowth during development (Chan et al., 1996; Keino-Masu et al., 1996), but not axon regeneration (Gabel, Antonie, Chuang, Samuel, & Chang,

2008). These “regeneration-specific” pathways suggest that axon outgrowth and innervation after injury is intrinsically and uniquely programmed.

The functional endpoint for axonal regeneration is to re-establish a functional circuit. Unless re-fusion occurs (as in Figure 2.1Cii) this requires a newly formed axon to re-form lost synaptic contacts (Figure 2.1Ci). While mechanisms that promote the growth of injured axons have been the topic of much investigation, there are very few studies to characterize whether and how synapses can be formed by regenerating axons. Studies of mammalian NMJ regeneration have provided insights into roles of extracellular matrix proteins (Skouras, Ozsoy, Sarikcioglu, & Angelov, 2011). But little is known about the intracellular pathways in neurons that promote regeneration of synapses. Synapse regeneration may share similarities in ‘programming’ with axon regeneration, with mechanisms that are both shared and distinct from developmental pathways. The field simply needs more studies and more information on this topic. Invertebrate model systems, in which functional regeneration can occur (which can result in readily screen-able behavioral phenotypes) have important contributions to make for these important future questions.

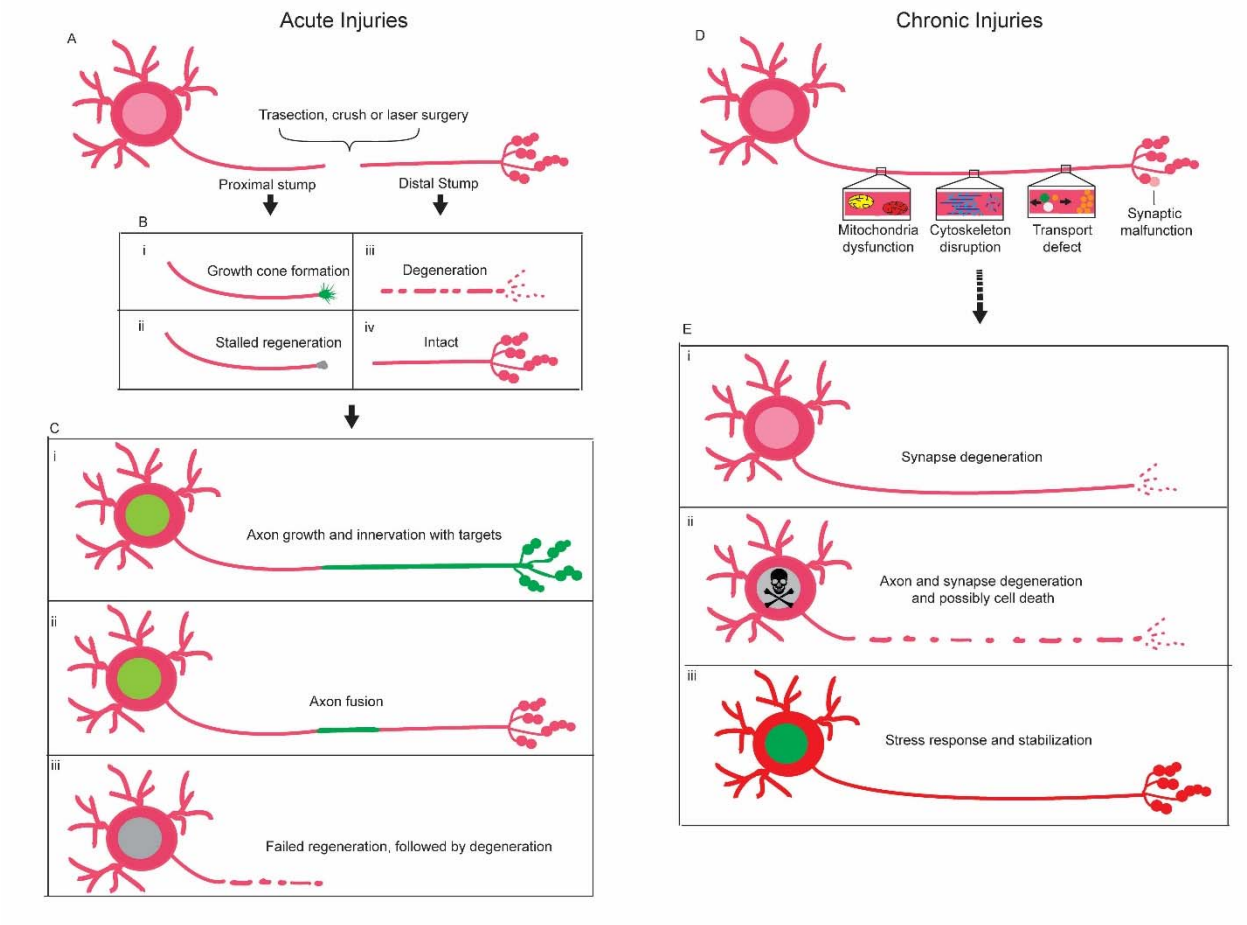

Figure 2.1: Axon regeneration and degeneration in response to acute and chronic injuries (A) Acute injuries physically break axons into two parts: a proximal stump which remains connected to the cell body and a distal stump which has lost this connection. In many cases the distal stump has presynaptic terminals (cartooned as button shaped boutons) that are made non-functional by the injury. (B) In response to acute injuries, the proximal stump either (i) succeeds or (ii) fails to form a new growth cone, and the distal axon either (iii) degenerates or (iv) stays intact. Responses vary in different injury models (**Table 2.1**), however in most cases, outcomes (i) and (iii) occur. (C) Ultimate outcomes of the injury responses include (i) new growth (in green) from the proximal stump to replace the lost distal stump. Alternatively some invertebrate neurons have been observed to undergo (ii) fusion of the two stumps, which requires less new growth from the proximal stump and the ability of the distal stump to remain intact until it can be reconnected. (iii) Failure to regenerate axons, followed by degeneration is another outcome for

some neuronal injuries. (D) Chronic injuries include long-term forms of stress that neurons may experience in their axons or synaptic terminals as the result of a genetic mutation or an environmental condition. Such stresses can include perturbations that impair mitochondrial function, organization of the cytoskeleton, long distance transport of proteins and organelles in axons, and impairments to synaptic transmission. (E) Responses to chronic injuries include degeneration of (i) synaptic terminals or (ii) entire axons and even cell death. However (iii) neurons may also initiate stress response pathways which may allow for an enhanced resiliency to degeneration. This likely involves transcriptional and translational events in the cell body and transport of newly synthesized proteins into axons (hence the green nucleus and red cytosol).

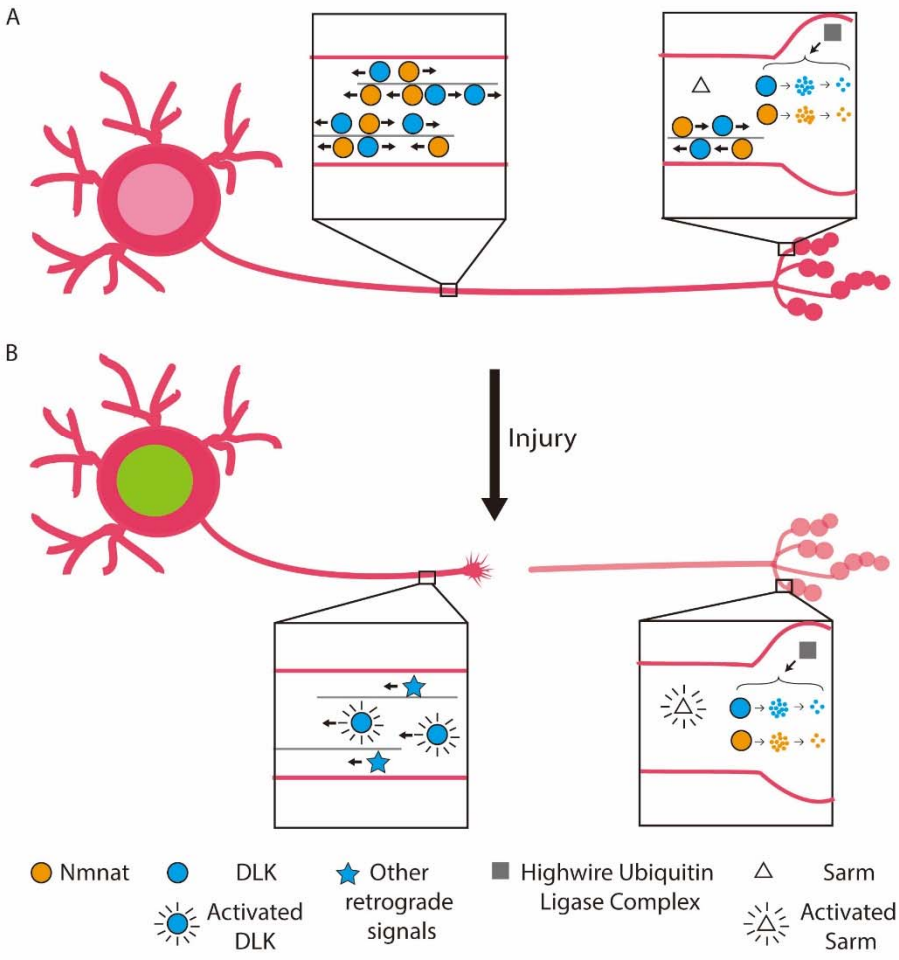

Figure 2.2: Molecular mechanisms during axon and synapse regeneration and degeneration

(A) In uninjured neurons, several critical factors for regeneration or degeneration are present in axon and synapses. These include Nmnat (orange circle) and DLK (blue circle) which are transported (associated with vesicles) in axons, and which are also turned over in axons, most likely in distal axon and synaptic locations by the Hiw ubiquitin ligase complex (gray squares). (B) Upon injury, the DLK kinase becomes activated, and in the proximal stump can signal retrogradely to the cell body to initiate a transcriptional response (green nucleus). Retrograde signaling by DLK and other factors (indicated with stars (Rishal & Fainzilber, 2014)) are required for later axon regrowth. In the distal stump, 'survival' factors such as Nmnat become depleted because their turnover continues while the supply of new molecules from the cell body is cut off. Sarm (triangle) becomes activated in the injured distal stump, and promotes a rapid rundown in intracellular NAD+ and ultimately axonal degeneration.

Table 1 Axon response to acute injury in different models

Species	Neurons	assay	CNS/PNS	Degeneration of distal stump	Regeneration of proximal stump	Ref
Drosophila melanogaster (fruit fly)	Olfactory Recptor neuron (adult)	transection	CNS	fragmentation starts 1 day after injury and completes by a week	N.A.	Macdonald et al., 2006; Hoopfer et al., 2006
	motor neuron (larva)	crush/laser surgery	PNS	fragmentation initiates 4 hours after injury and continues for up to a day	forming growth cones 10-14 hours after injury, followed by axon growth	Xiong et al., 2010; Xiong et al., 2012
	sensory neuron (adult wing)	trasection/laser surgery	CNS/PNS	fragmentation initiates within a day and completes by around a week	(laser surgery):regeneration initiates by 3 days	Fang et al., 2012; Neukomm et al., 2014
	DA sensory neuron (larva)	laser surgery	CNS/PNS	fragmentation starts 6 hours after injury for Class I neurons	regeneration observed for Class IV neurons (3 days after injury) and some Class I neurons (1-3 days) but not for Class III; limited CNS regeneration versus prominent peripheral regeneration	Stone et al., 2010 & 2012; Song et al., 2012
	mushroom body neuron (larva, pupa and adult)	disassociation (in vitro)	CNS	N.A.	neurites sprout 1 day after dissociation in culture	Marmor-Koller et al. 2016
	sLNv neuron (adult brain explant)	trasection by microdissection device (in vitro)	CNS	fragmentation starts 1 day after injury	filopodia sprouts observed 2 days after injury in a portion of axons while a majority of axon do not regenerate	Ayaz et al., 2008
Periplaneta americana (cockroach)	motor neuron	transection	PNS		reinnervation by 4 weeks and recovery of circuits by 7-9 weeks	Bodenstein, 1957; Case, 1957
Acheta domestica (cricket)	medial giant interneuron (giant fibre system)	crush or cut	CNS		sprouting; crush near cell body induces dendritic branching	Roederer and Cohen, 1983
	sensory neuron	trasection of cerci	PNS		sprouting; target to the same giant fibre	Edwards and Sahota, 1967
Procambarus clarkii (crayfish)	motor neuron	crush or transection	PNS	not oberved for 3 months	fusion occurs; a majority of injured axons establish reconnection by 30 days	Hoy et al., 1967

Table 1 Axon response to acute injury in different models (continued)

Species	Neurons	assay	CNS/PNS	Degeneration of distal stump	Regeneration of proximal stump	Ref
Caenorhabditis elegans	mechanosensory neuron (ALM, PLM, AVM); Chemosensory neuron (ASH, ASJ); GABAergic motor neuron (DD, VD); Cholinergic motor neuron (DA/DB); HSN motor neuron	laser surgery	N.A.	axons become thin, beaded and invisible in ALM/PLM/DD neurons 24 hours for L1 or several days for L3 after injury	axon growth 12-24 hours after surgery; fusion observed with some mechanosensory neuron	Chen, Chrisholm 2011; Gabel et al., 2008; Wu et al., 2007; Yanik, 2004; Chung et al., 2016; Nichols et al., 2016; Details see Hammarlund and Jin, 2014
	GABAergic motor neuron (*β-spectrin* mutant)	spontaneous	N.A.	N.A.	70% axons regenerate	Hammarlund et al., 2009
Aplysia californica (California sea hare)	sensory neuron and motor neuron	dissociated or crush (in vitro)		degeneration does not occur for hours	sprouting and regrow axons	Schacher and Proshansky, 1983; Dash et al., 1998
	sensory neuron	crush	CNS		reinnervation and recovery of reflex behavior within 2-3 weeks	Dulin et al., 1995; Steffensen et al., 1995; Noel et al., 1995
	buccal motor neuron	crush	PNS	Degeneration observed 8 weeks after injury	Reinnervation to targets observed 3 weeks after injury	Ross et al., 1994
Lymnaea Stagnails (Great pond snail)	interneuron	crush	CNS		Sprouting more prominent when injured closer to soma; synaptic connections restored 3-6 days after injury	Allison and Benjamin, 1985; Benjamin and Allison, 1985
Helodrilus caliginosus and *Lumbricus terrestris* (earthworm)	giant axon	transection	CNS		fusion with high accuracy	Hall, 1921; Birse and Bittner, 1976
Hirudo medicinalis (leech)	interneuron	crush	CNS	Starts around 1 month after injury	sprouting and following the existing distal stump to innervate the target by 1 month and functional recovery by 2 months	Frank et al., 1975; Muller and Carbonetto, 1979

CHAPTER III

THE WALLENDA/DLK MAP KINASE SIGNALING CASCADE RESTRAINS THE EXPRESSION OF PRE-SYNAPTIC PROTEINS ACCORDING TO THEIR TRANSPORT BY THE KINESIN-3 MOTOR UNC-104/IMAC

3.1 Abstract

Synapse development requires the assembly of presynaptic active zones (AZs) and localization of synaptic vesicles (SVs). A kinesin-3 family member, Unc-104/Imac/KIF1A, is required for the delivery of synaptic components and SVs to nascent synapses. We found that the synaptic defects of *Drosophila unc-104* mutants could be rescued by inhibiting the Wallenda (Wnd)/DLK MAP kinase signaling pathway, which was previously identified as a regulator of axonal damage signaling. Wnd/DLK signaling becomes activated in *unc-104* mutants, and inhibits synapse formation independently of Unc-104's transport functions by controlling the levels and timing of expression of AZ and SV components. Our findings indicate that Wnd becomes activated when presynaptic proteins accumulate within cell bodies, and thereby regulates a stress response pathway to fine-tune the expression level of presynaptic proteins according to the neuron's capacity to transport them.

3.2 Introduction

Synapse development and plasticity involve highly orchestrated trafficking events in both pre and postsynaptic cells. In contrast to the postsynaptic receptors, whose trafficking and organization has been studied extensively in many different synapse types (Choquet and Triller, 2013), much less is known about the mechanisms that regulate the assembly and maturation of the neurotransmitter release machinery in the presynaptic neuron. This machinery includes the active zone (AZ), an electron-dense complex of structural proteins that scaffold both calcium channels and synaptic vesicles (SV) for the coordination of calcium-regulated exocytosis (Südhof, 2012). The protein components of the AZ are synthesized in cell bodies and trafficked together in association with vesicles (known as piccolo-bassoon transport vesicles (PTVs)) (Ahmari et al., 2000; Maas et al., 2012; Shapira et al., 2003). Likewise, synaptic vesicle precursors (SVPs) are also synthesized in cell bodies, and carried by kinesin motors to synapses (Hall and Hedgecock, 1991; Okada et al., 1995). Regulation of presynaptic assembly and maturation likely involves a global coordination of the synthesis and transport of both AZ and SV components. However the mechanisms that regulate these important steps in synapse development are poorly understood.

A critical role in synapse development has been assigned to the kinesin-3 family of motor proteins (Hall and Hedgecock, 1991; Kern et al., 2013; Niwa et al., 2016; Pack-Chung et al., 2007; Yonekawa, 1998). Mutations in the orthologous gene originally referred to as *unc-104* in *C. elegans, imac* in *Drosophila* and *Kif1a* in mammals cause severe defects in synaptogenesis: synaptic boutons fail to form, SVs and AZ components fail to localize to nascent synapses, and concomitantly, SV and AZ associated proteins accumulate in the cell body. It is therefore broadly accepted that the protein encoded by this gene (which is now referred to as *unc-104* in

both flies and worms) promotes presynaptic assembly by physically delivering presynaptic components to their destinations in the synaptic terminal (Goldstein et al., 2008). However, while there is biochemical evidence that KIF1A is a major carrier of SV precursors (Okada et al., 1995), there is very little evidence that KIF1A or Unc-104 directly carries AZ components. Studies in both *Drosophila* and *C. elegans* suggest that Unc-104 is not required for the initial localization of AZs to presynaptic terminals (Hall and Hedgecock, 1991; Pack-Chung et al., 2007), however *unc-104-null* mutants fail to add additional AZs during the expansion of the developing Neuromuscular Junction (NMJ) terminal. It is therefore possible that Unc-104 regulates AZ localization and assembly through an indirect mechanism.

Here we identified the Wnd/DLK kinase as a critical mediator of presynaptic assembly defects in *unc-104* mutants. This MAP kinase has recently received intense interest for its roles in regulating both regenerative and degenerative responses to axonal damage in vertebrate and invertebrate neurons (Gerdts et al., 2016; Tedeschi and Bradke, 2013). We find that Wnd/DLK signaling pathway is activated in *unc-104* mutants, and, mutations in *wnd* rescue the presynaptic assembly defects in *unc-104* mutants, yet do so without suppressing the defects in transport. Instead, suppression occurs by rescuing the levels of AZ and SV protein components, which are reduced in *unc-104* mutants. Our findings delineate a new role for the Wnd/DLK pathway in restraining the expression of key presynaptic proteins needed for AZ assembly and bouton maturation. We propose that the Wnd pathway functions to calibrate the expression of abundant presynaptic proteins according to their ability to be transported, which can play an adaptive role to stresses that disrupt intracellular transport.

3.3 Methods

Drosophila Stocks

The following strains were used in this study: *Canton-S*, *hiw*$^{\Delta N}$ (Wu et al., 2005), *wnd*^{1}, *wnd*^{3}, *wnd*^{dfED228}(Collins et al., 2006), UAS-*wnd*$^{\text{kinase dead}}$-GFP(Xiong et al., 2010), MiMIC-*wnd*-GFP (Venken et al., 2011), *unc-104*$^{O3.1}$, *unc-104*^{P350} (Barkus et al., 2008), *unc-104*^{bris} (Medina et al., 2006), *unc-104*^{d11204} (Thibault et al., 2004), *unc-104*^{52} (Pack-Chung et al., 2007); UAS-*cacophony*-GFP(Kawasaki et al., 2004), *OK6*-Gal4 (Aberle et al., 2002), *OK319*-Gal4, *OK371*-Gal4(Mahr and Aberle, 2006), *m12*-Gal4(Ritzenthaler et al., 2000), *Bg380*-Gal4(Budnik et al., 1996),*elav*-Gal4^{C155}(Lin and Goodman, 1994), UAS-*Fos*^{DN} (Eresh et al., 1997), UAS-*bsk*^{DN} (Weber et al., 2000),*khc*^{8}, *khc*^{27}(Brendza et al., 1999), *khc*^{k13314}(Spradling et al., 1999), *Liprin-α*^{F3ex15}, *Liprin-α*^{R60}(Kaufmann et al., 2002), UAS-VGlut-GFP, UAS-VGlut^{A470V}-GFP (Grygoruk et al., 2010), UAS-Brp-GFP (Bloomington (BL) 36291 and 36292), UAS-SytI-GFP (BL6925 and 6926), UAS-*liprin-α*-GFP(Fouquet et al., 2009), *Rab3*^{rup}(Graf et al., 2009), UAS-YFP-*Rab3*, UAS-YFP-*Rab3*^{Q80L}, UAS-YFP-*Rab3*^{T35N}(Zhang et al., 2007), uas-mcd8-ChRFP (Schnorrer, 2009.5.11), *puc*-lacZ^{E69}(Martín-Blanco et al., 1998), *vglut* promoter-DsRed (gifts from Daniels and Diantonio), RNAi lines: *moody* RNAi (control), *Octβ2R* RNAi (vdrc 104524, control), *unc-104* RNAi (vdrc 23465, I and TRiP BL43264, II), *wnd* RNAi (vdrc 103410 and vdrc 26910), *Rab3* RNAi (TRiP BL31691 and BL34655), UAS-*Dcr2* was a gift from Stephan Thor (Linköping Université, Linköping Sweden). Flies were raised at 25℃ or 29℃ (as indicated for certain RNAi knock-down) on standard yeast-glucose media (Backhaus et al. 1984).

To generate *vglut*-DsRed reporter flies, genomic sequence spanning 5.3 upstream of the ATG start codon for *vglut* (CG9887) was cloned into a plasmid derived from pCaSpeR-AUG-bGal

(Thummel et al., 1988), in which lacZ was replaced with DsRed.T4-NLS(Barolo et al., 2004) coding sequence, such that the expressed DsRed would concentrate in the nucleus.

Animal lethality, motility and size measurement

To determine the timing of lethality during larva stages, we measured the animal width of the latest stage before death. Crosses were set with at least 30 males and 30 females. 8-9 days later around 100 3rd instar offspring larvae of indicated genotype were selected and transferred to grape plates. The largest width of surviving 3rd instar larvae was determined as following: the 20 largest ones were selected among nearly 80 animals and each animal was pinned at head and tail to ensure its body was straight; then the body width was measured with a ruler under a dissecting microscope.

To determine puparium lethality (survival to adulthood), 60 offspring 3rd instar larvae of indicated genotype were transferred to grape plates and raised in 29℃ to increase RNAi knock-down efficiency. The number of adults emerging out of pupae was counted over the next 14 days. Adults with anterior half of their body (head, thorax and foreleg) out of pupae, but with the posterior half body (abdomen and posterior 4 legs) stuck in pupae were considered as halfway emerging adults. UAS-RNAi lines were driven by *OK371*-Gal4. UAS-*Octβ2R* RNAi and UAS-*moody* RNAi were used as a controls for UAS dosage, as expression of these 2 RNAi lines did not result in any phenotypes in neurons. The survival rate was measured as the number of emerged or halfway emerged adults divided by the total number of larvae.

To determine the motility, 10 3rd instar larvae of indicated genotype were selected and put on grape plates 1 hour to adapt before recording. A 2-minute video recording was made at 30 frames per second. For each larva, the distance and time traveled after it was released in a new

plate and before it reached the plate walls was measured with the MB-Ruler (Markus Bader). A marker point in the middle of movement was only applied if the larva moved 45 degree away from the current direction and 2-5 marker points were set to determine the path. A total of 60 larvae were recorded and analyzed for each genotype.

Axonal regeneration

The nerve crush assay was carried out as described (Xiong et al., 2010), and animals were fixed either 9 or 18 hours after the injury. Axonal regeneration was quantified by measuring the number of injured axons that contained more than 5 branches at 9 hours, and the length of the longest branch at 18 hours.

Immunocytochemistry

Third-instar larvae were dissected in ice-cold PBS, then fixed in 4% formaldehyde (FA) in PBS/HL3 solution for 3 minutes for Cac-GFP, 10 minutes for Brp and GluRIII/GluRIIC staining or 20 minutes for other antibody staining, followed by blocking in PBS with 0.1% Triton (PBT) containing 5% Normal Goat Serum (NGS) block for 30 minutes.

Embryos were dissected, fixed and stained as described in (Featherstone et al., 2009; Lee et al., 2009). In brief, embryos were collected for 30-60 minutes on Molasses plates and kept in 18℃ (for stage 14 to 16) or 25℃ (for stage 17) overnight. Early-stage embryos (14-16) were dechorionated, sorted (based on GFP), staged (based on gut morphology (Hartenstein, 1993)) and dissected (tungsten needles) on negatively charged slides. Stage 17 embryos (20-21 hours AEL) were dissected with Vet glue (Vetbond) in PBS (PH=7.3) on Sylgard-coated coverslips.

Bouin's fixation for 5 minutes was used for all antibodies staining but Synapsin staining (4% PFA for 25 minutes). The examined *unc-104-null* alleles include *P350/P350* and *52/52*.

Primary antibody and secondary antibody incubations were conducted in PBT containing 5% NGS at 4°C overnight and at room temperature for 2 hours, respectively, with three 10-minute washes in PBT after each antibody incubation. The following primary antibodies and dilutions were used: ms anti-Brp (NC82, Developmental Studies Hybridoma Bank (DSHB)), 1:200; ms anti-Synapsin (3C11, DSHB), 1:50; ms anti-CSP-1 (ab49, DSHB), 1:100; ms anti-DLG(4F3, DSHB), 1:1000; Rb anti-GluRIII (gift from Diantonio lab), 1:2500; Rb anti-SytI (gifts from Noreen Reist, (Mackler et al., 2002)), 1:400; Rb anti-Unc-104(imac, gift from Tom Schwarz), 1:500; ms anti-lac-Z (40-1a, DSHB), 1:100; Rb anti-Phospho-Smad1/5 (Cell signaling),1:100; Rb anti-DsRed (Clontech), 1:1000; Rat anti-elav (7E8A10, DSHB), 1:50; A488 rabbit anti-GFP (Invitrogen), 1:1000 and Alexa488/cy3/Alexa647 conjugated Goat anti-HRP (Jackson ImmunoResearch), 1:300. Rabbit anti-VGlut (gift from Diantonio lab), 1:10000, staining was carried as described in (Daniels et al., 2008). For secondary antibodies we used Cy3- or A488-conjugated goat anti-rabbit or anti-mouse 1:1000 (Invitrogen).

Imaging and analysis

Confocal images were collected as described in (Füger et al., 2012; Xiong et al., 2010). Similar settings were used to collect all compared genotypes and conditions.

The identification and quantification of the % unopposed PSD was based on manual counts of the total number of individual GluRIII-labeled puncta (on either muscle 4 or 26/27/29, where indicated), scored for the presence or absence of an apposing AZ component (Brp or Liprin-α-GFP). To affirm that AZ components were indeed completely absent, confocal settings and

brightness levels were optimized for the weakest signals in unc-104 mutants. Since the same settings were used for all genotypes some pixels for AZ components were necessarily over-exposed in the wt controls. For measurements of intensity levels, using Volocity software, only raw images acquired together using the same confocal settings were compared. At least 8 animals and 12 NMJs were examined per genotype. To measure VGlut and Brp levels in axons and NMJs, we used staining for HRP (which labels neuronal membrane) to define the region of interest. For cell bodies, we selected the signal above a specified threshold. To estimate the total VGlut or Brp level within a single motoneuron (Figure 3.12), we summed measurements of: (a) total intensity for individual cell bodies (located in the dorsal midline of the ventral nerve cord), (b) total intensity for individual NMJ nerve terminals at muscle 4, and (c) estimated total intensity within a motoneuron axon, calculated from mean intensity in axonal segments, based on the assumption of 32 motoneuron axons per nerve and an average axon length of 1mm.

When imaging nerve cord, we used 0.8 μm step size for the z-stack and focused on the posterior and central nerve cord, corresponding to A4-A8. When imaging axons or the NMJ, we used 0.4 μm step size for z-stacks. Axonal segments were imaged 900μm away from the nerve cord. NMJ images were collected at segment A3 for muscle 4 or (when using the m12Gal4 driver) for muscle 26, 27 and 29, which are innervated by the MNSNc neuron. *puc*-lacZ level was measured within the nucleus region for motoneurons, selected by P-smad staining in the dorsal regions of A4-A8 in the ventral nerve cord.

For live imaging analysis of GFP-wnd-KD transport, 3rd instar larvae were dissected in the center of a circle reinforcement label (Avery) in HL3 solution (Stewart et al., 1994) with 0.45 mM calcium. Larvae were pinned at the head, tail and 2 lower corners, the pins were then pushed into sylgard so that the coverslip could lie directly on top of the reinforcement label (and the larva),

and excess HL3 solution was removed before imaging on an inverted microscope. Images were collected at 0.3 Hz for 5 minutes at 40x magnification in segmental nerves at a location 900μm distal to the nerve cord. The images were then processed in imageJ with a kymograph plugin (Jens Rietdorf and Arne Seitz) and further analyzed in MATLAB with a program written to determine vesicle segmental speed and duration (described in (Ghannad-Rezaie et al., 2012)).

Western Blot

25-30 3rd brains were collected in PBS and homogenized for each sample. The following antibodies and dilutions were used: rb anti-Wnd 4-3 (Collins et al., 2006) 1:700; rb anti-VGlut ((Daniels et al., 2008), 1:10000; ms anti-Brp (NC82), 1:100; ms anti-β-tubulin (1E7, DSHB), 1:1000; and rb anti-unc-104 (Gift from Tom Schwarz lab), 1:500. The blots were probed with HRP conjugated secondary antibodies: Gt at-ms and Gt at-rb at the dilution of (1:5000) and imaged with either film or an Odyssey CLx imager (LI-COR).

Real-time PCR

30 third-instar larvae brains were collected and homogenized in Trizol (Invitrogen) and the total RNA was extracted using PicoPure RNA Isolation kit (KIT0204, ThermoFisher). Samples were then treated with DNase (Invitrogen). The First-strand cDNA was synthesized with VILO kit (Life technologies). 5-10ng of cDNA was used per RT-PCR reaction for all test samples. A standard curve was established for all primer sets, and analysis was restricted to primers and samples that yielded an R^2 of least 0.99. The Pfaffl method was used to calculate the mRNA expression level of a gene in experimental samples relative to that in control sample (wild type), using RP49 and α-Tub84B as endogenous reference genes. Expression levels were averaged for at least 2 biological replicates. Primers were chosen from FlyPrimerBank (Hu et al., 2013), and

the optimal primer concentration was determined for the lowest dimer formation and high amplicon yield. The following primers were used:

rp49, For: GCCCAAGGGTATCGACAACA, Rev: GCGCTTGTTCGATCCGTAAC.

α-tub84B, For: GATCGTGTCCTCGATTACCGC, Rev: GGGAAGTGAATACGTGGGTAGG.

brp, For: GCAGTCCATACTACCGCGAC, Rev: TTGGATAGTCCATGGCATGGG.

vglut, For: CCTTCGGCATGAGGTGCAATA, Rev: CGAGTCCACATGGCTCTCC.

liprin-α, For: CCTTTTGGAACGTGACGAGGA, Rev: ACCAAGCACTCCAGATGTTCG.

cacophony, For: TTCGGGCGCACTGCATAAG, Rev: GGTGGCCTTTTCCAGGATGT.

Electrophysiology

Third instar larvae were dissected within 3 minutes in HL3 solution containing 0.65 mM Calcium at 22°C. Muscle 6 at segment A3 was located by the use of an OLYMPUS BX51WI scope with a 10x water objective and then recorded intracellularly with an electrode made of thick wall glass (1.2mmx0.69mm) pulled by SUTTER PULLER P-97. Amplifier GeneClamp 500B and digitizer Digidata 1440A were used. The recording was only used if the resting potential was negative to -60mV and muscle resistance was > 5mΩ. A GRASS S48 STIMULATOR was used to obtain a large range of stimulation voltage range (1-70V). We noticed that *hiw* mutants and *unc-104* mutants required a higher stimulus to recruit the 2nd axon that intervenes Muscle 6 (10-40V were required in *hiw* and *unc-104* mutants, as opposed to 2-8V in wild type). To ensure that we could always recruit both axons, for each muscle we tested a range of stimulation voltage (1-70V) to find the threshold which triggered the largest response

within the testing range. A stimulus slightly larger than this threshold was then used at a frequency of 0.2Hz and duration of 1ms for EJP measurements. Axon Laboratory software was used for acquisition and the Mini Analysis program (Synaptosoft Inc) was used for analysis of mEJP frequency and amplitude (Parameters for Mini Analysis were set as: 0.2 (threshold) and 1 (area threshold)). 35 individual EJP traces and a 45s-long mEJP trace per muscle were analyzed for at least 15 muscles per genotype. Quantal content was corrected for non-linear summation using the revised Martin correction factor as described in (Kim et al., 2009; Morgan and Curran, 1991).

Data analysis

Data was analyzed by either Student's t-test (two groups) or one-way ANOVA followed by Tukey test (multiple groups). p values smaller than 0.05 were considered statistically significant. All p values are indicated as * $p < 0.05$, ** $p < 0.01$, and *** $p < 0.001$ and **** $p<0.0001$. Data are presented as mean ± SEM.

3.4 Results

The Wnd signaling pathway mediates presynaptic assembly defects in *unc-104* mutants

Mutations in *Drosophila unc-104* lead to striking impairments in the synapse structure and function at the NMJ (Pack-Chung et al., 2007; Kern et al., 2013; Zhang et. al. 2016; Zhang et al., unpublished data and Figures 3.1 and 3.3). Surprisingly, we found that the structural and functional synaptic defects caused by severely hypomorphic mutations in *unc-104* could be

rescued to near completion by mutations in *wnd* (Figure 3.1 and 3.3). The defects that could be rescued include: (1) a reduction in the localization of AZ components at NMJ terminals. Up to 50% of synapses (identified by postsynaptic GluRIII clusters) in *unc-104* mutants appear to lack presynaptic AZs, based on the absence of multiple presynaptic AZ components (including the cytomatrix component Brp/ELK/CAST (Figure 3.1A and E), Liprin-α (Figure 3.1B and 3.2A) and voltage gated calcium channel Cacophony (Cac) (Figure 3.2E)). Brp intensity was also reduced within synapses that contained presynaptic components (Figure 3.1D and 3.2C), and across NMJ terminals (Figure 3.1D and F). *Wnd* mutants also suppressed (2) reduced levels of SV associated proteins, such as the vesicular glutamate transporter VGlut, across NMJ terminals (Figure 3.1C and F); (3) aberrant bouton morphology (Figure 3.1C and D); (4) impaired synaptic transmission (Figure 3.3 and 3.2H) including reduced quantal content and strongly reduced mini frequency; (5) defects in larval motility (Figure 3.2I, partial rescue); and (6) lethality at late 3rd instar and pupal stages (Figure 3.1G and 3.2F, partial rescue). Throughout all results, we noticed similar rescue effects for two different *unc-104-hypomorphic* alleles (*bris* and *O3.1*), which were tested as trans-heterozygotes over different *unc-104-null* alleles (*P350* and *d11204*). Likewise, different *wnd* alleles (*1* and *3*) and RNAi knockdown of *unc-104* or *wnd* (Figure 3.1 and 3.2, and data not shown), led to similar suppression. Results using RNAi knock-down (Figure 3.1B, G and 3.2A, B, F and I), including use of a single-neuron Gal4 driver (Figure 3.2G) indicate that both Unc-104 and Wnd function cell-autonomously for the synaptic phenotypes. Altogether, these observations reveal a critical role for Wnd in regulating the presynaptic assembly defects, transmission failures and lethality of *unc-104* mutants.

In axonal regeneration and synaptic overgrowth, Wnd has been shown to act in a signaling pathway consisting of a cascade of MAP kinases and transcription factors (Tedeschi

and Bradke, 2013). We found that inhibition of the downstream MAPK JNK (Bsk) and Fos transcription factor, via expression of dominant-negative (DN) isoforms in neurons, could rescue the assembly defect for release machinery components Brp and Cac (Figure 3.1E, 3.2D and E). These results imply that a signaling pathway consisting of Wnd, JNK and Fos inhibits presynaptic assembly, in a cell-autonomous manner, in *unc-104* mutants.

The Wnd signaling pathway is restrained by Unc-104

To assess whether Wnd signaling is activated in *unc-104* mutants, we utilized a transcriptional reporter of JNK signaling, the *puckered* (*puc*)-lacZ enhancer trap (Martín-Blanco et al., 1998), which has been previously shown to report Wnd signaling activity in motoneurons (Xiong et al., 2010). Reduction of *unc-104* expression by RNAi in motoneurons (using 2 independent RNAi lines) led to a significant increase in *puc*-lacZ expression (3-5 fold, depending on the RNAi line). This increase was abolished when *wnd* was concomitantly knocked-down by RNAi (Figure 3.4A and B), hence reflects activation of a Wnd-mediated nuclear signaling cascade.

When the Wnd signaling pathway is activated in motoneurons, nerve terminals undergo overgrowth characterized by more boutons and longer branches at the NMJ (Collins et al., 2006). Similar overgrowth was reported in *unc-104* mutants (Kern et al., 2013). We found that inhibition of Wnd, JNK or Fos in presynaptic motoneurons could all suppress the overgrowth defect in *unc-104* mutants (insets in Figure 3.1C and D; Figure 3.5A and B). This further implies that the Wnd signaling pathway is activated in *unc-104* mutants.

Previous studies have shown that activation of Wnd/DLK signaling enhances the ability of axons to initiate regenerative axonal growth after injury (Hammarlund et al., 2009; Shin et al., 2012; Xiong et al., 2010; Yan et al., 2009). Consistent with these findings, we found that *unc-104* mutants showed an enhanced axonal regeneration response compared to wild type animals. By 9 hours after nerve crush injury, axons in wild type animal initiate new growth via short filopodia-like branches from the proximal axonal stump. At 18 hours, a few branches are stabilized and grow either towards the distal axon or the cell body (Figure 3.4C). In comparison, *unc-104* mutants showed a marked increase in new axonal branches at 9 hours (Figure 3.4C and D), and at 18 hours these new axonal branches showed similar stabilization but extended nearly twice as far as wild type axons (Figure 3.4C and E). We observed similar enhancement of regeneration cell autonomously when *unc-104* expression was reduced by RNAi (Figure 3.4E). These observations imply a non-intuitive role for the Unc-104 motor in restricting the ability of axons to regenerate by inhibiting Wnd signaling.

Previous studies have suggested links between JNK signaling and the regulation of axonal transport (Verhey and Hammond, 2009). It is therefore interesting that other mutations that disrupt axonal transport, including mutations which inhibit kinesin-1, dynein and dynactin did not significantly affect the expression of *puc*-lacZ ((Figure 3.4B) and (Xiong et al., 2010)). This specificity suggests a unique functional interdependence between Wnd and the Unc-104 kinesin.

Wnd is mis-localized to the cell body in *unc-104* mutants

Wnd and its DLK homologues in mammals and *C. elegans* are known to be highly regulated at the protein level (Feoktistov et al., 2016; Hao et al., 2016; Huntwork-Rodriguez et al., 2013) which includes regulation by a highly conserved ubiquitin ligase domain protein Hiw/Rpm-1/Phr1 (Babetto et al., 2013; Collins et al., 2006; Nakata et al., 2005; Xiong et al., 2010). In contrast, mutations in *unc-104* did not lead to a detectable increase in global levels of endogenous Wnd protein (Figure 3.5H), or in synaptic Wnd protein level (Figure 3.5D and G). However, using a MiMIC-*wnd*-GFP line (Venken et al., 2011), in which a GFP tag is inserted via an exon trap within the *wnd* genomic locus (Figure 3.5C), and a UAS-GFP-wnd^{kd} (kinase dead Wnd) transgenic line, we observed that *unc-104* mutations caused an increase in the level of Wnd protein in motoneuron cell bodies (Figure 3.4F-I) and axons (Figure 3.5E and F). We considered the possibility that Unc-104 directly transports Wnd-associated vesicles. However, we observed no impairment of Wnd's transport in *unc-104* mutants (Figure 3.6A-D), and no co-localization for Wnd and Unc-104 (Figure 4.1), so we interpret that Wnd is unlikely to be a direct cargo of Unc-104.

Wnd inhibits presynaptic assembly independently of Liprin-α and Rab3

We then considered the possibility that Unc-104 regulates Wnd signaling indirectly via the transport of another cargo. We focused upon two previously identified cargos/adaptors of Unc-104 with known roles in presynaptic assembly: Liprin-α (Shin et al., 2003) and Rab3-GEF (Niwa et al., 2008). Liprin-α is recruited to the AZ at early stages of synapse assembly and is required for normal morphology of the presynaptic terminal (Südhof, 2012). Rab3-GEF and its target, the small GTPase Rab3 plays an important role in regulating presynaptic assembly in

Drosophila (Graf et al., 2009). Moreover, ectopic overexpression of Rab3 can ameliorate some of the synaptic defects caused by impaired Unc-104 function (Zhang et al., 2016). We observed that *liprin-α* mutant NMJs contain a large portion of unopposed GluRIII-labeled PSDs, resembling the defects in *unc-104* mutants (Figure 3.7A). Similar defects were reported for *rab3* and *rab3-gef* mutants (Bae et al., 2016; Graf et al., 2009). However, in contrast to *unc-104*, the *liprin-α* and *rab3* synaptic defects were not suppressed by mutations in *wnd* (Figure 3.7A-C). Furthermore, the increased Brp intensity per AZ and reduced AZ number due to *liprin-α* and *rab3* mutations was not suppressed by *wnd* mutations (Figure 3.7A, B and D). This suggests that Liprin-α and Rab3 regulate presynaptic assembly via pathways that are either independent or downstream of Wnd. In addition, the *puc*-lacZ transcriptional reporter for Wnd/JNK signaling was only slightly activated in *liprin-α* and *rab3-gef*/*rab3* mutants, far less than the activation by *unc-104* knock-down (Figure 3.7E). Collectively, these data indicate that Rab3 and Liprin-α are not responsible for Wnd activation in motoneurons.

Activation of the Wnd signaling pathway in neurons is sufficient to impair presynaptic assembly and synaptic transmission

If activated Wnd signaling is responsible for the synaptic defects in *unc-104* mutants, then ectopic activation of Wnd should mimic the *unc-104* mutant phenotype. Indeed, expression of *wnd* alone in motoneurons resulted in a cell-autonomous presynaptic defects that are comparable to *unc-104* mutants: many synapses lacked Brp (Figure 3.8A and C), and synapses that contained Brp had reduced Brp intensity (Figure 3.8B), which resulted in a global 70%

reduction in Brp intensity across the entire NMJ terminal (Figure 3.8B). VGlut intensity within NMJ terminals was also reduced (Collins et al., 2006).

Hiw is a negative regulator of the Wnd protein (Collins et al., 2006; Nakata et al., 2005) and *hiw* mutants displayed strikingly similar presynaptic defects to *unc-104* mutants, all of which were suppressed in *hiw;wnd* double mutants (Figure 3.9) . These included 60% of synapses lacking AZ proteins, Brp, Liprin-α and Cac (Figure 3.9A, B and D), a reduction of total Brp intensity at individual synapses and across the NMJ terminal (Figure 3.8G and 3.9C), and, as previously reported, overgrowth of synaptic boutons, decreased VGlut levels, and impaired spontaneous synaptic transmission (Collins et al., 2006; Nakata et al., 2005). We also observed that both *hiw* and *unc-104* mutant nerves showed reduced excitability, requiring a higher stimulus to evoke a synaptic response. In addition, we found that the activation of Wnd accounts for a significant portion of the reduced quantal content observed in *hiw* mutants (Figure 3.8D-F and 3.9E-G). This result differed from a previous study which found that Wnd did not affect quantal content in *hiw* mutants(Collins et al., 2006), and may be related to different alleles used. (We used null alleles ($wnd^{3/3}$ and wnd^{3}/Df), while the previous study used an allele that may be hypomorphic (wnd^{1})). Taken together, these observations indicate that activation of the Wnd signaling pathway leads to significant presynaptic defects in synaptic structure and synaptic transmission.

Wnd inhibits synapse assembly independently of cargo transport downstream of Unc-104

The above findings indicate that Wnd signaling is regulated by Unc-104, and that loss of this regulation is sufficient to impair synapse formation. However a recent study has suggested an opposite relationship, that Unc104 may be regulated by Wnd/JNK signaling (Voelzmann et al., 2016). To more firmly understand the relationship of Unc-104 and Wnd, we tested whether *wnd* mutations could suppress the synaptic and/or transport defects of *unc-104* null mutants during the earliest stages of synaptic formation.

Consistent with previous studies (Pack-Chung et al., 2007), homozygous null mutants of *unc-104* failed to form NMJ synapses and died at the late embryonic stage (stage 17). The nascent presynaptic terminal had very few AZs, and failed to form mature synaptic boutons. In $unc\text{-}104^{null};wnd^{3/3}$ double mutants, the bouton morphology defects and the AZ defects were suppressed (Figure 3.10A and C), with an increase in the number of Brp puncta (Figure 3.10D) and total intensity of Brp at NMJ terminals (Figure 3.10E). While the $unc\text{-}104^{null};wnd^{3/3}$ mutants still failed to hatch and died at the late embryonic stage, we noticed a modest rescue of muscle contraction when the mutant were assisted out of their vitelline membrane (Figure 3.11D), consistent with the rescue of synaptic defects.

Despite the pronounced rescue of presynaptic structure, and in contrast with the strong suppression of *unc-104* hypomorphic mutants (Figures 3.1 and 3.3), *wnd* mutations failed to rescue the defective localization of SV components in $unc\text{-}104^{null}$ mutants (Figure 3.10). VGlut, synaptotagmin-I (sytI) and CSP (cysteine string protein) were almost completely depleted from NMJ and accumulated at the cell body, and this defect persisted in $unc\text{-}104^{null};wnd$ double mutants (Figure 3.10B, C and E, 3.11C, 3.12A, 3.13A and B). In contrast to the complete failure of *wnd* mutants to rescue SV protein localization, the localization of synapsin, which can

associate with SVs and AZs in a regulated (non-obligate) manner (Baitinger and Willard, 1987; Easley-Neal et al., 2013), was weakly suppressed (Figure 3.10E and 3.11A).

Taken together, the genetic interactions with Wnd allow us to parse the synaptic phenotypes of *unc-104* mutants into two separable mechanisms (Figure 3.14H). The first is a consequence of Unc-104's direct role in transporting SV components to synaptic terminals, and the second comes from the activation of Wnd signaling when *unc-104*'s function is lost.

Wnd regulates the expression level of presynaptic proteins downstream of Unc-104

Consistent with the interpretation that Unc-104 is an important transporter of pre-synaptic proteins, reductions in synaptic localization of Brp, VGlut, and other synaptic proteins in *unc-104* mutants are accompanied by an accumulation of these proteins in cell bodies (Hall and Hedgecock, 1991; Pack-Chung et al., 2007). We noticed that this accumulation was enhanced in *unc-104;wnd* double mutants (Fig.7A). This suggests that the Wnd pathway may inhibit synapse assembly by restraining total levels of presynaptic proteins in motoneurons. Since motoneurons represent only a small component of the *Drosophila* nervous system, we carried out quantitative immunohistochemistry to compare total protein levels in motoneuron cell body, axonal and synaptic compartments (described further in Methods). In both *unc-104*-null (stage 17 embryos, Figure 3.12A-B, and 3.13A-B) and hypomorphic (3rd instar larvae, Figure 3.12C-E) mutants, we observed reductions in intensity of SytI, VGlut, CSP and Brp. In all cases this reduction was largely suppressed in *unc-104;wnd* double mutants. The increased intensity of synaptic proteins was restricted to cell bodies in *unc-104^{null};wnd* double mutants (Figure 3.12A, 3.13A and B), but appeared in axons and synaptic terminals in the *unc-104^{hypomorph};wnd* double mutants (Figure

3.12E, 3.1F and 3.13I), likely the result of residual Unc-104 transport function in the hypomorphic mutants.

These observations build a model that Wnd signaling, which becomes activated in *unc-104* mutants, inhibits synapse assembly by down-regulating the expression of multiple pre-synaptic proteins. In support of this, *unc-104* mutations led to decreased expression of a *vglut*-DsRed transcriptional reporter in motoneurons, in a Wnd-dependent manner (Figure 3.12C, G and 3.13H). We also detected changes in total mRNA levels for Brp, VGlut and Cac in *unc-104;wnd* double mutants via RT-PCR (Figure 3.13G), suggesting possible transcriptional regulation of multiple presynaptic genes. Neuronal genes and proteins, including Elav (Figure 3.13F) and Liprin-α (Figure 3.13G), and general synaptic markers, including HRP (Figure 3.13D) and GluRIII (Figure 3.13E), appeared unaffected by Wnd.

Wnd restrains the expression of presynaptic proteins at early stages of synaptogenesis

Since the expression of presynaptic proteins is critical for the development, function and plasticity of synapses, we asked whether Wnd regulates the expression of presynaptic proteins in a developmental context. Since unrestrained Wnd signaling in *unc-104* mutants inhibits presynaptic assembly during early stages of NMJ development (Figure 3.10), we investigated the phenotype of *wnd-null* mutants in embryos during stages of axonal outgrowth and synapse formation (stages 14 through 17). We observed a modest but statistically significant role for Wnd in restricting pre-synaptic protein expression in early developmental stages. For VGlut, the differences between wild type and *wnd* mutant were observed only in motoneuron cell bodies in

early stage 15 embryos (Figure 3.14A-C). We note this is the time point at which VGlut protein first becomes expressed in motoneurons, which precedes the time of its delivery to presynaptic terminals (Figure 3.14C, D and 3.15A), and coincides with the time at which most motoneuron axons are first reaching their target muscles (Johansen et al., 1989). SytI intensity was also increased in *wnd* mutants at early (stage 16, Figure 3.14E-F and 3.15B) but not late (3rd instar larvae, Figure 3.15C) time points. In contrast, we observed no significant increase in Synapsin intensity during early development and a modest but significant decrease in Brp at stage 16 (Figure 3.15A, D and E). However we noted that Brp, VGlut (Horiuchi et al., 2007), Syt1 and Synapsin (Figure 3.15F) showed elevated intensity in axons of *wnd* mutants. These early and transient changes of in *wnd* mutants suggest that Wnd may be required for refining the timing and/or degree of expression of presynaptic proteins at specific developmental stages.

Wnd signaling is sensitive to misregulated presynaptic proteins

Across our cumulative observations, we noticed an interesting correlation between the function of Wnd and the appearance of presynaptic proteins localized in motoneuron cell bodies. During development, the role of Wnd in restraining VGlut was most significant immediately after the onset of VGlut expression and before its transport to synaptic terminals (Figure 3.14B-D). In *unc-104* mutants, the highly elevated function of Wnd to restrain the expression of presynaptic components coincided with their accumulation in cell bodies (Figure 3.12A and 3.13B). We propose that Wnd signaling controls the expression of abundant presynaptic proteins to levels appropriate for their transportation (Figure 3.14H).

This model predicts that Wnd signaling, which is highly restrained in wild type uninjured neurons, would become activated when the levels of presynaptic proteins are in excess. We therefore tested whether ectopic over-expression of SV or AZ component proteins had any effect upon Wnd signaling in uninjured neurons. Each of the three proteins tested, Brp, SytI and VGlut, caused a significant induction of the *puc*-lacZ reporter (Figure 3.14G), while over-expression of other proteins (Luciferase (Figure 3.14G) and membrane localized GFP (Figure 3.4B)), had no effect. In order to determine whether this is due to altered synaptic activity, we over-expressed a non-functional VGlut transgene, $VGlut^{A470V}$, which has no effect upon synaptic physiology (Daniels et al., 2011). This mutated VGlut caused a similar induction in *puc*-lacZ expression (Figure 3.14G). These results, taken together with the cell autonomous nature of Wnd activation in *unc-104* mutants (Figure 3.4A), suggest that Wnd signaling is sensitive to a trafficking aspect of misregulated presynaptic proteins.

3.5 Discussion

Synaptic defects in *unc-104* mutants are caused by activation of the Wnd/DLK signaling pathway independently of impaired cargo transport.

The kinesin-3 family member Unc-104/Imac/KIF1A is known to be an important mediator of presynaptic assembly: mutations in *unc-104* and its homologues inhibit the localization of SV and AZ precursors to nascent synapses, causing profound defects in synapse development and function (Barkus et al., 2008; Hall and Hedgecock, 1991; Kern et al., 2013; Li et al., 2016; Niwa et al., 2016; Otsuka et al., 1991; Pack-Chung et al., 2007; Yonekawa, 1998; Zhang et al., 2016). While these synaptic defects have been considered logical outcomes of

defective transport, we found that major aspects, including impaired AZ addition and maturation of synaptic boutons, are not mediated by a direct transport role for the Unc-104 protein. Rather, the *unc-104^{null};wnd* double mutants reveal separable functions for Unc-104: (1) Transport of SVPs to synaptic terminals is likely a direct function, since it persists in *unc-104^{null};wnd* double mutants, and is consistent with previous biochemical data. (2) Localization of AZs is unlikely to be a direct transport role, but is instead mediated by the Wnd/DLK signaling pathway, which becomes activated when Unc-104 function is impaired (Figure 3.14H).

With the knowledge that the Wnd/DLK signaling pathway is activated in *unc-104* mutants, it is now worth considering whether it contributes to other phenotypes previously described for Unc-104 and its homologues in other species. These include impaired dendritic branching (Kern et al., 2013), increased microtubule dynamics (Chen et al., 2012), failed neuronal remodeling (Park et al., 2011), which may be related to Wnd/DLK's ability to alter microtubule growth (Hirai et al., 2011; Lewcock et al., 2007), neuronal remodeling (Kurup et al., 2015; Marcette et al., 2014) and dendrite growth (Wang et al., 2013). *Unc-104/Kif1a* mutants also show accelerated motor circuit dysfunction in aging animals (Li et al., 2016), impaired BDNF-stimulated synaptogenesis (Kondo et al., 2012) and neuronal death (Yonekawa, 1998). These phenotypes may also be facilitated by activation of DLK, which impairs synaptic development and function (this study and Nakata et al., 2005), and has also been shown to mediate neuronal death in some contexts (Chen et al., 2008; Pozniak et al., 2013; Welsbie et al., 2013). Human mutations in *KIF1A* have been associated with hereditary spastic paraplegia (SPG30) (Fink, 2013), and hereditary sensory and autonomic neuropathy type IIC (HSN2C) (Rivire et al., 2011). The possibility that DLK activation mediates deleterious aspects of these disease pathologies becomes an interesting future question.

Wnd/DLK pathway is sensitive to defects in Unc-104-mediated transport

How does the Wnd pathway become activated in *unc-104* mutants? The mechanism(s) that lead to activation of Wnd and its DLK homologues are of general interest for their roles in axonal regeneration as well as degeneration and neuronal death. In addition to axonal injury (Watkins et al., 2013; Welsbie et al., 2013; Xiong et al., 2010), disruption of microtubule and/or actin/cortical cytoskeleton can lead to activation of DLK (Valakh et al., 2013, 2015). Moreover, many studies have noted a role for DLK signaling in mediating structural changes in neurons downstream of manipulations that disrupt cytoskeleton (Bounoutas et al., 2011; Marcette et al., 2014; Massaro et al., 2009). Since the cytoskeleton is a closely functioning partner of all motor proteins, and is also implicitly affected by axonal injury, it is possible that these manipulations share a similar underlying mechanism with that of *unc-104* mutations. While disruption of cytoskeleton should impair transport by many motor proteins, mutations that impair kinesin-1 and dynein do not lead to activation of Wnd (Figure 3.4 and (Xiong et al., 2010)). This specificity suggests that disruption of Unc-104 mediated transport, potentially via mislocalization of Unc-104's cargo, mediates Wnd/DLK's activation after cytoskeletal disruption and potentially after axonal injury.

This line of reasoning leads to further consideration of Unc-104's cargo. Our live imaging data do not support a simple model that Wnd is a cargo of Unc-104 (Figure 3.6). Known cargo of Unc-104 are important for the assembly and function of synapses (Goldstein et al., 2008), so does Wnd activation occur in response to an impairment in synaptic assembly or function? We think this is unlikely, since mutations in *rab3-gef*, *liprin-α* (Figure 3.7E) and *vglut*

(data not shown), which impair presynaptic assembly and function, do not cause activation of Wnd (Figure 3.7E).

Instead, we note an intriguing correlation between the localization and abundance of presynaptic proteins with Wnd's activation: Wnd signaling becomes activated in *unc-104* mutants, which accumulate presynaptic proteins in the neuronal cell body. We noticed a similar role for endogenous Wnd in wild type neurons during the onset of embryonic NMJ development. These stages correspond to the onset of synaptic protein expression, before substantial transport to synaptic terminals, hence represent a time in which levels are high in the cell body. Consistent with the idea that Wnd signaling is sensitive to mislocalized presynaptic proteins, ectopic overexpression of several different presynaptic proteins caused an elevation in Wnd signaling in uninjured neurons (Figure 3.14G). These observations suggest a model that accumulations of presynaptic proteins, as a feature of aberrant cargo transport, are 'sensed' by Wnd signaling (Figure 3.14H).

Wnd/DLK signaling restrains the expression of presynaptic proteins: mechanism and relevance.

While previous studies in *C. elegans* (Nakata et al., 2005; Yan et al., 2009) have suggested that DLK activation may impair synaptic development (altering the size and spacing of active zones), the regulation of total levels of presynaptic proteins and the relationship with Unc-104 provides a new view into Wnd/DLK's function and mechanism. In addition to VGlut, SytI, CSP-1, Brp, Liprin-α and Cac, we suspect that Wnd inhibits the expression of a larger cohort of presynaptic proteins. Regulation of multiple targets required for synapse development

can explain the severe defects in *unc-104-hypomorph* mutants, and the dramatic suppression by disruption of the Wnd pathway (Figure 3.1 and 3.3). In support of this idea, presynaptic defects in *unc-104-hypomorph* mutants can be partially rescued by overexpressing Brp (Kern et al., 2013) or Rab3 (Zhang et al., 2016).

It is interesting to consider that the targets of Wnd regulation are also abundant presynaptic proteins, and are thought to be major cargo for axonal transport. Down-regulation of these proteins in response to defects in their transport or after axonal damage may comprise an adaptive response mechanism to prevent unwanted buildup or wasted cellular resources. This role of Wnd, together with its "sensing" role, likely serves as a mechanism to prevent cargo buildup in *unc-104* mutants (Figure 3.14H).

How does Wnd signaling regulate presynaptic proteins? The regulation of the *vglut*-promoter-DsRed reporter suggests the involvement of transcriptional regulation (Figure 3.12F-G), and we also noticed increased levels of Brp, VGlut and Cac transcripts in *unc-104;wnd* double mutants (Figure 3.13G). We are limited in our ability to detect total changes in mRNA and protein levels from whole nerve cord preparations by the fact that the Wnd signaling pathway may not be acting in all cell types. It is also possible that additional post-transcriptional mechanisms, such as regulation of protein stability or translation, factor into the regulation of presynaptic proteins by Wnd.

Many previous studies have reported links between JNK signaling and kinesin-driven transport (Verhey and Hammond, 2009), with some observations suggesting that JNK signaling may directly regulate the function of kinesin-1, modulating its cargo binding, affinity for microtubules and its processivity (Fu and Holzbaur, 2013; Horiuchi et al., 2007; Morfini et al.,

2006; Stagi et al., 2006; Sun et al., 2011). Our finding of a separate role for JNK signaling in regulating the abundance of transported cargo adds a new layer of complexity to interpreting phenotypes of axonal transport defects. A commonly described defect is the presence of accumulations of cargo within axons, referred to as 'traffic jams'. These defects have been noted for many different mutations, including kinesin-1 and dynein subunits (Gindhart et al., 1998; Kurd and Saxton, 1996; Martin et al., 1999), and also in mutants for *wnd* and other members of JNK signaling pathways (Bowman et al., 2000; Horiuchi et al., 2005, 2007). Does a failure to regulate excess protein cargo contribute to the presence of the jams? Intriguingly, *unc-104* mutations do not cause 'traffic jams' in axons, but instead leads to accumulate of synaptic proteins in cell bodies, which correlates with the activation of Wnd signaling.

Finally, it is interesting to compare Wnd's role in fine-tuning levels of presynaptic proteins with previously identified roles for DLK in promoting cell death (Chen et al., 2008; Huntwork-Rodriguez et al., 2013; Pozniak et al., 2013; Watkins et al., 2013; Welsbie et al., 2013). While *Kif1a* mutant mice show early signs of neuronal death and degeneration, which may potentially be mediated by activation of DLK, *unc-104* mutants in *C. elegans* and *Drosophila* lack hallmarks of cell death and synaptic degeneration (Hall and Hedgecock, 1991; Kern et al., 2013; Pack-Chung et al., 2007). In analogy with other stress response pathways, regulation of presynaptic proteins may comprise a first order response that facilitates adaptation to stress, while cell death can be used as the more extreme response of 'last resort'. Inhibition of synaptic proteins is, alone, a pathology that becomes relevant for long term maintenance of synapses and their function over time, since synthesis and transport of new synaptic proteins likely needs to occur throughout the long lifespan of a neuron. Interestingly, previous studies have linked activation of JNK signaling to synapse loss in aged animals (Ma et al., 2014; Sclip et

al., 2014; Voelzmann et al., 2016). Exciting future work lies ahead to further understand DLK's activation and its consequences in different models of neuronal injury, disease, and aging.

3.6 Figures

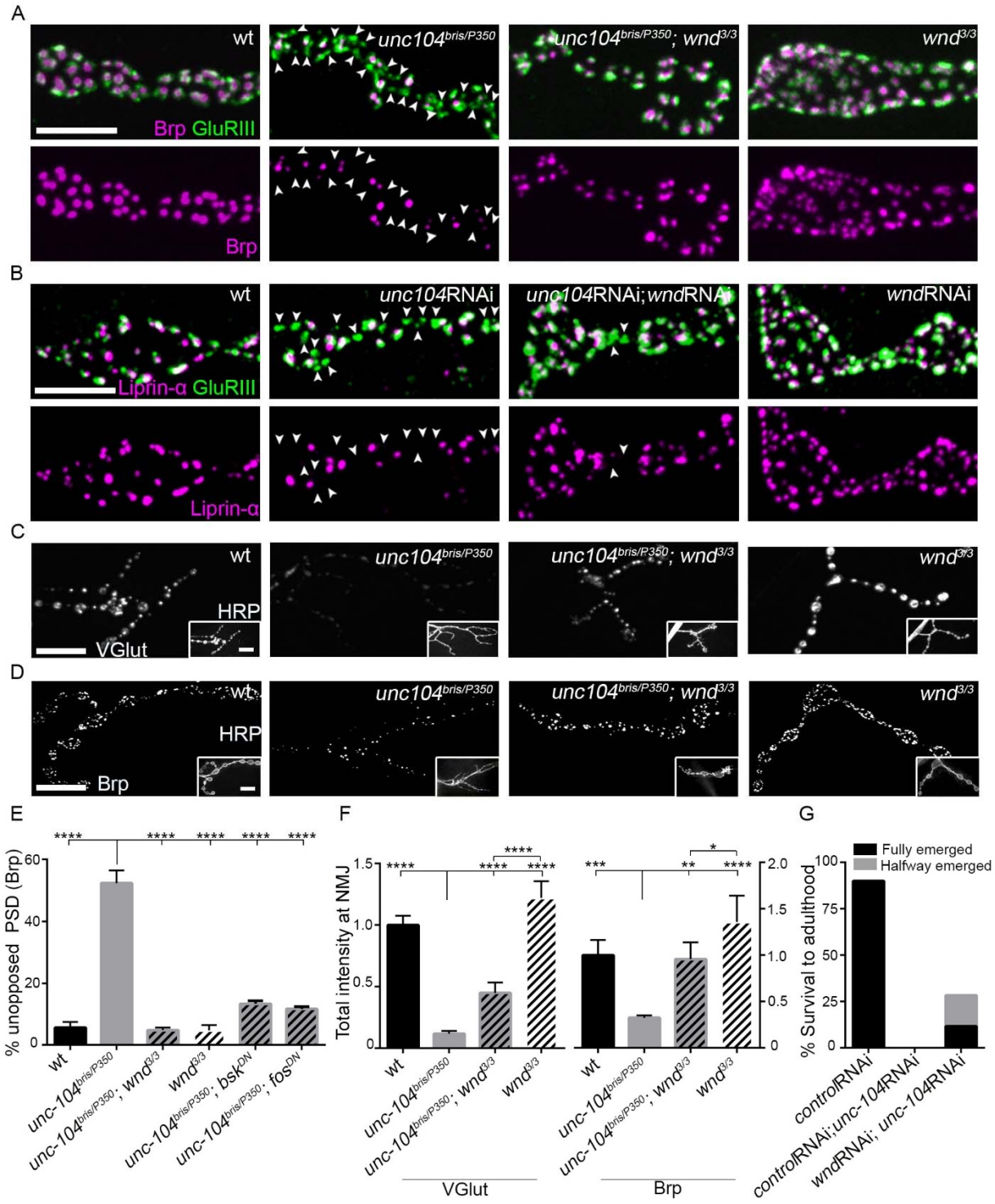
A
wt
unc104bris/P350
unc104bris/P350; wnd3/3
wnd3/3
Brp GluRIII
Brp
B
wt
unc104RNAi
unc104RNAi;wndRNAi
wndRNAi
Liprin-α GluRIII
Liprin-α
C
wt
unc104bris/P350
unc104bris/P350; wnd3/3
wnd3/3
HRP
VGlut
D
wt
unc104bris/P350
unc104bris/P350; wnd3/3
wnd3/3
HRP
Brp
E
% unopposed PSD (Brp)
wt
unc-104bris/P350
unc-104bris/P350; wnd3/3
wnd3/3
unc-104bris/P350; bskDN
unc-104bris/P350; fosDN
F
Total intensity at NMJ
wt
unc-104bris/P350
unc-104bris/P350; wnd3/3
wnd3/3
VGlut
Brp
G
% Survival to adulthood
Fully emerged
Halfway emerged
controlRNAi
controlRNAi;unc-104RNAi
wndRNAi; unc-104RNAi

Figure 3.1: Wnd signaling pathway is required for the presynaptic assembly defect in *unc-104* mutant NMJs.
(A-D) Representative confocal images of third instar larval neuromuscular junctions (NMJ) at muscle 4. Postsynaptic densities (PSDs) identified by GluRIII staining (Green) that lacked apposing AZ components Brp (magenta in A), or Liprin-α (magenta in B) are highlighted by arrowheads. Note that when determining the absence of AZ, the pixel saturation threshold was reduced to reveal any AZ of weak signal. (This resulted in saturation of certain pixels in wt controls. For more details, see Experimental Procedures.)
(A) Alignment of postsynaptic GluRIII (green) with presynaptic AZ component Brp (magenta) in *Canton-S* (wt), $unc\text{-}104^{bris/P350}$, $unc\text{-}104^{bris/P350};wnd^{3/3}$ and $wnd^{3/3}$. $Unc\text{-}104^{P350}$ is a null allele.
(B) Alignment of postsynaptic GluRIII (green) with presynaptic AZ component Liprin-α (magenta). Liprin-α-GFP was driven by rab7 promoter and UAS-*unc-104* RNAi and UAS-*wnd* RNAi were driven by neuronal *elav*-Gal4.
(C-D) VGlut (C) and Brp (D) distribution at one NMJ terminal at Muscle 4. The motoneuron membrane was labeled by HRP (inset).
(E) The percentage of unopposed GluRIII-labeled PSDs from 1A, 3.2C and D. The unopposed PSDs were defined by the GluRIII-labeled PSDs that lacked any trace of the presynaptic AZ protein Brp.
(F) Quantification of the total intensity of VGlut (C) and Brp (D) immunostaining within the entire synaptic NMJ terminal at the muscle 4, normalized to that in wild type animals.
(G) Percentage survival of larvae to adulthood. For details, see Supplemental Experimental Procedures.
All data are represented as mean ± SEM; At least 8 animals and 12 NMJs were examined per genotype; **** $P<0.0001$, *** $P<0.001$, ** $P<0.01$, *$P<0.05$. Scale bar, 5μm (A-B) and 20μm (C-D). For additional data, see Figure 3.2.

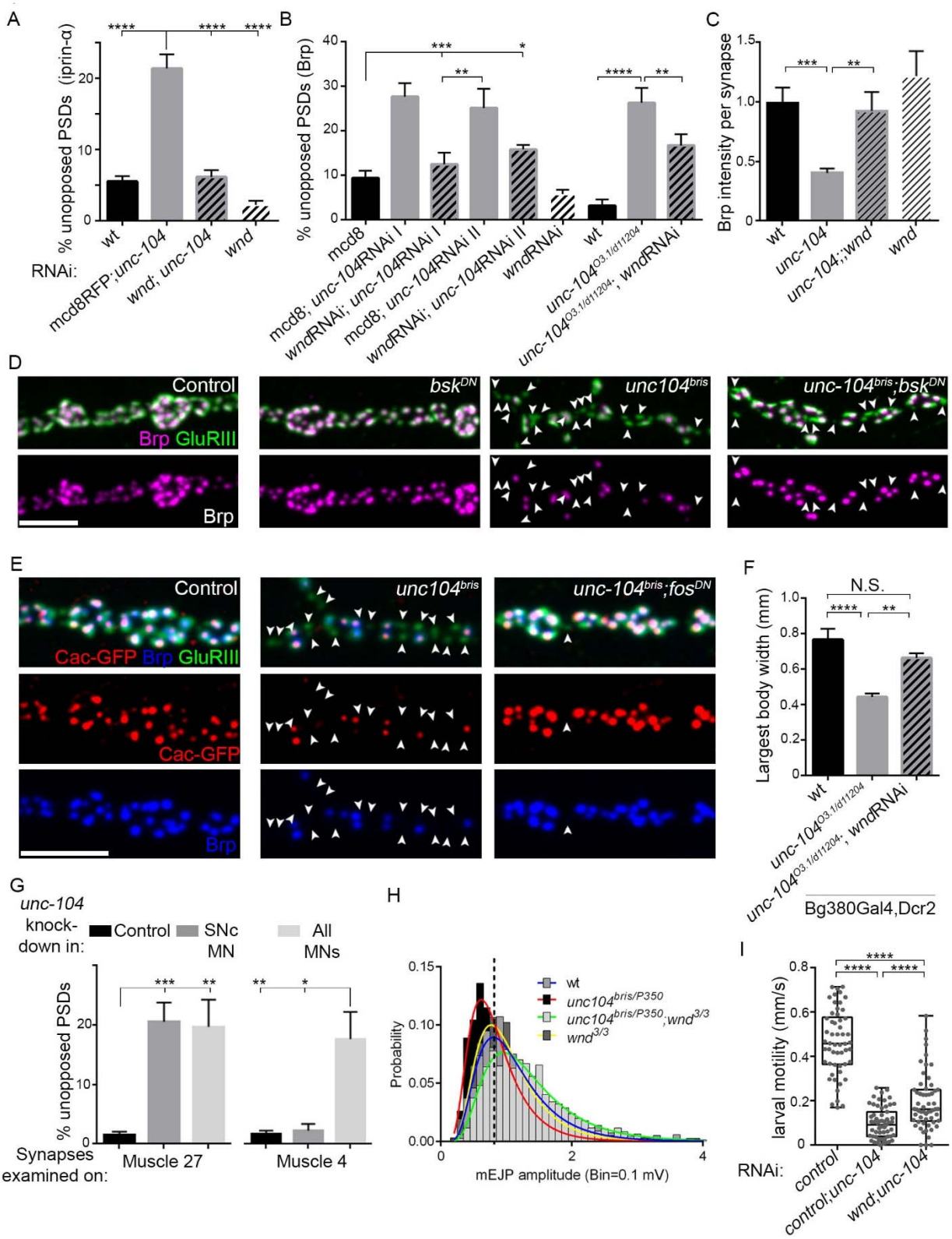
A
% unopposed PSDs (iprin-α)
RNAi:
wt
mcd8RFP;unc-104
wnd; unc-104
wnd
B
% unopposed PSDs (Brp)
mcd8
mcd8; unc-104RNAi I
wndRNAi; unc-104RNAi I
mcd8; unc-104RNAi II
wndRNAi; unc-104RNAi II
wndRNAi
wt
unc-104Q3.1/d11204
unc-104Q3.1/d11204; wndRNAi
C
Brp intensity per synapse
wt
unc-104
unc-104;;wnd
wnd
D
Control
Brp GluRIII
Brp
bskDN
unc104bris
unc-104bris;bskDN
E
Control
Cac-GFP Brp GluRIII
Cac-GFP
Brp
unc104bris
unc-104bris;fosDN
F
N.S.
Largest body width (mm)
wt
unc-104Q3.1/d11204
unc-104Q3.1/d11204; wndRNAi
Bg380Gal4,Dcr2
G
unc-104 knock-down in:
Control
SNc MN
All MNs
% unopposed PSDs
Synapses examined on:
Muscle 27
Muscle 4
H
Probability
mEJP amplitude (Bin=0.1 mV)
wt
unc104bris/P350
unc104bris/P350;wnd3/3
wnd3/3
I
larval motility (mm/s)
RNAi:
control
control;unc-104
wnd;unc-104

Figure 3.2: The Wnd signaling cascade is required in neurons for *unc-104* mutant's defects in presynaptic assembly, animal growth, quantal content and mEJP amplitude, (related to Figures 3.1 and 3.3).
(A) The percentage of unopposed PSDs, defined by the absence of presynaptic Liprin-α-GFP at synapses labeled by GluRIII, increased when *unc-104* was knocked down in motoneurons, using the Rab7 promoter driver. This defect was suppressed when *wnd* was knocked down at the same time.
(B) Showing the cell autonomy of the *unc-104* synaptic defect and the role of Wnd, the percentage of unopposed PSDs, defined by the absence of BRP at synapses labeled by GluRIII, was rescued when Wnd was neuronally knocked down by RNAi together with *unc-104* (2 independent RNAi lines: vdrc 23465, I and TRiP BL43264, II) or *unc-104-hypomorph* mutants. All UAS-RNAi were driven by *Bg380*-Gal4. UAS-Dicer was co-expressed to enhance RNAi efficiency with *unc-104*RNAi II.
(C) Total Brp intensity at individual synapses was reduced in *unc-104$^{bris/P350}$-hypomorph* mutants and restored in *unc-104$^{bris/P350}$;wnd$^{3/3}$* double mutants.
(D-E) Representative confocal images of NMJ synapses labeled with Brp (D) and the L-type calcium channel Cacophony (cac)-GFP (E). Inhibition of JNK/bsk (D) or Fos (E) via expression of a Dominant Negative (DN) transgene rescued the synaptic apposition defect of *unc-104* mutants. (D): Control (*OK319*-Gal4), *bsk^{DN}* (*OK319*-Gal4*;* UAS-*bsk^{DN}*), *unc-104^{bris} (OK319*-Gal4, *unc104$^{bris/d11204}$*) and *unc-104^{bris}; bsk^{DN}* (*OK319*-Gal4, *unc104$^{bris/d11204}$*; UAS-*bsk^{DN}*). (E): Control (*OK319*-Gal4; UAS-*cac*-GFP), *unc-104^{bris}* (*OK319*-Gal4, *unc104$^{bris/d11204}$*; UAS-*cac*-GFP) and *unc-104^{bris}; fos^{DN}* (*OK319*-Gal4, *unc104$^{bris/d11204}$*; UAS-*bsk^{DN},* UAS-*cac*-GFP). GluRIII-labeled PSDs that lack apposing AZs (Cac-GFP or Brp) are highlighted by arrowheads. *unc104^{d11204}* is a null allele.
(F) The largest body width measured in surviving 3rd instar larvae, as described in Supplemental Experimental Procedures, was reduced in *unc-104* mutants and restored when *wnd* was neuronally knocked down. UAS-*wnd*RNAi expression was driven by *Bg380*-Gal4 together with UAS-Dicer2.
(G) Knockdown of *unc-104* causes cell autonomous defects in presynaptic assembly. Two different Gal4 drivers were used to express *unc-104* RNAi, either specifically in SNc neurons, which innervate muscle 26, 27 and 29 (*m12-gal4*) or all motoneurons (*OK6*-Gal4). Knockdown in SNc neurons caused synaptic assembly defects on innervated muscles (quantified for muscle 27) but not other muscles (quantified for muscle 4).
(H) Distribution of mEJP amplitudes in *unc-104* mutants fit with log Gaussian. The center amplitude was determined by the peak of curve: wild type (0.80 mV), *unc104$^{bris/P350}$* (0.61 mV), *unc104$^{bris/P350}$; wnd$^{3/3}$* (0.95mV) and *wnd$^{3/3}$* (0.76 mV). Note that both the center amplitude and the amplitude distribution were restored in double mutants.
(I) Motility of 3rd instar larvae was defective when *unc-104* was knocked down, but was significantly rescued when *wnd* concomitantly inhibited by co-expression of UAS-*wnd*-RNAi but not a control RNAi. UAS-RNAi were driven by *OK371*-Gal4 (See Supplemental Experimental Procedures, below).
All data are represented as mean ± SEM; N.S., not significant; **** P<0.0001, *** P<0.001, ** P<0.01,*P<0.05; Tukey test for multiple comparison; Scale bar, 5μm.

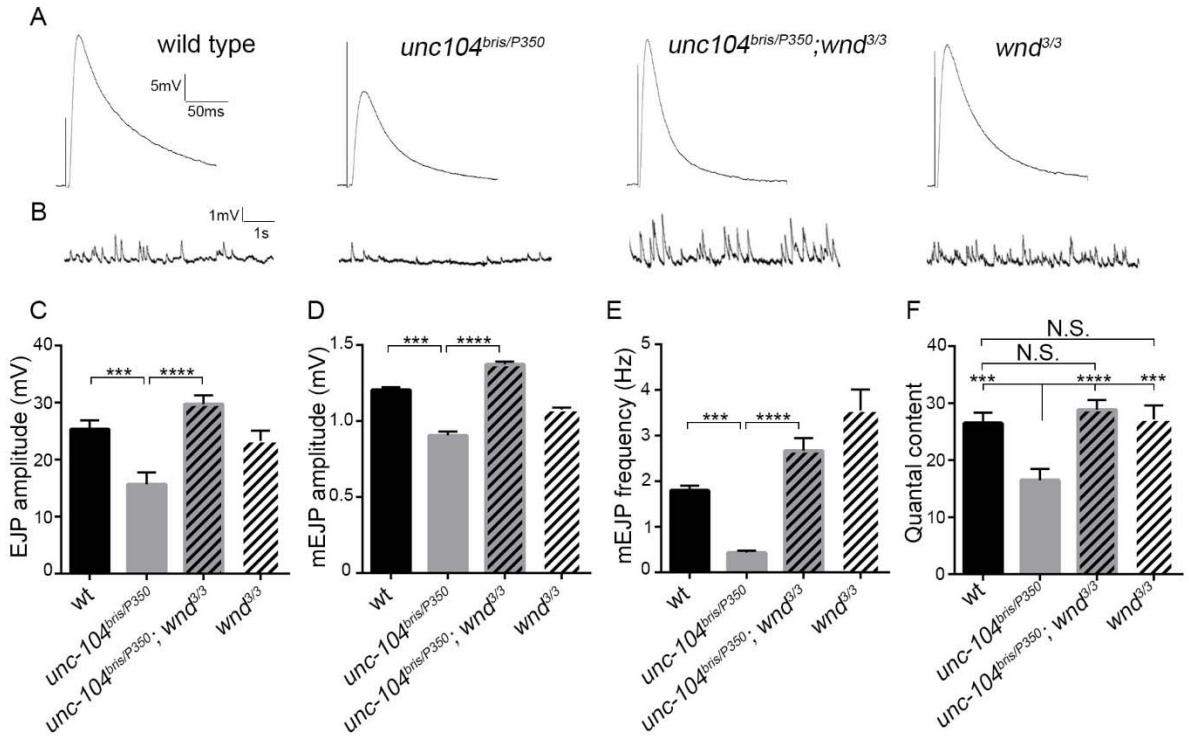

Figure 3.3: The synaptic transmission defect in *unc-104* mutants is suppressed by *wnd* mutations
(A and B) Representative electrophysiological traces of (A) Evoked Excitatory Junctional Potentials (EJP) and (B) miniature Excitatory Junctional Potentials (mEJP) recorded from muscle 6 of third instar larvae
(C-F) Quantification of (C) the average EJP, (D) average mEJP, (E) average mEJP frequency and (F) average quantal content (corrected for nonlinear summation).
All data are represented as mean ± SEM; N.S., not significant; **** P<0.0001, *** P<0.001; Tukey test for multiple comparison. For additional data, see Figure 3.2.

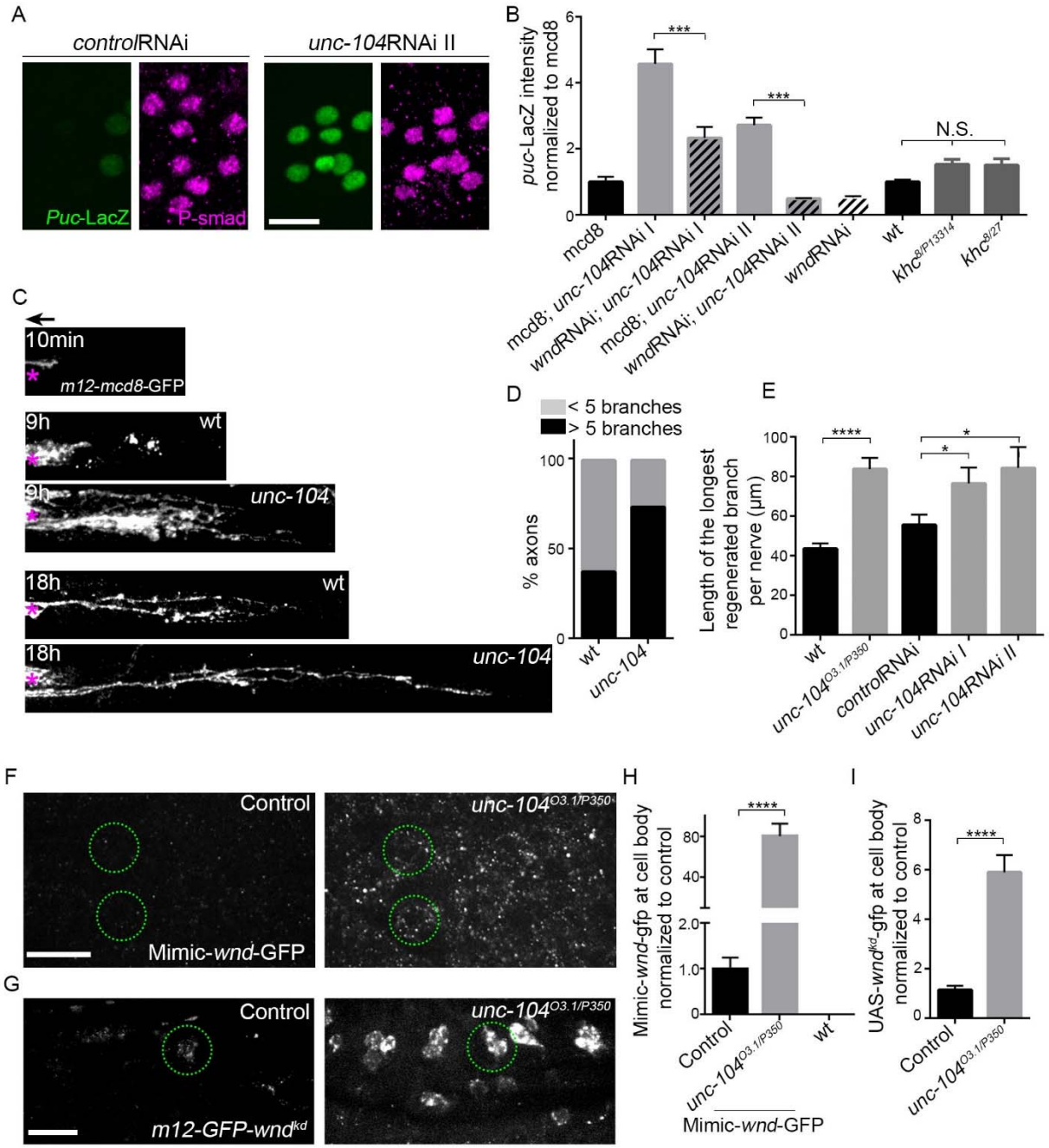
A
controlRNAi
unc-104RNAi II
Puc-LacZ
P-smad
B
puc-LacZ intensity normalized to mcd8
***
***
N.S.
mcd8
mcd8; unc-104RNAi I
wndRNAi; unc-104RNAi I
mcd8; unc-104RNAi II
wndRNAi; unc-104RNAi II
wndRNAi
wt
khc8/P13314
khc8/27
C
10min
m12-mcd8-GFP
9h
wt
unc-104
18h
wt
unc-104
D
< 5 branches
> 5 branches
% axons
wt
unc-104
E
Length of the longest regenerated branch per nerve (µm)
****
*
*
wt
unc-104O3.1/P350
controlRNAi
unc-104RNAi I
unc-104RNAi II
F
Control
unc-104O3.1/P350
Mimic-wnd-GFP
G
Control
unc-104O3.1/P350
m12-GFP-wndkd
H
Mimic-wnd-gfp at cell body normalized to control
****
Control
unc-104O3.1/P350
wt
Mimic-wnd-GFP
I
UAS-wndkd-gfp at cell body normalized to control
****
Control
unc-104O3.1/P350

Figure 3.4: The Wnd signaling pathway is activated in *unc-104* mutants
(A) Expression of the *puc*-lacZ reporter for Wnd/JNK signaling was induced in *unc-104* mutants. Nuclear lacZ (green), expressed from the *puckered* promoter, was evaluated in motoneuron nuclei marked by Phospho-SMAD staining. UAS-RNAi lines (including UAS-*moody* RNAi as a control) were driven by *BG380*-Gal4.
(B) Quantification of *puc*-lacZ expression from (A) showing a Wnd-dependent regulation. UAS-*mcd8*-ChRFP was used as a control for dosage of UAS lines. *Unc-104* RNAi II was accompanied with Dicer2 expression to facilitate the knock-down.
(C) Regenerative axonal sprouting of *m12*-Gal4, UAS-*mcd8*-GFP labeled axons 10 minutes, 9 hours or 18 hours after nerve crush from wt and *unc-104*$^{O3.1/P350}$ mutant animals. Asterisk (*) indicates the injury site and arrow indicates the direction of the cell body.
(D) 9 hours after injury, the percentage of axons with more than 5 branches per nerve were enhanced in *unc-104* mutants.
(E) The axon regeneration was enhanced in *unc-104* mutants, measured by the length of the longest branch per nerve at 18 hours after injury. 2 independent *unc-104* RNAi lines and *control* RNAi (*moody*-RNAi) were driven by *m12*-Gal4.
(F) Endogenously tagged Wnd protein (MiMIC-*wnd*-GFP) increased in motoneuron cell bodies of *unc-104*$^{O3.1/P350}$mutants, compared to that of wild type. Two representative cell bodies are marked by green circles.
(G) Ectopically expressed GFP-*wnd*$^{kinase\ dead}$ increased in cell bodies of MNSNc motoneurons, compared to that of wild type. A representative cell body is marked by a green circle.
(H-I) Quantification of GFP signal intensity from (F) and (G) in cell bodies.
All data are represented as mean ± SEM; N.S., not significant; **** $P<0.0001$, *** $P<0.001$,*$P<0.05$, Tukey test for multiple comparison; Scale bar, 20μm. For additional data, see Figure 3.5 and 3.6.

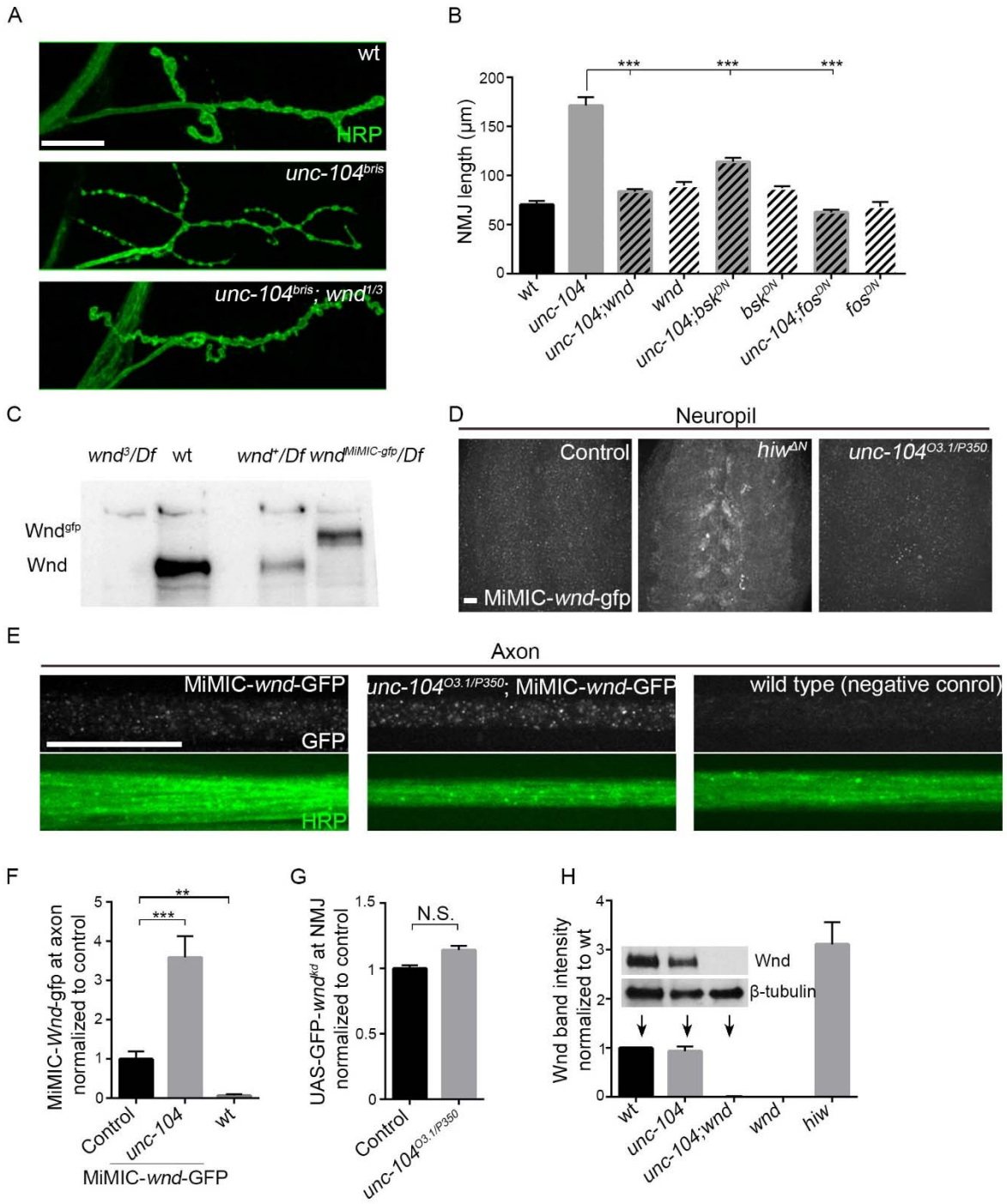
A
wt
HRP
unc-104bris
unc-104bris; wnd1/3
B
NMJ length (μm)
200
150
100
50
0
***
***
***
wt
unc-104
unc-104;wnd
wnd
unc-104;bskDN
bskDN
unc-104;fosDN
fosDN
C
wnd3/Df
wt
wnd+/Df
wndMiMIC-gfp/Df
Wndgfp
Wnd
D
Neuropil
Control
hiwΔN
unc-104O3.1/P350
MiMIC-wnd-gfp
E
Axon
MiMIC-wnd-GFP
GFP
HRP
unc-104O3.1/P350; MiMIC-wnd-GFP
wild type (negative conrol)
F
MiMIC-Wnd-gfp at axon normalized to control
5
4
3
2
1
0
**
***
Control
unc-104
wt
MiMIC-wnd-GFP
G
UAS-GFP-wndkd at NMJ normalized to control
1.5
1
0.5
0
N.S.
Control
unc-104O3.1/P350
H
Wnd band intensity normalized to wt
4
3
2
1
0
Wnd
β-tubulin
wt
unc-104
unc-104;wnd
wnd
hiw

Figure 3.5: The Wnd signaling pathway was activated in *unc-104* mutants, in a different manner than that in *hiw* mutants, (related to Figure 3.4).
(A) Presynaptic bouton morphology and branching at the NMJ, viewed via immunostaining for HRP (which labels axonal membrane) at muscle 4. The presynaptic arbor was over-branched in *unc-104* ^{bris} mutants, and this was rescued in *unc-104*^{bris}*;wnd*$^{1/3}$ double mutants.
(B) The total NMJ length (from the most proximal to the most distal bouton of the presynaptic nerve terminal at muscle 4, labeled via anti-HRP staining) was increased in *unc-104* mutants, and this increase was suppressed with mutations that inhibit the Wnd pathway. UAS-*bsk*^{DN} and UAS-*fos*^{DN} were driven by *elav*-Gal4 and *unc-104*$^{bris/bris}$*; wnd*$^{1/3}$ were used.
(C-D) Characterization of the MiMIC-wnd-GFP as a tag for endogenous Wnd.
(C) Western blot with anti-Wnd antibody for larval brain extracts from *wnd*^{3}*/Df*, wt, *wnd*$^{+}$*/Df* and *wnd*$^{MiMIC\text{-}gfp}$*/Df* animals. Endogenous Wnd protein runs at approximately 130kDa, while the MiMIC-Wnd-GFP fusion protein can be detected at an appropriately larger molecular weight (160kDa) for the GFP-fusion, confirming the expression and stability of the fusion protein.
(D) MiMIC-*wnd*-GFP in neuropil was enhanced in *hiw* mutants, but not control or *unc-104* mutants. This also indicates that the MiMIC-*wnd*-GFP is, like endogenous Wnd (Collins et al., 2006), subject to regulation by Hiw.
(E) Axonal MiMIC-*wnd*-GFP within larval segmental nerves (containing motoneuron axons) was enriched in *unc-104* mutants. Neuronal membrane (green) was identified via anti-HRP staining.
(F) Quantification of MiMIC-*wnd*-GFP signal intensity from axons in segmental nerves, shown in (E).
(G) Total intensity of UAS-GFP-*wnd*^{kd} (driven by *m12*--Gal4) divided by the total NMJ terminal area at muscles 26, 27 and 29.
(H) Representative Western blot of larval whole brain extracts for endogenous Wnd and β-tubulin, and quantification of Wnd levels normalized to β-tubulin band intensity (n≥3). Mutants examined include *unc-104*$^{bris/P350}$*; wnd*$^{3/3}$ and *hiw*$^{\Delta N}$.
All data are represented as mean ± SEM; N.S., not significant, *** P<0.001, **P<0.01, *P<0.05, Tukey test for multiple comparison; Scale bar, 20μm.

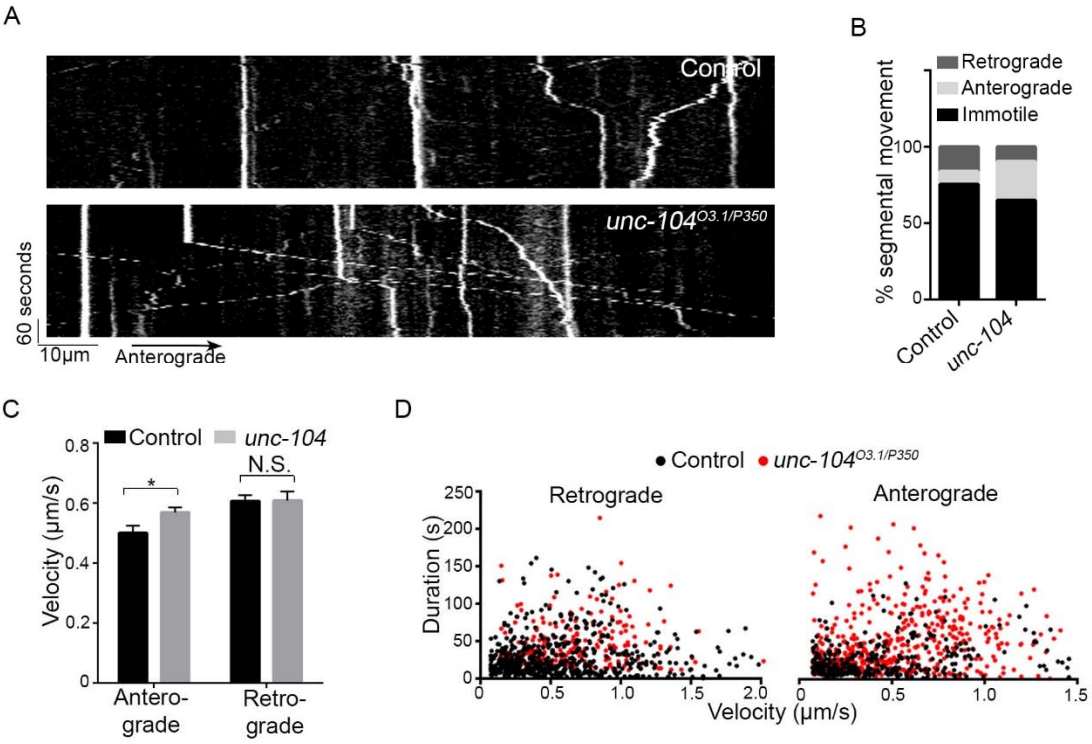

Figure 3.6: Wnd transport was not impaired in *unc-104* mutants, (related to Figure 3.4).
(A) Kymograph of GFP-wnd^{KD} particle movement in SNc motoneuron axons (using the *m12*-Gal4 driver). Axons were imaged 900 µm distal to cell bodies at 0.3 Hz for 5 minutes in wild type and $unc\text{-}104^{O3.1/P350}$ mutant animals. Anterograde particles (which were more abundant in *unc-104* mutants) moved from left to right.
(B-D) Measurement of GFP-wnd^{KD} particle movement by (B) the distribution of particles across retrograde, anterograde and immotile categories, (C) velocity, and (D) scatter plot showing both duration (y-axis) and velocity (x-axis) of all anterograde and retrograde particles. In *unc-104* mutants anterogradely-moving particles are more abundant and move in longer duration at higher velocity.
All data are represented as mean ± SEM; N.S., not significant, *** P<0.001, **P<0.01, *P<0.05, Tukey test for multiple comparison.

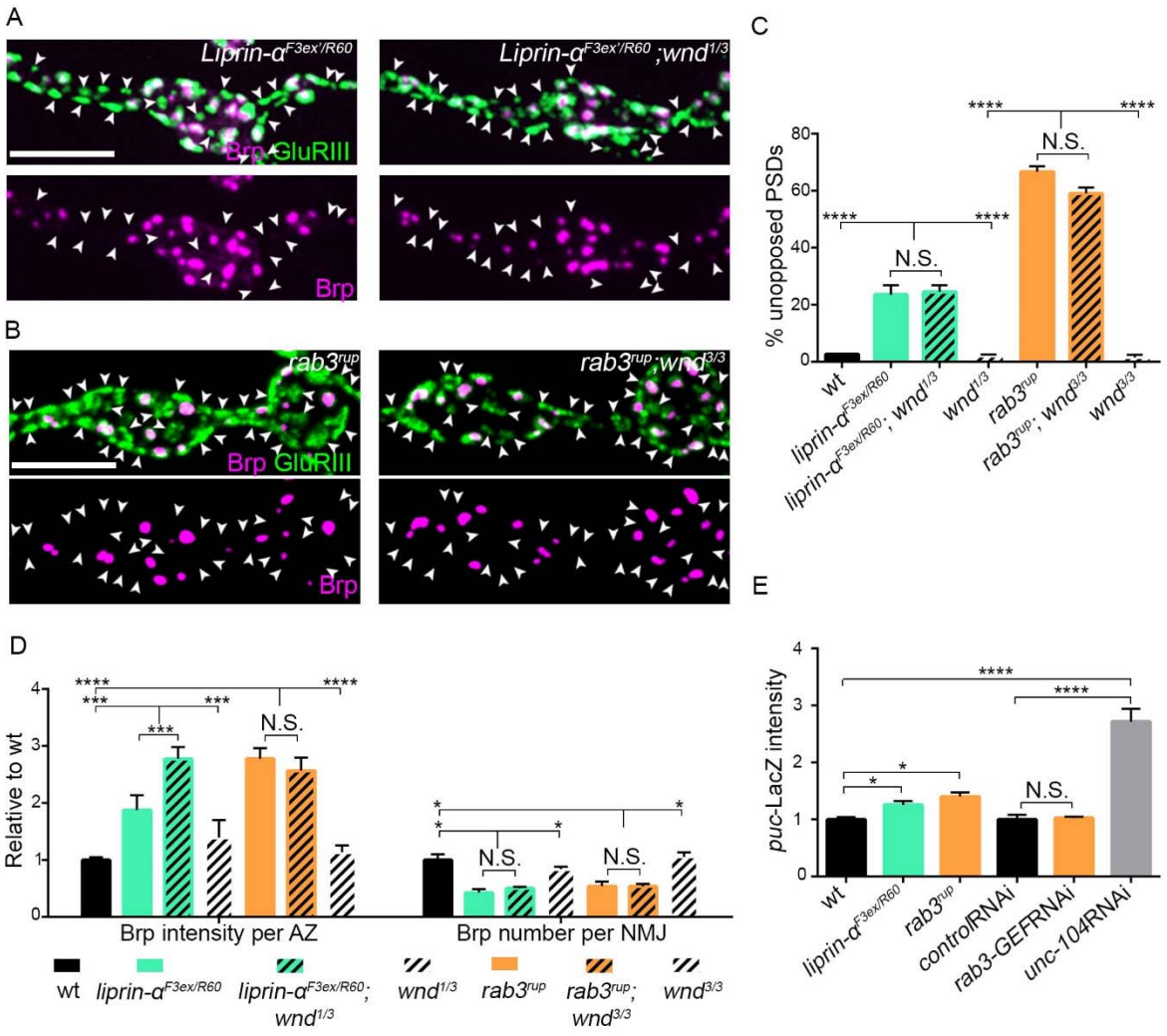

Figure 3.7: Liprin-α and Rab3 control presynaptic assembly independently of Wnd
(A-B) Representative images of presynaptic Brp and postsynaptic GluRIII from (A) *liprin-α* and *liprin-α ;wnd* and (B) *rab3* and *rab3;wnd*. Unopposed GluRIII-labeled PSDs are highlighted by arrowheads.
(C) Percentage of unopposed GluRIII-labeled PSDs from (A) and (B)
(D) The evaluation of BRP at present AZ by the intensity per AZ and the number per NMJ. Increased Brp intensity of individual AZ and reduced Brp number per NMJ in either *liprin-α* or *rab3* mutants were not suppressed by *wnd* mutations.
(E) *puc*-lacZ intensity in *liprin-α*and *rab3* mutants and *rab3-GEF* knock-down, normalized to wild type and *control*RNAi (*moody*-RNAi).
All data are represented as mean ± SEM; N.S., not significant, **** P<0.0001, *** P<0.001, * P<0.05; Tukey test for multiple comparison; Scale bar 5μm.

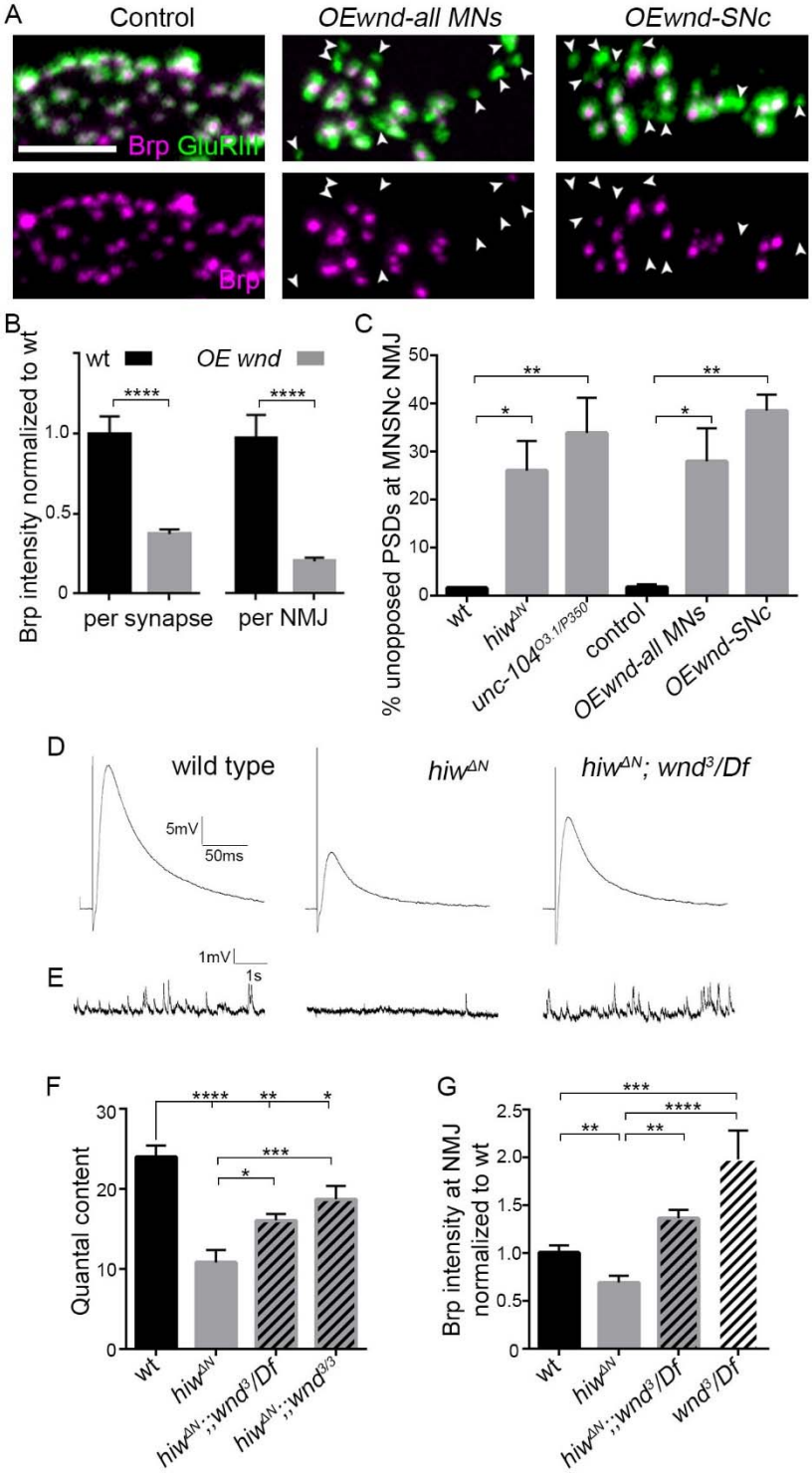
A
Control
OEwnd-all MNs
OEwnd-SNc
Brp GluRIII
Brp
B
wt
OE wnd
Brp intensity normalized to wt
per synapse
per NMJ
C
% unopposed PSDs at MNSNc NMJ
wt
hiwΔN
unc-104O3.1/P350
control
OEwnd-all MNs
OEwnd-SNc
D
wild type
hiwΔN
hiwΔN; wnd3/Df
5mV
50ms
E
1mV
1s
F
Quantal content
wt
hiwΔN
hiwΔN;;wnd3/Df
hiwΔN;;wnd3/3
G
Brp intensity at NMJ normalized to wt
wt
hiwΔN
hiwΔN;;wnd3/Df
wnd3/Df

Figure 3.8: Over-active Wnd signaling is sufficient to induce defects in presynaptic assembly and transmission
(A) Representative images of MNSNc synapses at muscle 26, 27 and 29 with Brp and GluRIII staining. GluRIII-labeled PSDs that lack opposed AZs (highlighted by arrowheads) increased when Wnd was over-expressed. Similar defects were observed using a pan-motoneuron driver (*OK6*-Gal4), and in driver line specific to the MNSNc motoneuron (m12-Gal4), indicating the cell autonomy of Wnd's effect upon synapse assembly.
(B) Brp protein intensity at individual synapses and across entire NMJ terminals (at muscle 4) was reduced when Wnd was over-expressed in motoneurons (using the *OK6*-Gal4 driver).
(C) The percentage of unopposed GluRIII-labeled PSDs at the MNSNc NMJ terminals in $hiw^{\Delta N}$, $unc\text{-}104^{O3.1/P350}$ and when UAS-*wnd* was over-expressed using either pan-motoneuron driver (*OK6*-Gal4) or a driver specific to MNSNc motoneurons (*m12*-Gal4).
(D-E) Representative electrophysiological traces of (D) EJP and (E) mEJP on muscle 6 of third instar larvae in wild type, $hiw^{\Delta N}$ and $hiw^{\Delta N};;wnd^{3/deficiency}$.
(F) Average quantal content (corrected for nonlinear summation) reduced significantly due to activation of Wnd in *hiw* mutants.
(G) The total amount of Brp intensity across NMJ synaptic terminals was inhibited by over-activation of Wnd in *hiw* mutants.
All data are represented as mean ± SEM; N.S., not significant, **** P<0.0001, *** P<0.001, ** P<0.01, *P<0.05, Tukey test for multiple comparison; Scale bar, 2μm. For additional data, see Figure 3.9.

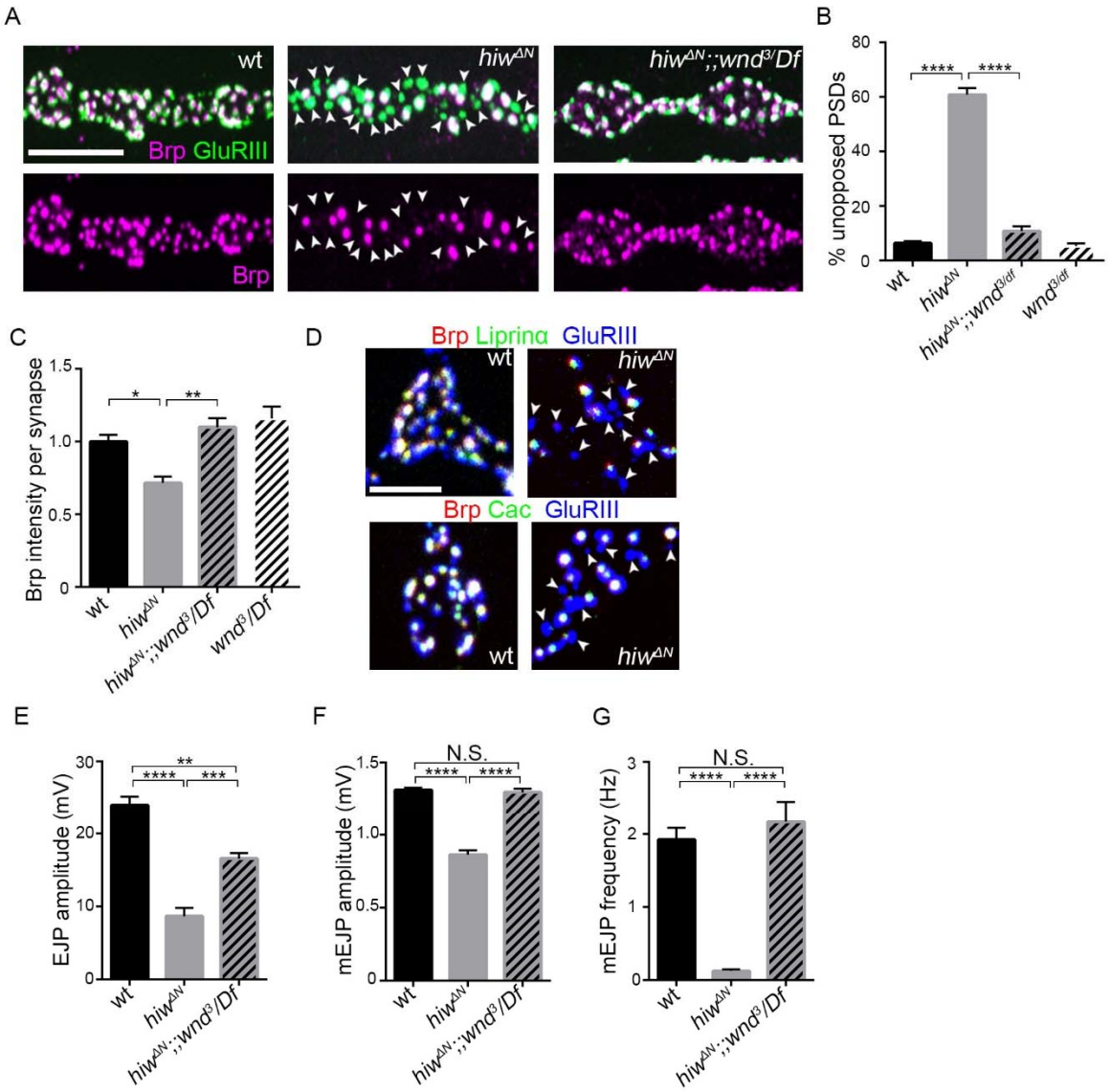

Figure 3.9: Wnd activation inhibits presynaptic assembly, (related to Figure 3.8).
(A) Representative images of presynaptic Brp (magenta) and postsynaptic GluRIII (green) from wild type, *hiw$^{\Delta N}$* and *hiw$^{\Delta N}$;;wnd^{3}/Df*. GluRIII-labeled PSDs that lack opposed AZs are highlighted by arrowheads.
(B) Quantification of (B) the percentage of unopposed GluRIII-labeled PSDs, normalized to wt.
(C) The total intensity of Brp measured at individual synapses was reduced *hiw* mutants, and this reduction required *wnd*.

(D) Triple labeling of Brp (red), GluRIII (blue) and either Liprin-α-GFP or Cacophony-GFP (green) from wild type and $hiw^{\Delta N}$. The co-localization of three markers resulted in white while "half synapses" resulted in blue only, highlighted with arrowheads. Notice the co-disappearance of all presynaptic markers in *hiw* mutants.
(E-G) Electrophysiology recordings from NMJs at muscle 6. Quantification of the (E) average EJP, (F) average mEJP and (G) average mEJP frequency.
All data are represented as mean ± SEM; **** P<0.0001, *** P<0.001, ** P<0.01, *P<0.05; Tukey test for multiple comparison, Scale bar, (A) 5μm and (D) 2μm

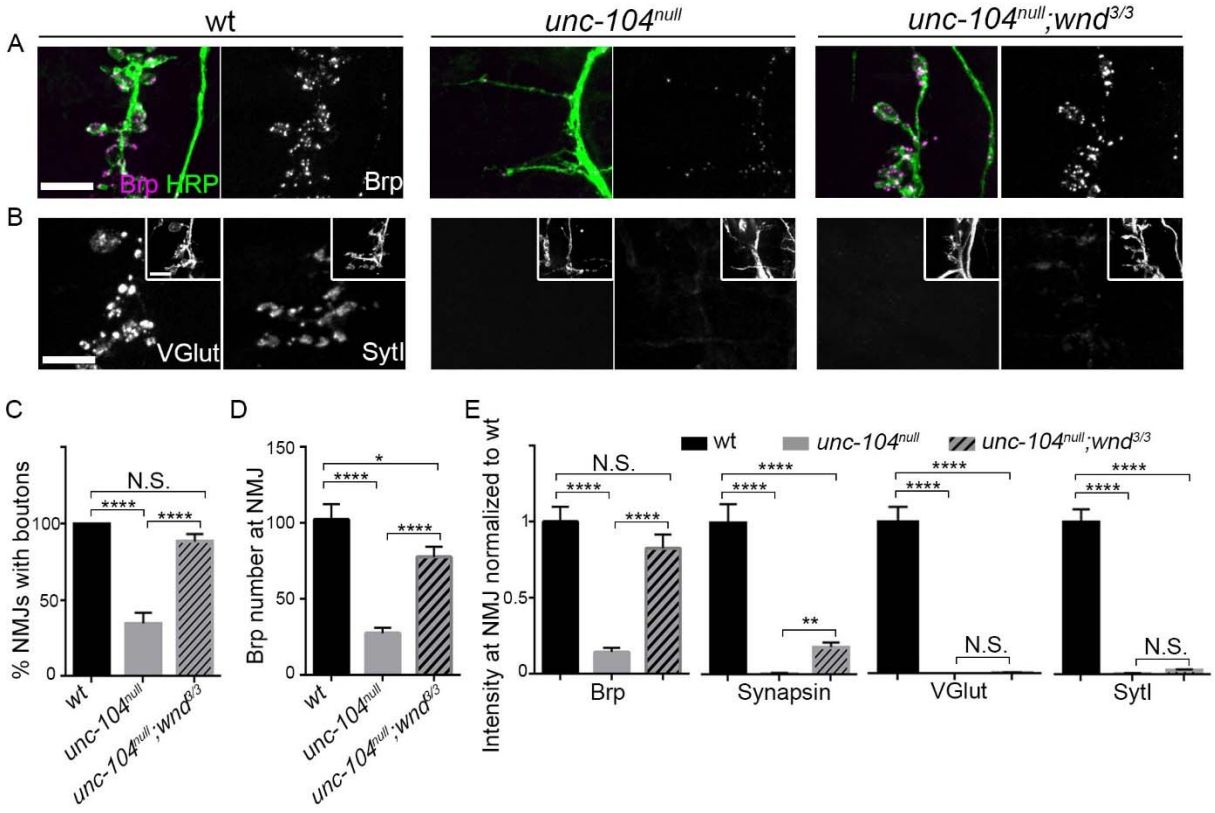

Figure 3.10. Synaptic bouton and AZ formation but not SV transport defects in *unc-104*^{null} mutants are rescued by mutations in *wnd*

(A-C) Representative images of ISNb NMJ terminals at muscle 6/7/12/13 at embryonic stage 17 (20-21 hours AEL). The examined *unc-104*^{null} alleles include *P350/P350* and *52/52*.

(A) In *unc-104*^{null} mutants, boutons (identified by HRP staining) failed to form, and AZs (Brp) failed to localize to NMJ. Both of the defects were largely suppressed in *unc-104*^{null}*;wnd* double mutants.

(B) Presynaptic vesicle proteins VGlut and SytI failed to localize to presynaptic terminals (NMJ) in both *unc-104* and *unc-104; wnd* mutants. NMJ membrane was labeled by HRP (inset)

(C) The percentage of NMJs with boutons reduced in *unc-104*^{null} mutants and largely restored in *unc-104*^{null}*;wnd*$^{3/3}$ double mutants.

(D) The number of AZs (identified by Brp) formed at a NMJ was strongly reduced in *unc-104*^{null} mutants, but was largely restored in *unc-104; wnd* double mutants.

(E) The intensity of Brp, Synapsin, VGlut and SytI at NMJ terminals was reduced in *unc-104* mutants. In *unc-104;wnd* double mutants, Brp intensity was largely restored and Synapsin was mildly restored. No significant suppression was observed for VGlut and SytI.

All data are represented as mean ± SEM; At least 9 animals and 20 NMJs were examined per genotype; **** P<0.0001, *P<0.05; Tukey test for multiple comparison; Scale bar, 10 μm. For additional data, see Figure 3.11.

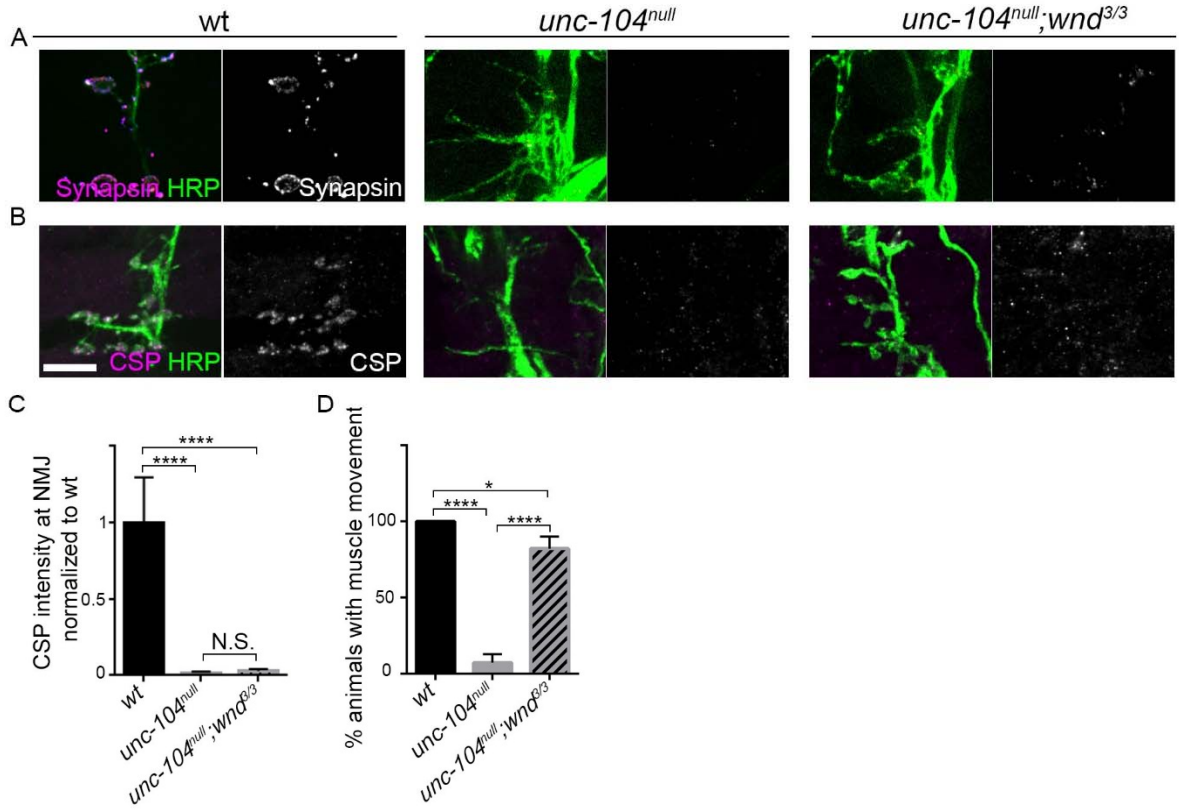

Figure 3.11: Transport defects of presynaptic vesicle proteins largely persisted *in unc-104^{null};wnd* mutants, (related to Figure 3.10).

(A-B) Representative images of ISNb NMJs at muscle 6, 7, 12 and 13 at embryonic stage 17 (21 hours AEL). In *unc-104^{null}* mutants, presynaptic vesicle proteins (A) Synapsin and (B) CSP failed to localize to NMJ. Synapsin localization was mildly suppressed in *unc-104^{null};wnd* mutants, while CSP was not.

(C) The total intensity of CSP measured at NMJ terminals (shown in B) were reduced in *unc-104* mutants and in *unc-104;wnd* double mutants.

(D) Transient rescue of muscle contraction defects in early embryos. Embryos with visible muscle contraction were scored immediately after dissection from the vitelline membrane at stage 17 (20-21 AEL). Contractions were mostly absent in *unc-104* mutants however were present in *unc-104; wnd* double mutants. The degree of contraction in double mutants was less robust than wildtype and was transient – animal were still within 3 minutes.

All data are represented as mean ± SEM; At least 4 animals and 10 NMJs were examined per genotype; **** P<0.0001, *P<0.05; Tukey test for multiple comparison; Scale bar, 10 μm.

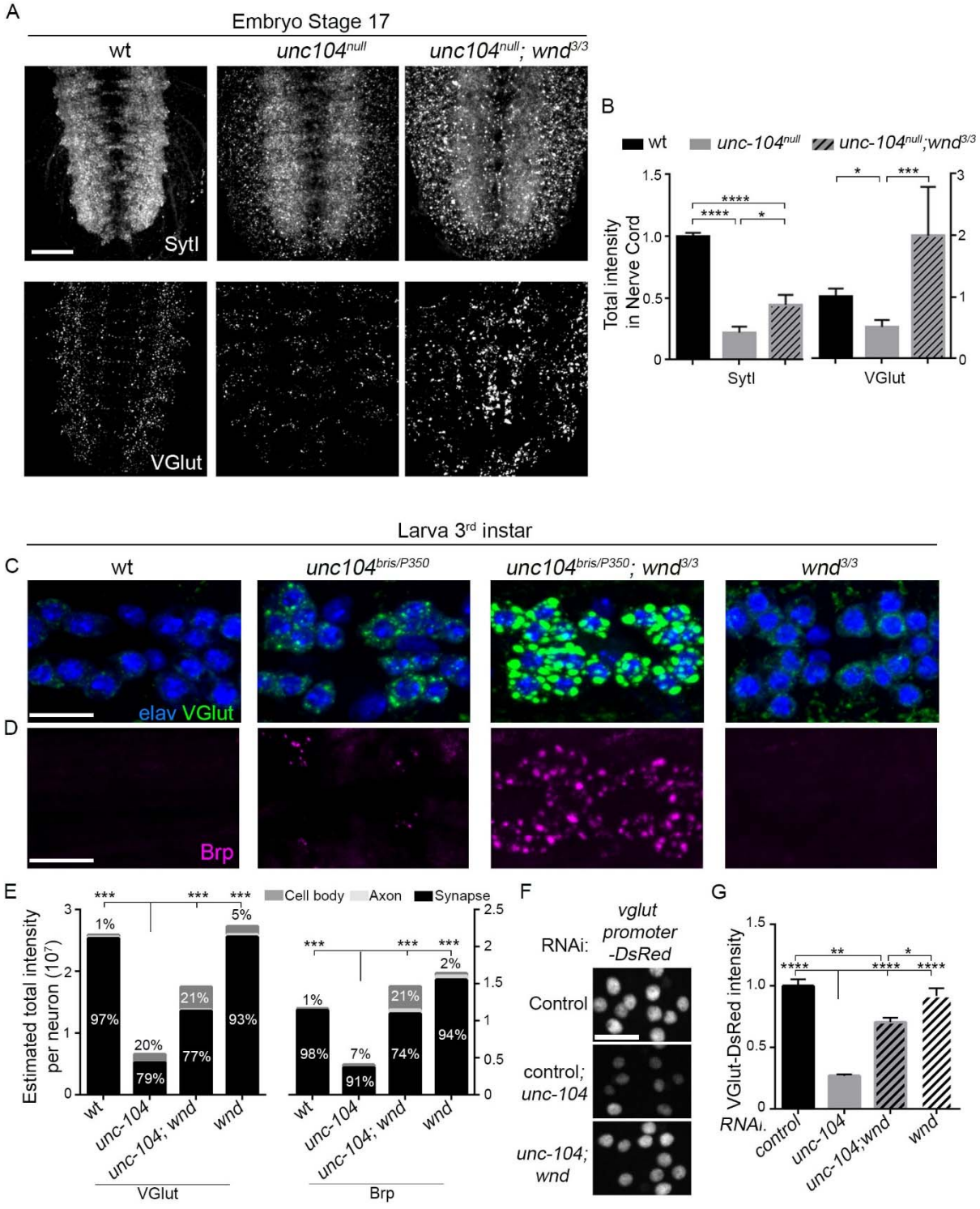
A
Embryo Stage 17
wt
unc104null
unc104null; wnd3/3
SytI
VGlut
B
wt
unc-104null
unc-104null;wnd3/3
Total intensity in Nerve Cord
SytI
VGlut
Larva 3rd instar
C
wt
unc104bris/P350
unc104bris/P350; wnd3/3
wnd3/3
elav VGlut
D
Brp
E
Cell body
Axon
Synapse
Estimated total intensity per neuron (10^7)
wt
unc-104
unc-104; wnd
wnd
VGlut
Brp
F
RNAi:
vglut promoter -DsRed
Control
control; unc-104
unc-104; wnd
G
VGlut-DsRed intensity
RNAi:
control
unc-104
unc-104;wnd
wnd

Figure 3.12: Wnd restrains total levels of presynaptic components downstream of Unc-104.
(A-B) SytI and VGlut immunostaining in stage 17 embryonic nerve cord (20-21 AEL) in *unc-104*^{null} mutants. Quantification in (B) shows an increase in total intensity in *unc-104*^{null}*;wnd* double mutants. Increased staining is noted in the cell body region (A, and Figure 3.15A). Additional data is shown in Figure 3.15B.
(C-D) In *unc-104*$^{bris/P350\ (hypmorph)}$*; wnd* double mutants, increased intensity of VGlut (C) and Brp (D) is observed in motoneuron cell bodies of 3rd instar larvae (see also Figure 3.15). In each image, two groups of motoneuron cell bodies were shown with their nuclei identified by Elav staining (blue in C).
(E) Estimates of the total intensity of VGlut and Brp (described in methods), showing the relative percentage from each compartment (cell body (gray), axons (light gray) and synaptic terminals (black)).
(F) The expression of *vglut* promoter-DsRed reporter was down-regulated via Wnd when *unc-104* is knocked-down. (H) Quantification of *vglut*-DsRed intensity in (H) is normalized to *control*RNAi. UAS-*RNAi* lines were driven by *OK6*-Gal4.
All data are represented as mean ± SEM; **** P<0.0001, *** P<0.001, ** P<0.01, *P<0.05, Tukey test for multiple comparison; Scale bar, 20μm. For additional data, see Figure 3.13.

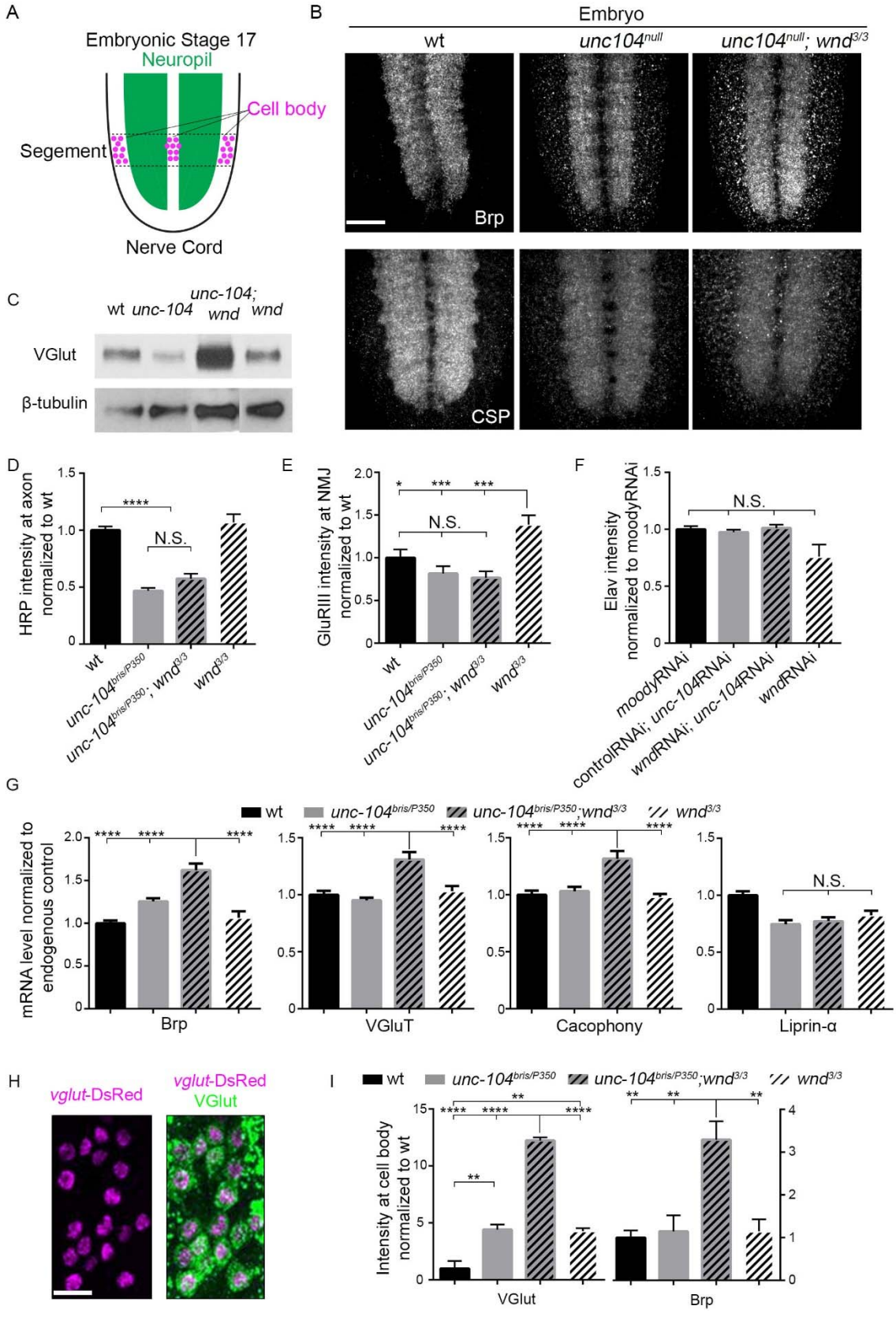
A
Embryonic Stage 17
Neuropil
Cell body
Segement
Nerve Cord
B
Embryo
wt
unc104null
unc104null; wnd3/3
Brp
CSP
C
wt unc-104 unc-104; wnd wnd
VGlut
β-tubulin
D
HRP intensity at axon normalized to wt
****
N.S.
wt
unc-104bris/P350
unc-104bris/P350; wnd3/3
wnd3/3
E
GluRIII intensity at NMJ normalized to wt
*
***
***
N.S.
F
Elav intensity normalized to moodyRNAi
N.S.
moodyRNAi
controlRNAi; unc-104RNAi
wndRNAi; unc-104RNAi
wndRNAi
G
wt
unc-104bris/P350
unc-104bris/P350;wnd3/3
wnd3/3
mRNA level normalized to endogenous control
Brp
VGluT
Cacophony
Liprin-α
N.S.
H
vglut-DsRed
vglut-DsRed
VGlut
I
wt
unc-104bris/P350
unc-104bris/P350;wnd3/3
wnd3/3
Intensity at cell body normalized to wt
VGlut
Brp

Figure 3.13: In *unc-104* mutants, a specific cohort of synaptic proteins were down-regulated by Wnd, (related to Figure 3.12).
(A) Schematic cartoon showing the locations of motoneuron cell bodies (within one segment, denoted by dotted lines) and Neuropil (green) in the nerve cord at embryonic stage 17.
(B) Immunostaining for Brp, CSP and Synapsin in the nerve cord at embryonic stage 17 (20-21 AEL). In *unc-104* mutants, Brp, CSP and Synapsin protein accumulated in cell bodies and their total protein levels were slightly reduced. Both the accumulation and the total levels were enhanced in *unc-104; wnd* double mutants.
(C) Representative Western blot of 30 larval brains for VGlut and β-tubulin from wild type (wt), $unc\text{-}104^{bris/P350}$, $wnd^{3/3}$ and $unc\text{-}104^{bris/P350};wnd^{3/3}$.
(D-E) Quantification of (D) mean HRP intensity measured in segmental nerve axons and (E) the total GluRIII levels of individual NMJ terminals (at muscle 4) from wild type (wt), $unc104^{bris/P350}$, $wnd^{3/3}$ and $unc104^{bris/P350};wnd^{3/3}$. Note that HRP intensity was reduced in a Wnd-independent manner.
(F) Quantification of nuclear Elav levels in animals carrying UAS-RNAi lines driven by *OK371*-Gal4
(G) Relative mRNA levels measured by quantitative RT-PCR for Brp, VGlut, Cacophony and Liprin-α from whole larval brains. Similar results were observed with both Tubulin and RP49 as normalization controls, so the mean fold change using both is reported. Note mRNA level of Brp, VGlut and Cac, but not Liprin-α, increased in *unc104; wnd* double mutants.
(H) Validation that the *vglut*-DsRed (magenta) reporter is accurately expressed in cells that express VGlut protein, detected by anti-VGlut antibody staining (green).
(I) Quantification of total intensity measurements for VGlut and Brp in motoneuron cell bodies, normalized to wild type.
All data are represented as mean ± SEM; N.S., not significant, **** $P<0.0001$, *** $P<0.001$, * $P<0.05$, Tukey test for multiple comparison; Scale bar, 20μm.

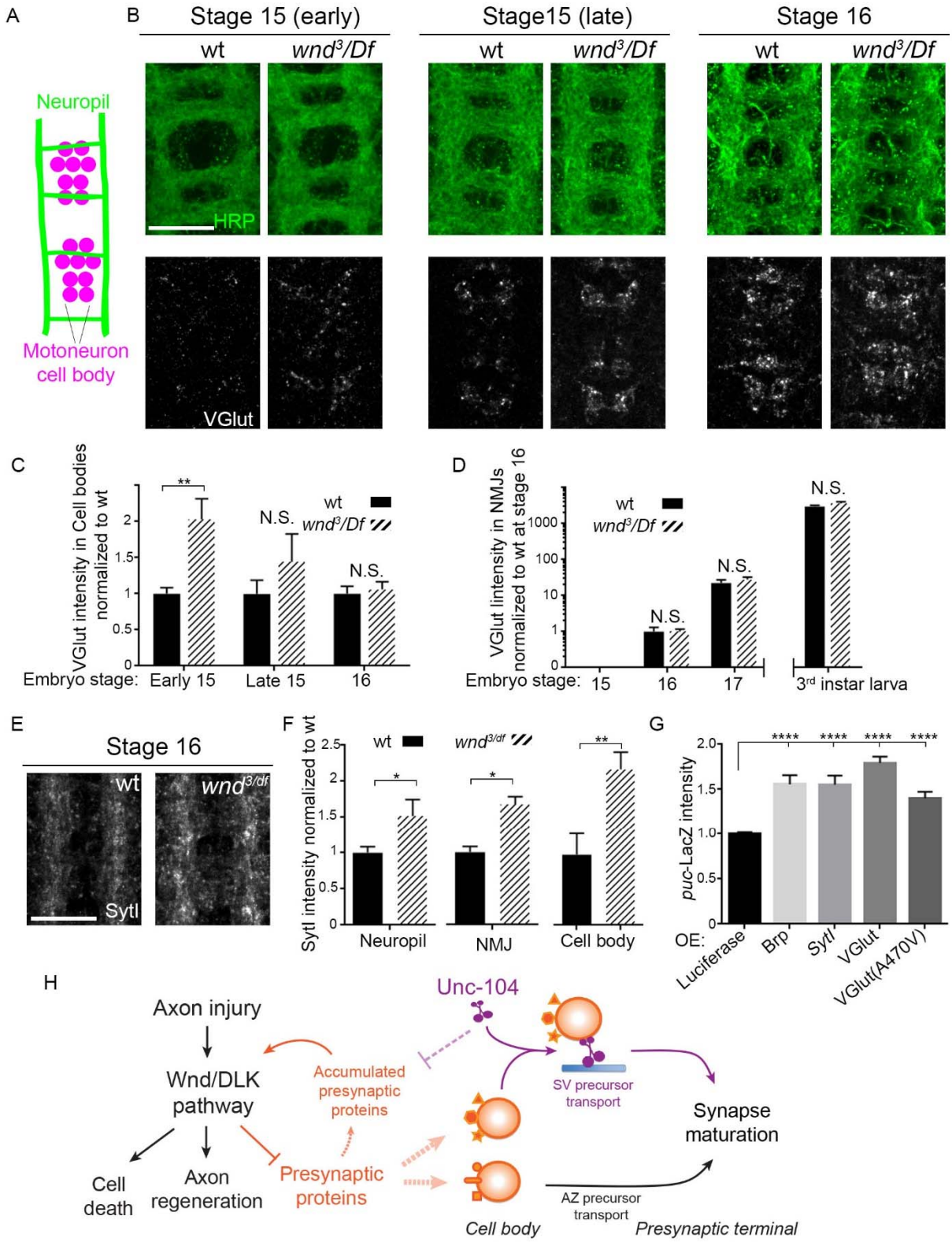
A
B
Stage 15 (early)
Stage15 (late)
Stage 16
wt
wnd3/Df
Neuropil
HRP
Motoneuron cell body
VGlut
C
VGlut intensity in Cell bodies normalized to wt
**
N.S.
N.S.
wt
wnd3/Df
Embryo stage: Early 15 Late 15 16
D
VGlut lintensity in NMJs normalized to wt at stage 16
N.S.
N.S.
N.S.
Embryo stage: 15 16 17 3rd instar larva
E
Stage 16
wt
wnd3/df
Sytl
F
Sytl intensity normalized to wt
wt
wnd3/df
*
*
**
Neuropil
NMJ
Cell body
G
puc-LacZ intensity
****
****
****
****
OE:
Luciferase
Brp
Sytl
VGlut
VGlut(A470V)
H
Axon injury
Wnd/DLK pathway
Cell death
Axon regeneration
Presynaptic proteins
Accumulated presynaptic proteins
Unc-104
SV precursor transport
Synapse maturation
AZ precursor transport
Cell body
Presynaptic terminal

Figure 3.14: Wnd's role in synapse development.
(A) Schematic cartoon of the embryonic nerve cord showing the neuropil (the location of neurites and developing synapses in the CNS) and motoneuron cell bodies in 2 segments at late embryonic stages (15 to 16).
(B) Representative images of VGlut (white, bottom row) expression in motoneuron cell bodies of wild type and *wnd-null* mutants (*wnd*^{3}/*Df*) at embryonic stage early 15, late 15 and 16. Analogous segments are identified by neuropil HRP staining (top row).
(C-D) Quantification of VGlut intensity in (C) motoneuron cell bodies and (D) NMJ presynaptic terminals for wt and *wnd-null* mutants at different embryonic stages and in 3rd instar larvae. VGlut expression first appears in cell bodies at embryonic stage 15 (C), corresponding with the onset of NMJ synaptogenesis, but does not appear at NMJ terminals until stage 16 (D). As the NMJ matures and expands throughout development, VGlut intensity, which is predominantly localized to NMJ terminals, continues to increase (note the logarithmic scale). Quantification (D) is normalized to intensity at stage 16.
(E-F) SytI intensity is elevated in *wnd-null* mutants at embryonic stage 16. (E) Representative images of SytI immunostaining in CNS neuropil. Additional images for quantification in (F) are shown in Figure 3.15C.
(G) Ectopic over-expression of presynaptic components (Brp, SytI, VGlut and VGlut^{A470V}) led to increase of Wnd-JNK signaling reporter, *puckered*-lacZ. Pan neuronal Gal4 (*bg380*) was used to drive their expression.
(H) Model for the relationship between Wnd/DLK signaling and Kinesin-3-mediated transport. In purple, the kinesin-3 family motor protein Unc-104/Imac plays an important role in synaptic assembly by carrying synaptic vesicle precursors to nascent synapses. It also plays indirect roles in synaptic assembly via the Wnd/DLK signaling pathway, which becomes activated when Unc-104-mediated transport is impaired. Wnd/DLK activation also becomes activated after axonal injury, and is previously known for roles in promoting axonal regeneration, and also in cell death in some models of axonal stress. Here we have found that Wnd restrains the expression of presynaptic proteins to prevent their excess build-up when Unc-104 function is inhibited.
All data were represented as mean ± SEM; **** $P<0.0001$, ** $P<0.01$, *$P<0.05$, Tukey test for multiple comparison; Scale bar, 20μm (B and E). For additional data, see Figure 3.15.

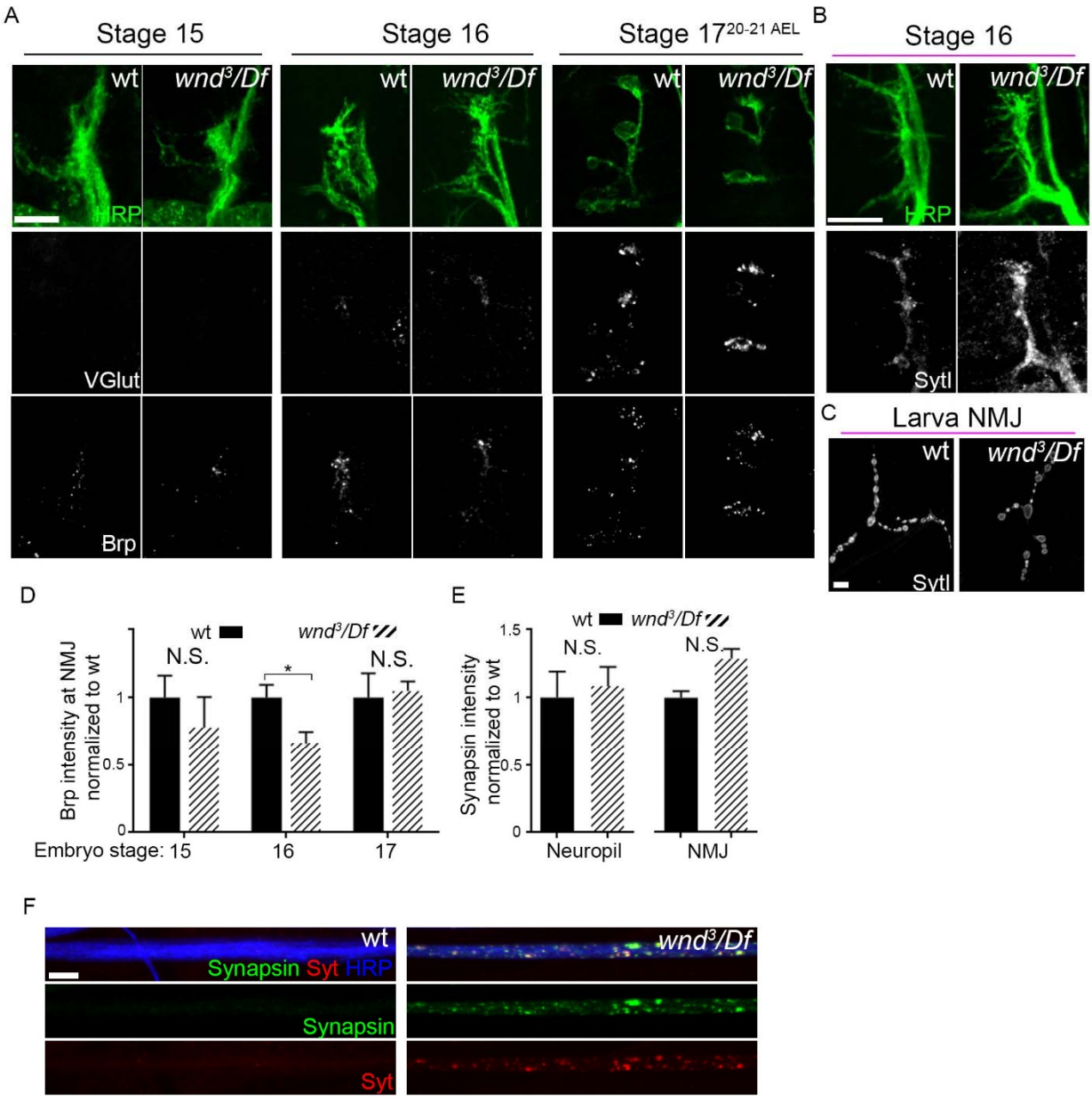
A
Stage 15
Stage 16
Stage 17 20-21 AEL
wt
wnd3/Df
HRP
VGlut
Brp
B
Stage 16
Sytl
C
Larva NMJ
D
Brp intensity at NMJ normalized to wt
N.S.
*
Embryo stage: 15
16
17
E
Synapsin intensity normalized to wt
Neuropil
NMJ
F
Synapsin Syt HRP
Synapsin
Syt

Figure 3.15: Wnd's role in synapse development, (related to Figure 3.14).
(A) VGlut (second row) and Brp (third row) expression at ISNb NMJs for wild type and *wnd* null mutants at embryonic stage 15, 16 and 17. Top row shows the NMJ morphology at each stage based on staining with HRP which reveals the axonal and nerve terminal membrane.
(B) SytI intensity, detected at NMJ terminals at embryonic stage 16, was increased in *wnd* mutants compared to wt.
(C) SytI intensity, detected at NMJ terminals (M4) was similar between wt and *wnd* mutants in 3rd instar larvae.
(D) Quantification of Brp total intensity at ISNb NMJ terminals in wt and *wnd* mutants. A mild decrease was observed at this stage 16 in *wnd* mutants.
(E) Total intensity of Synapsin detected in Neuropil and in NMJ terminals was similar between wt and *wnd* mutants at embryonic stage 16.
(F) Synapsin and Syt1 intensity within segmental nerves (containing motoneuron axons) are increased in *wnd* mutants (3rd instar larvae).
All data are represented as mean ± SEM; N.S., not significant, * $P<0.05$, Tukey test for multiple comparison; Scale bar, 10μm (A, B, C and F).

CHAPTER IV

INVESTIGATING MECHANISMS THAT MEDIATE THE ACTIVATION OF WALLENDA/DLK SIGNALING IN *UNC-104* MUTANTS

The loss of presynaptic AZs and SVs from individual synapses, when Wnd signaling is activated or *unc-104* is mutated, is unique. Importantly, the activation of Wnd signaling is only observed in *unc-104* mutants, but not kinesin-1 or dynein mutants. This suggests a specific relationship between the activation of Wnd signaling and the loss of *Unc-104* function. To gain an understanding of this relationship I have considered several different hypotheses and in this chapter I report my findings in evaluating them. I considered: first (in section 4.1) whether Wnd is a direct cargo of Unc-104; then (in section 4.2) whether dysfunctional synapses in *unc-104* mutants lead to activation of Wnd signaling; then (in section 4.3) whether the accumulated cargo in the cell body contributes to the activation; lastly (in section 4.4) whether defective autophagy plays a role in activating Wnd signaling.

4.1 Is Wnd a direct cargo of Unc-104?

Wnd and its DLK homologues localize to axons and this appears critical for their signaling function. It has been shown that at least a population of Wnd is actively transported in vesicles anterogradely and retrogradely in axons (Holland et al., 2015; Xiong et al., 2010). The retrograde transport machinery is required for the activation of Wnd/DLK's downstream targets in response to injury (Holland et al., 2015; Shin et al., 2012; Watkins et al., 2013; Xiong et al.,

2010). DLK localize to vesicles via palmitoylation and this likely also occurs for Wnd via a conserved consensus palmitoylation motif (Holland et al., 2015). It remains unclear what motor is responsible for transport of Wnd/DLK-associated vesicles and whether this transport may be regulated as part of injury signaling.

The increased levels of Wnd protein in the cell bodies observed in *unc-104* mutants (Figure 3.4) suggests that Wnd's transport may be influenced by Unc-104. However, the examination of GFP-Wnd^{kd} transport in axons showed no obvious impairment (Figure 3.6). These results suggest that either Wnd is not a cargo of Unc-104, or Wnd is transported by multiple motors including Unc-104.

To further test the cargo possibility I examine the co-localization and co-transport of Wnd and Unc-104 *in vivo*. Unc-104 movement had not been examined in Drosophila and the imaging turns out to be challenging. Most studies (including mine) are carried out with exogenously expressed fluorescent protein-tagged Unc-104 and a large pool of the expressed protein is cytosolic, which mask the signals from Unc-104 that moves along with vesicles (Figure 4.1A). Unc-104's movement has previously been successfully examined in cultured neurons (Hung and Coleman, 2016; Lee et al., 2003). *In vivo* it has been documented in two studies in *C. elegans* via direct live-imaging, despite its high cytosolic signal. However the two studies generated very distinct histograms of Unc-104's transport velocities (Wagner et al., 2009; Zhou et al., 2001). For example, Unc-104's greatest velocity is 0.8~1 μm/s in one study compared to 0.2~0.4 μm/s in the other. This difference could be due to the difficulty in accurately identifying moving Unc-104-associated particles from cytosolic pool of Unc-104. Another study in *C. elegans* reported this problem on cytosolic signal and could not conclude on Unc-104's velocity based on live imaging data (Klopfenstein and Vale, 2004). Therefore, the live

imaging of Unc-104 has not been well established because of the high background signal. In order to solve it, I decided to locally photobleach Unc-104-mCherry fluorescence to reduce background from the cytosolic pool, before acquiring images of its movement.

In order to do live imaging of the Drosophila larval nervous system, I developed a simple set-up that exposes the nervous system, including axons, to light microscopy while keeping larvae fully immersed in physiological solutions, such as HL3 or PBS buffer, which is tightly sealed in between coverslip and dissection plate. It allows for live imaging with inverted microscope for up to 1 hour. In this set-up I was able to observe robust fast transport of Wnd vesicles at single-axon resolution, labeled by GFP conjugated to a kinase dead version of Wnd (Figure 4.1A and B). For Unc-104, without photobleaching, only a few occasional particles were observed, and these particles did not cotransport with Wnd-GFP; however Unc-104-mCherry particles were still difficult to distinguish from the fluctuations in the background signal (Figure 4.1C). Interestingly, a strong signal comes from retrograde transport of Unc-104, which may imply the existence of a particle with multiple motors attached (Figure 4.1A and B). This retrograde 'bulk' may potentially serve to recycle Unc-104 motors after they reach the distal end.

Within 10 seconds after photobleaching a 170 um length of the segmental nerve, Unc-104-mcherry particles could be spotted entering the photobleached area in the anterograde direction. However these particles were rarely spotted in consecutive frames and instead disappeared within three frames (Figure 4.1D), likely due to photobleaching and/or overwhelmingly high background signal from the cytosolic pool. With the caveats that very few transport particles were spotted, no obvious colocalization was observed with Wnd-GFP (Figure 4.1D).

Given the challenge in doing live imaging of Unc-104, I also carried out further genetic analysis to test the cargo hypothesis. If Wnd is a direct cargo of Unc-104, then over-expression of Unc-104 might alter Wnd signaling. A previous study in *C. elegans* has described a gain-of-function mutation in *unc-104* which appears to enhance its transport and cargo binding, and affect synapse distribution (Niwa et al., 2015; Zheng et al., 2014). Over-expression of wild type Unc-104 behaves similarly to gain-of-function mutation to suppress synaptic defects caused by mutations in its adaptor Liprin-α (Zheng et al., 2014). After driving over-expression of Unc-104 in all neurons I observed no changes in expression from the puc-lacZ reporter, including in animals after axonal injury, which induces endogenous Wnd signaling (Figure 4.2A). Furthermore, overexpression of Unc-104 caused no changes to the number of Brp-marked AZs (Figure 4.2C) and no changes in the levels of VGlut and Brp measured at NMJ synapses (Figure 4.2B and D). These negative observations suggest that Wnd signaling is unlikely to be directly inhibited by Unc-104.

From my observations thus far, I cannot rule out some remaining possibilities for a direct relationship between Unc-104 and Wnd. For example, (a) Wnd may be transported by a small population of Unc-104 motors, which falls below the limits of my detection in live imaging; (b) Unc-104 may function near the cell body to transport Wnd before its entry into axons, rather than in the axon shaft where my imaging focused; or (c) Unc-104 transports Wnd at an early stage of development, that was not detected in my experiments. These possibilities are in line with our current understanding of motors, which is that a cargo is bound by multiple motors and motor-cargo binding is dynamically regulated (Hirokawa et al., 2009). Future work to carry out live imaging of Wnd-GFP in embryos of *unc-104*-null mutants could further address these possibilities.

4.2 Does synapse dysfunction activate Wnd signaling?

If Wnd is not itself a direct cargo of Unc-104, the next logical possibility is that one of Unc-104's cargo functions to regulate Wnd pathway. Previous work has suggested that DCVs and SVs are major cargo of Unc-104. In the *unc-104* mutants, these vesicles and associated proteins are depleted from synapses and accumulate in the cell body (Gong et al., 1999; Hall and Hedgecock, 1991; Pack-Chung et al., 2007; Yonekawa, 1998). Hence there are two simultaneous defects in these unc-104 cargo: depletion from synapses and accumulations in the cell body. We endeavored to tease apart which (synaptic depletion or cell body accumulation) was responsible for the activation of the Wnd pathway.

The depletion of DCVs and SVs and their associated proteins from synapses in *unc-104* mutants directly impair exocytosis of these vesicles, So the synaptic transmission in *unc-104* mutants is severely weakened (Figure 3.3). It is known that vesicle release from synapses is critical for synaptic morphology and structure: SV release is important for synaptic homeostasis and maintenance (Verhage et al., 2000); DCVs upon fusion at synapses release neuropeptides, many of which have been shown to be important for synapse growth (Chen and Ganetzky, 2012; Nässel and Winther, 2010); Octopamine, a neurotransmitter carried in DCVs, influences synapse formation (Koon et al., 2011); Neuropeptides and morphogens such as BDNF are also transported in the form of DCVs (Dieni et al., 2012). From these possible cargo, both cell-autonomous and non-cell-autonomous mechanisms can be envisioned for their roles in synapse formation. To test whether disruption of synaptic release mediates the activation of Wnd signaling in *unc-104* mutants, I attempted to specifically impair DCV and SV release.

4.2.1 SV release impairment did not activate Wnd activation

Since Drosophila motoneurons are mostly glutamatergic, I first examined the mutants of *vesicular glutamate transporter (vglut)*. These mutants are semi-lethal and a few animals that survive to 3rd instar larva stage, show reduced mEJP frequency and EJP amplitude (Daniels et al., 2006). I found that *vglut* mutants or knock-down showed no change of expression of puc-lacZ (Figure 4.3A), which faithfully reports Wnd signaling (Xiong et al., 2010), contrasting its dramatic upregulation in *unc-104* mutants. In a different approach to silence synaptic transmission, Tetanus Toxin Light Chain (TeTxLC), which cleaves synaptobrevin (v-SNARE) and inhibit SV exocytosis, was expressed in all motoneurons. Again no change to the puc-lacZ expression was observed (Figure 4.3A).These suggest that reduced synaptic transmission (both spontaneous and evoked release) in *unc-104* mutants is unlikely the cause of Wnd pathway activation.

4.2.2 Octopaminergic signaling did not mediate Wnd signaling activation

Octopamine, which is close to mammalian norepinephrine, is also released by a few motoneurons in Drosophila. It exhibits autoregulatory and paracrine control of NMJ growth (Koon et al., 2011). This makes it an interesting target since Wnd/DLK pathway also acts to regulate NMJ morphology (Collins et al., 2006). A straightforward model would be that octopaminergic signaling inhibits Wnd signaling and its loss in *unc-104* mutants activates Wnd signaling. In order to mimic this downregulation, I expressed neuronal RNAi to knock down the octopamine synthesis enzyme (tyrosine beta-hydroxylase (tbh)) and two receptors (Octβ1R and Octβ2R), all of which were shown to play important roles in NMJ growth (Koon et al., 2011). No activation of Wnd pathway using puc-lacZ reporter was observed (Figure 4.3B). A noticeable

reduction of puc-lacZ expression was observed when tbh was knock-down, but this was non-motoneuron specific, and distinctly from Unc-104 (Figure 4.3.B).

Another possibility is that the failed delivery of octopamine to synapses activates, instead of inhibits, its receptors. If so, one would predict that the knock-down of these receptors in *unc-104* mutant would suppress the activation of Wnd. However, I observed no obvious reduction of the Wnd signaling (Figure 4.3C). Furthermore, the synaptic assembly defects evaluated by the number of unapposed PSDs was also not affected (Figure 4.3D and E). Altogether these suggest that Octopaminergic transmission does not mediate the activation of Wnd pathway in *unc-104* mutants.

4.2.3 Accumulation, rather than release impairment of DCVs/neuropeptides, activates Wnd signaling

Neuropeptides from DCVs are another potential candidate for Wnd activation. An early observation I made hints that Wnd is more enriched in terminals (Type III) that are positive for neuropeptide storage and release. Further, when Unc-104 is overexpressed, it only appears in Type III terminals, but not others, suggesting a likely more important role for Unc-104 in peptidergic neurons (Figure 4.4). I therefore hypothesized that lack of neuropeptide release leads to synaptic defects in *unc-104* mutants.

To directly test whether the impaired release of neuropeptides are linked to Wnd activation and synaptic defects, I investigated a role for the Calcium activated protein for secretion (CAPS), which is required for regulated release of DCVs. CAPS has a conserved sequence and functions in Bilateria with homologues Unc-31 in *C. elegans* and Calcium-dependent secretion activator (Cadps) in mammals. CAPS and its homologues facilitate the

release of DCVs at synapses and mutations in *caps* and its homologues lead to impaired release of DCVs, which is often accompanied by impaired SV release (Ann et al., 1997; Berwin et al., 1998; Grishanin et al., 2004; Liu et al., 2008; Renden et al., 2001; Tandon et al., 1998). In my findings, knocking down of *caps* in neurons leads to phenotypes that are strikingly similar to *unc-104* mutants: defects in synapse apposition, Brp intensity at NMJ and activation of puc-lacZ expression (Figure 4.5A-C). Moreover, the puc-lacZ activation was inhibited by wnd knock-down (Figure 4.5A), suggesting that Wnd signaling is activated when *caps* function is disrupted. Furthermore, axon regeneration was substantially enhanced when *caps* was knocked down, with many injured axons regenerating and growing a much further distance than wild type (Figure 4.5D and E), indicating an activation of Wnd signaling.

These results are particularly interesting, however I noticed that these phenotypes are cell-autonomous, because knock-down of *CAPS* in single motoneuron led to synaptic defects (Figure 4.5B) and enhanced axon regeneration (Figure 4.5D). This cell-autonomy suggests that either neuropeptide release is important for regulating Wnd signaling through autocrine manner, or neuropeptide release does not directly affect the Wnd signaling.

To further determine the role of neuropeptide release in synaptic defects of *unc-104* mutants, I sought to examine whether knocking down *unc-104* specifically in neuropeptidergic neurons, which should impair neuropeptide release in these neurons, can cause synaptic defects. The knock-down was driven by 3 neuropeptidergic Gal4, C929 (most peptidergic neurons) (Hewes et al., 2003; Vömel and Wegener, 2008), CCAP (a subset of peptidergic neurons) (Dewey et al., 2004; Hewes et al., 2003; Vömel and Wegener, 2007) and Bursicon (a subset of peptidergic neurons) (Dewey et al., 2004; Lee et al., 2013; Peabody et al., 2008). Notably, both CCAP and Bursicon drives expression in Type III peptidergic motoneurons (Loveall and

Deitcher, 2010). In summary of results, examining two separate muscle regions, including one that is innervated by Type III peptidergic motoneurons, I did not observe any obvious synaptic defects in these conditions (Figure 4.6A and B). In contrast, single motoneuron knock-down of *unc-104* is sufficient to cause synaptic defects (Figure 3.2). These results suggest that loss of *unc-104* in peptidergic neurons alone is not sufficient to induce synaptic defects. A caveat of these experiments is that the knock-down of *unc-104* by RNAi may not be efficient if these Gal4s are not strong enough, however these Gal4 have shown prominent expression in other studies and accumulation of presynaptic proteins in cell body was observed in these conditions (not shown), indicating an at least partial loss of Unc-104 function.

Since neuropeptide release impairment by *caps* mutations is unlikely to be the cause of Wnd signaling activation and synaptic defects, it raises the possibility that other roles of CAPS may be in play. In fact, some recent studies show a role for CAPS in trafficking and Golgi morphology (Sadakata et al., 2013, 2010). In *caps* knock-down neurons, I noticed that Brp accumulated in the cell body (Figure 4.5F), in a similar way as in *unc-104* mutants. These accumulations of presynaptic proteins in the cell body of *caps* and *unc-104* mutants may affect the function of the secretory pathway, including the ER and Golgi and a defect in the secretory pathway may trigger a response. Interestingly, I found that in both *caps* and *unc-104* mutants, Phosphorylated eukaryotic initiation factor 2 α (P-eIF2α), which is highly elevated in scenarios of ER stress, is dramatically upregulated (Figure 4.7A). This suggests an association of cellular stress with loss of *unc-104* and *caps*. This led me to consider the possibility that presynaptic protein accumulation in the cell body leads to the activation of Wnd signaling.

4.3 Does the accumulation of presynaptic proteins induce UPR and activate Wnd signaling in *unc-104* mutants?

As mentioned above, a significant elevation of P-eIF2α was observed in *unc-104* mutants globally in the Nervous System, including motoneurons and sensory neurons (Figure 4.7A and B), which exhibit synaptic defects. eIF2α is essential for translation and upon ER stress can be phosphorylated at Serine 51 (S51) (Pakos-Zebrucka et al., 2016). P-eIF2α disrupts the ternary complex that is required for initiating translation, thus inhibiting global translation process. The RNA and the translation initiation components that remains associated with transcripts are then routed to form stress granules (Bellato and Hajj, 2016; Buchan and Parker, 2009). eIF2α phosphorylation can occur as a consequence of ER stress, as one arm of an unfolded protein response (UPR) pathway. Interestingly, the P-eIF2α observed in *unc-104* mutants appears to colocalize well with accumulated Brp in cell body in both motoneurons and sensory neurons (Figure 4.7C). This raises the possibility that accumulated Brp in *unc-104* mutants resides in association with P-eIF2α-containing stress granules. I also observed in *unc-104* mutants that some of these Brp puncta are located in close proximity to puncta containing Wnd (labeled by endogenous tagging by MiMIC, Figure 4.7D). Does this location relationship have anything to do with the activation of Wnd signaling? These observations suggest a possible role for P-eIF2α and UPR in activating Wnd signaling.

In order to examine the role of P-eIF2α in *Unc-104* mutants and activation of Wnd signaling, I first tested the involvement of UPR and whether UPR activation could activate Wnd signaling; then I tested roles of kinases that phosphorylate eIF2α.

4.3.1 P-eIF2α but not IRE1 is induced in unc-104 mutants

The UPR is induced by ER stress and entails three branches: PERK/P-eIF2α, IRE1/XBP1 and ATF6 (Gardner et al., 2013). If P-eIF2α is induced in *unc-104* mutants via accumulated presynaptic proteins in the ER, then other branches of the ER stress response are likely activated as well. Since it is unclear whether the ATF6 pathway is conserved in Drosophila (Ryoo, 2015), I set out to examine the IRE1 branch. The IRE1 branch, upon ER stress, is able to activate JNK signaling via the TNF-receptor-associated factor (TRAF) (Urano, 2000), making it an interesting candidate. Unfolded proteins in the ER induce IRE1, which induces alternative splicing of XBP-1. This event can be detected using a reporter which contains a GFP tag in the intron region, which, upon IRE1-induced alternative splicing, can be incorporated into the mature mRNA, allowing for expression of XBP1-GFP (Ryoo et al., 2007; Sone et al., 2013). XBP1-GFP and P-eIF2α are two common markers for UPR. In contrast to P-eIF2α, I saw no significant increase of XBP1-GFP expression in *unc-104* mutant larval motoneurons (Figure 4.8A). This suggests that the IRE1 branch is not activated by *unc-104* mutants while the P-eIF2α is. In line with the lack of IRE1 activation, the elevated puc-lacZ expression in *unc-104* mutants was not suppressed when TRAF1/4 or TRAF2/6 was knocked down in neurons (Figure 4.8B). No suppression of synaptic apposition defects in *unc-104* mutants was observed for knock-down of TRAF1/4 (Figure 4.8C). It is currently unknown whether one branch of UPR can be activated independently from the others during ER stress. But it is known that P-eIF2α can be induced by a range of signal besides ER stress (Pakos-Zebrucka et al., 2016).

4.3.2 UPR induction mildly activates Wnd signaling

I also examined whether the Wnd pathway becomes activated when the UPR is induced via several known approaches. Most assays for the UPR to date have been carried out in cultured cells following drug treatment. Some studies in *Drosophila* neurons in vivo center on responses to overexpressing mutated proteins (e.g. rhodopsin-1) in Drosophila photoreceptors, or overexpressing disease associated protein, such as TDP-43, which is associated with ALS (Kim et al., 2013; Ryoo, 2015). TDP-43 overexpression exhibits an elevation of P-eIF2α (Kim et al., 2013). I over-expressed TDP-43 or its mutated form in all neurons and observed a mild increase of puc-lacZ expression (Figure 4.9A). In contrast, over-expression of mutated rhodopsin-1 (G69D) in all neurons did not cause synaptic defects (Figure 4.9B). These mixed results may reflect differences in the extent that different UPR pathways are activated in these still poorly characterized models. Notably rhodopsin-1 (G69D) overexpression has been found to activate the IRE1/XBP1 branch (Ryoo et al., 2007) and I found no elevation of P-eIF2α (Figure 4.9C). Though further characterization is needed, these results imply that a potential P-eIF2α specific mechanism may partly contributes to the activation of Wnd activation.

Compared to in vivo assays, pharmacological UPR-induction assays in vitro are better characterized. Three common inducers can effectively induce a UPR in vitro: DTT (a reducing agent that inhibits disulfide bond formation, resulting in misfolded proteins), tunicamycin (an inhibitor of N-linked glycosylation, causing accumulation of unfolded glycoproteins in the ER) and thapsigargin (an inhibitor for ER calcium pumps, which is critical for Calcium-dependent ER chaperones) (Oslowski and Urano, 2011). I first tested whether a 4-hour incubation of larval brains with each of these agents was sufficient to induce P-eIF2α and found, except in a few neurons, no obvious increase of XBP1-GFP in motoneurons (Figure 4.9D). I noticed that the

simple incubation of dissected brains in solution triggers XBP1-GFP to relocalize from the nucleus to cell body, suggesting a XBP1 response to the incubation procedure.

In an alternative approach, DTT was fed to the animal from embryo to 3rd instar larvae for a duration of 6 days at a series of concentrations (0, 50uM, 500uM, 5mM, 50mM). In contrast to one study that shows elevation of XBP-1 (Debattisti et al., 2014), none of these concentrations significantly induce formation of P-eIF2α puncta (5mM was shown as an example, Figure 4.9E). None of these manipulations induced puc-lacZ (5mM was shown as an example, Figure 4.9E).

4.3.3 eIF2α phosphorylation kinases PERK, unlikely contributed to synaptic defects in unc-104 mutants

Since several pieces of evidence emphasize the role of P-eIF2α, I then considered whether upstream kinases of eIF2α play a role in the *unc-104* mutant phenotypes. PERK mediates phosphorylation of eIF2α during ER stress. Knock-down of PERK in neurons did not suppress the synaptic defects in *unc-104* mutants (Figure 4.10A). However, these manipulations failed to reduce the elevated P-eIF2α staining that occurs in *unc-104* mutants (Figure 4.10B), raising the possibility that other kinases may mediate the phosphorylation. Three additional kinases were found in mammals with the capability to phosphorylate eIF2α in other scenarios, such as amino acid deprivation (Ryoo, 2015). Whether these kinases are involved in Wnd activation and synaptic defects in *unc-104* mutants could be a subject of future investigation.

4.3.4 Promoting ER protein degradation did not suppress defects in unc-104 mutants

If the accumulation of presynaptic proteins mediates Wnd signaling activation and synaptic defects in *unc-104* mutants, promoting their degradation might relieve the stress and

rescue the phenotypes in *unc-104* mutants. During the UPR, HRD1, (an E3 ubiquitin ligase for ER associated Degradation (ERAD)), functions in the removal and degradation of unfolded proteins from the ER. HRD1 overexpression has been used to successfully reduce ER stress and ER stress-associated neurodegeneration in the Drosophila retina (Kang and Ryoo, 2009). I found that over-expression of HRD1 in neurons did not rescue the synaptic apposition defects, reduced Brp intensity at NMJ, or the activation of Wnd pathway in *unc-104* mutants (Figure 4.11A-C). Therefore, overexpression of HRD1 (which should promote ERAD) did not suppress phenotypes of *unc-104* mutants.

However when I examined P-eIF2α as a control for its effects, I observed that HRD1 overexpression caused a surprising enhancement of P-eIF2α rather than the expected reduction (Figure 4.11D). These confusing results could be due to the current lack of knowledge of how HRD-1 functions in these Drosophila assays and whether it interacts with other UPR components. From cultured cell assays, it is noted that overactive ERAD can lose its selectivity in substrate degradation via currently unknown mechanisms (Ruggiano et al., 2014). More importantly, the observation that no synaptic defects are observed when P-eIF2α is elevated by HRD-1 uncouples P-eIF2α induction and synaptic defects. Together with the mild effect on Wnd signaling by TDP-43 overexpression, I suspect that P-eIF2α elevation is not a major mediator of Wnd signaling activation and synaptic defects in *unc-104* mutants.

4.4 Does defective autophagy mediate the Wnd signaling activation in *unc-104* mutants?

The accumulation of presynaptic proteins in cell bodies of *unc-104* mutants may reflects= a defective degradation system. A recent study suggests that Unc-104 is important for autophagosome formation at presynaptic terminals (Stavoe et al., 2016). Mutations in *unc-104* lead to reduced number of autophagosome in neurites. This study and others have also linked

autophagy to synapse function (Binotti et al., 2014; Hernandez et al., 2012; Shen and Ganetzky, 2009; Torres and Sulzer, 2012). One study proposes that autophagy regulates synapse morphology via Highwire, a potent regulator of Wnd/DLK (Shen and Ganetzky, 2009). I therefore further probed the role of autophagy in *unc-104* mutant phenotypes and Wnd activation.

To test whether defective autophagy mediates the activation of Wnd pathway, I sought to impair autophagy function. Autophagy entails a series of highly orchestrated events, facilitated by a number of molecules. Atg1, Atg13, FIP200 and other autophagy components forms a complex that is required for autophagy initiation. Upon initiation, a phagophore forms, which later expands and matures into an autophagosome, which then fuses with a lysosome to form an autolysosome, in which protein and organelle degradation takes place. Atg7 is required for phagophore expansion(Ariosa and Klionsky, 2016; Stanley et al., 2014). In order to disrupt autophagy in neurons, I knocked down Atg1, Atg13, FIP200 and Atg7, all of which are known to play important roles in autophagosome formation. Atg1 knock-down leads to an elevation of puc-lacZ expression, which is mediated by Wnd (Figure 4.12A). This is interesting, especially considering that the loss of atg1 in Drosophila exhibits synaptic apposition defects that resemble *unc-104* mutants (Wairkar et al., 2009). In contrast, knock-down of the other components (Atg13, FIP200 and Atg7) did not lead to change of puc-lacZ expression (Figure 4.12A).

To confirm that my experimental manipulations indeed caused impairments to autophagy in Drosophila neurons, I used an Atg8 reporter to examine autophagosome/autolysosome formation. Atg8 is an LC3 homologue which is an integral component of the autophagosome membrane. The reporter contains a dual fluorescent tag of both GFP and mCherry. In autolysosomes, the GFP signal becomes quenched by the acidic environment. This reporter has been used to monitor autophagy induction and flux (Devorkin and Gorski, 2014). In the

Drosophila nervous system, many Atg8-positive puncta can be found in CNS and PNS cell body and nerves (Figure 4.12B-D). These puncta are mostly red, indicating a fully formed autolysosome. When FIP200 was knocked down, there are still number of Atg8-positive puncta across the nervous system; however, most of them are both red and green (Figure 4.12C and D), suggesting frequent presence of immature autophagosome or phagophore likely due to defective autophagy. This suggests that autophagy is indeed impaired by FIP200 knock-down.

Though further studies are needed to rule out the involvement of autophagy, my results suggests an alternative role of Atg1 in Wnd signaling activation. Besides autophagy, Atg1 has been implicated in trafficking in neurons. Work from *C. elegans* and Drosophila has identified multiple non-autophagic substrates of Atg1 and its homologues, and these substrates are all linked to kinesins (Joo et al., 2016; Lai and Garriga, 2004; Levy-Strumpf and Culotti, 2007; Toda et al., 2008; Watari-Goshima et al., 2007). Among them, unc-76 binds to SV protein, Synaptotagmin-1 and, together with Atg1 regulates SV transport along axons (Toda et al., 2008). Interestingly, a recent study found that ULK1/2, the mammalian homologue of Atg1, regulates ER-to-Golgi trafficking, independently from autophagy. The loss of ulk1/2 also activates the UPR (Joo et al., 2016). Possibly, the role of Atg1 in intracellular trafficking may crosstalk to Unc-104 or its cargos and the loss of them leads to similar defects. A specific model for my cumulative observations is that ER/Golgi malfunction caused by the loss of Atg1, *caps* or possibly *unc-104* accounts for the activation of Wnd signaling and its associated synaptic defects. Given Atg1's connection to kinesins, it would be future interest to study whether it interacts with Unc-104.

4.5 Figures

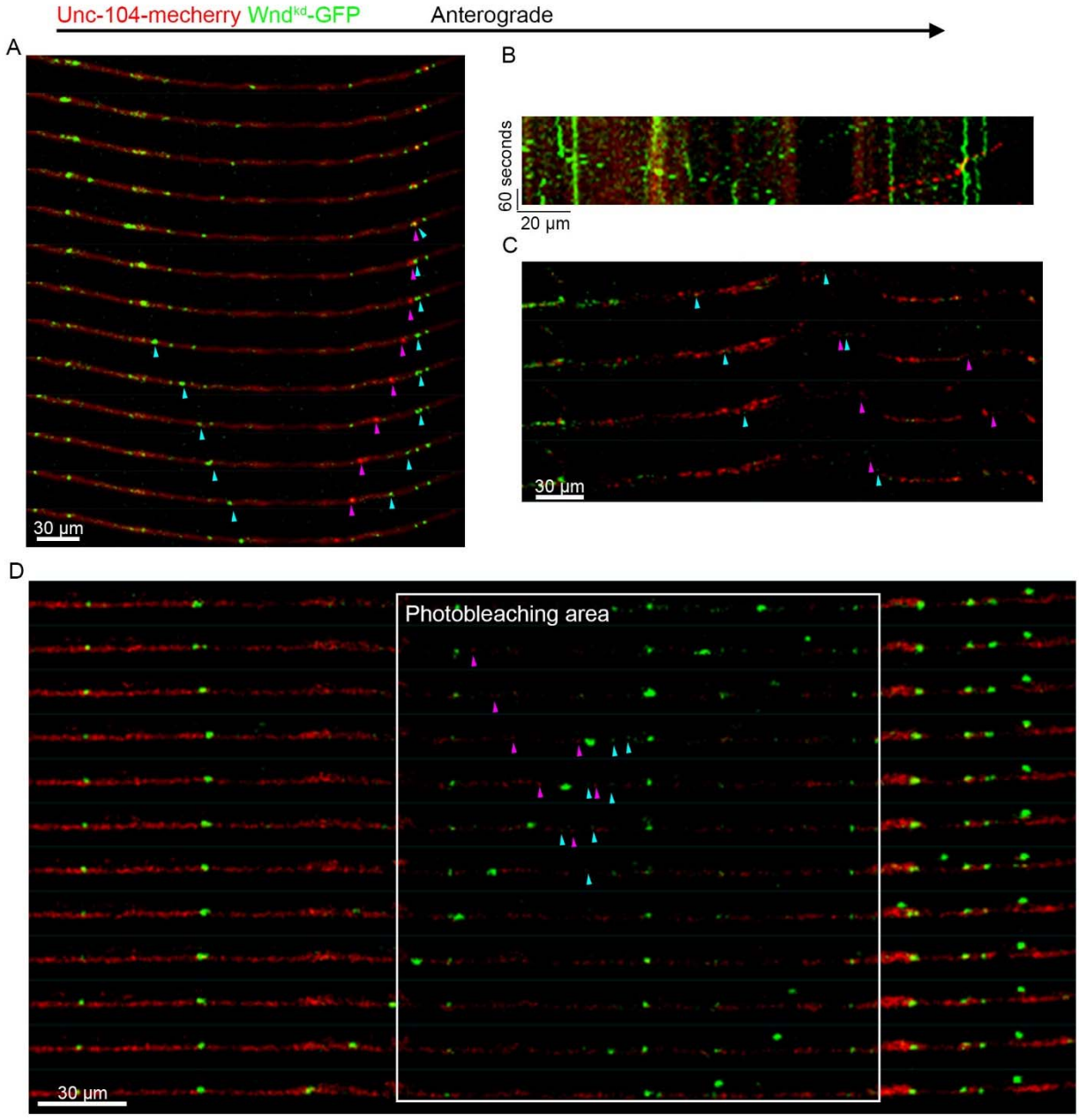
Unc-104-mecherry Wnd^kd-GFP
Anterograde
A
B
60 seconds
20 µm
C
30 µm
30 µm
D
Photobleaching area
30 µm

Figure 4.1: Live imaging of Unc-104-mCherry and GFP-Wnd^{kd} in Drosophila larval axons
(A, C and D) Stack of representative confocal images of Unc-104-mCherry and GFP-Wnd^{kd} acquired at a frequency of 0.25Hz in SNc motoneuron axons (using the *m12*-Gal4 driver)
(A) Without photobleaching, most Unc-104-mCherry reside in diffuse cytosolic pool. Retrogradely transported Unc-104-mCherry with strong fluorescence was occasionally observed (purple arrowheads). GFP-Wnd^{kd} (blue arrowheads) moves in both directions and do not colocalize with Unc-104-mCherry.
(B) Kymograph of GFP-*wnd*^{KD} and Unc-104-mCherry particle movement. Axons were imaged 900 μm distal to cell bodies at 0.25 Hz for 2-3 minutes. Anterograde particles moved from left to right.
(C) Rare identification of Unc-104-mCherry anterograde-moving particles that appear in a few frames and disappear. Note GFP-Wnd^{kd} (blue arrowheads) do not colocalize with Unc-104-mCherry.
(D) After photobleaching a region of 150 um long, a few anterograde-moving particles enters the region, but no colocalization with GFP-Wnd^{kd} was observed,
Scale bar, 30μm (A, C and D) and 20μm (B)

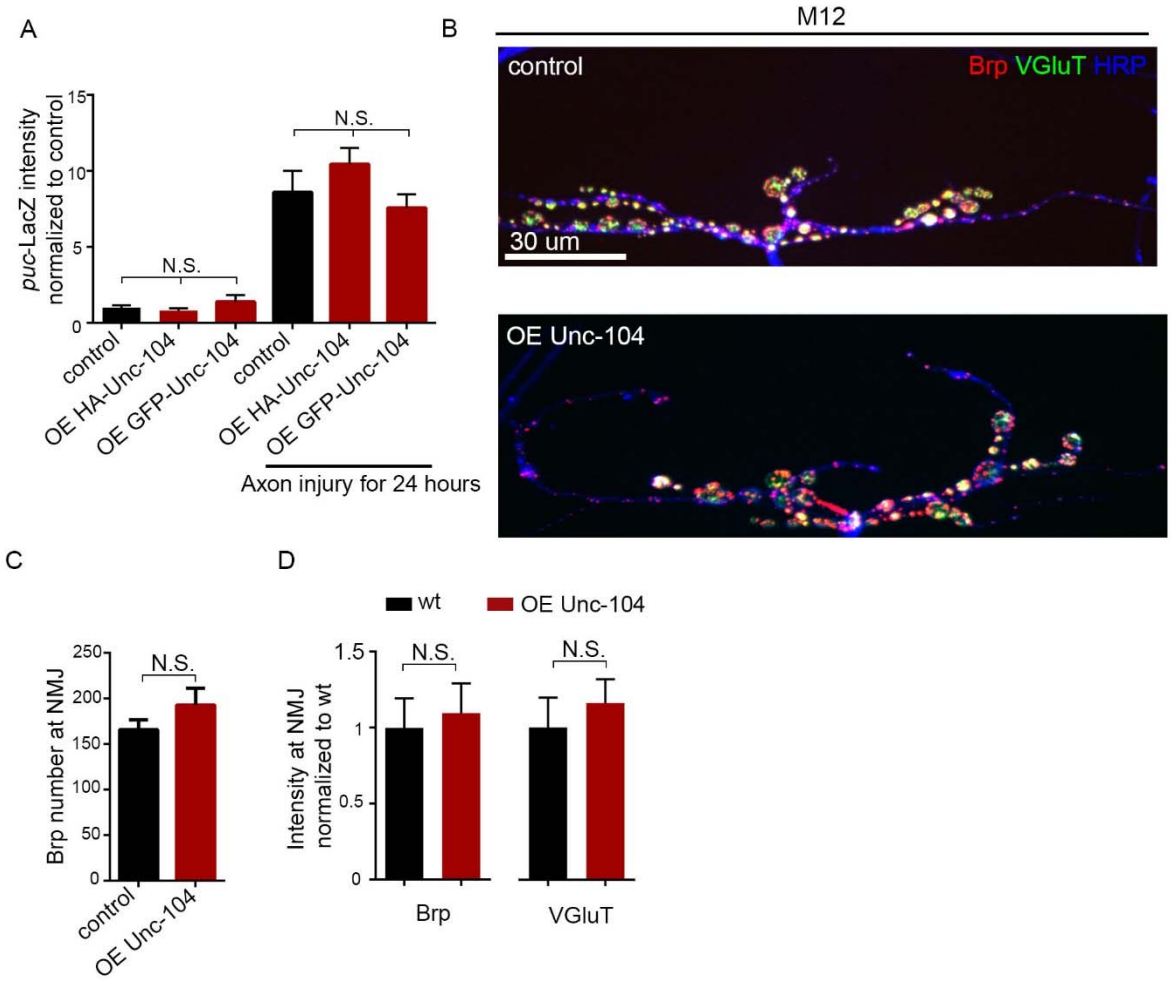

Figure 4.2 Overexpression of Unc-104 does not alter puc-lacZ expression and the intensity of Brp and VGlut at NMJ terminals.
(A) Expression of the *puc*-lacZ reporter for Wnd/JNK signaling was not affected by overexpression of two independent alleles of wild type Unc-104. Upon injury, puc-lacZ is elevated similarly between control and Unc-104 overexpression. Over expression were driven by *elav*-Gal4.
(B) VGlut (green) and Brp (red) distribution at one NMJ terminal at Muscle 12 in wild type and Unc-104 overexpression animals. The motoneuron membrane was labeled by HRP (Blue).
(C) Quantification of the total number of Brp-containing AZ puncta within the entire synaptic NMJ terminal at the Muscle 4.
(D) Quantification of the total intensity of VGlut and Brp immunostaining within the entire synaptic NMJ terminal at the Muscle 4, normalized to that in wild type animals.
All data are represented as mean ± SEM; N.S., not significant, Tukey test for multiple comparison; Scale bar, 30μm.

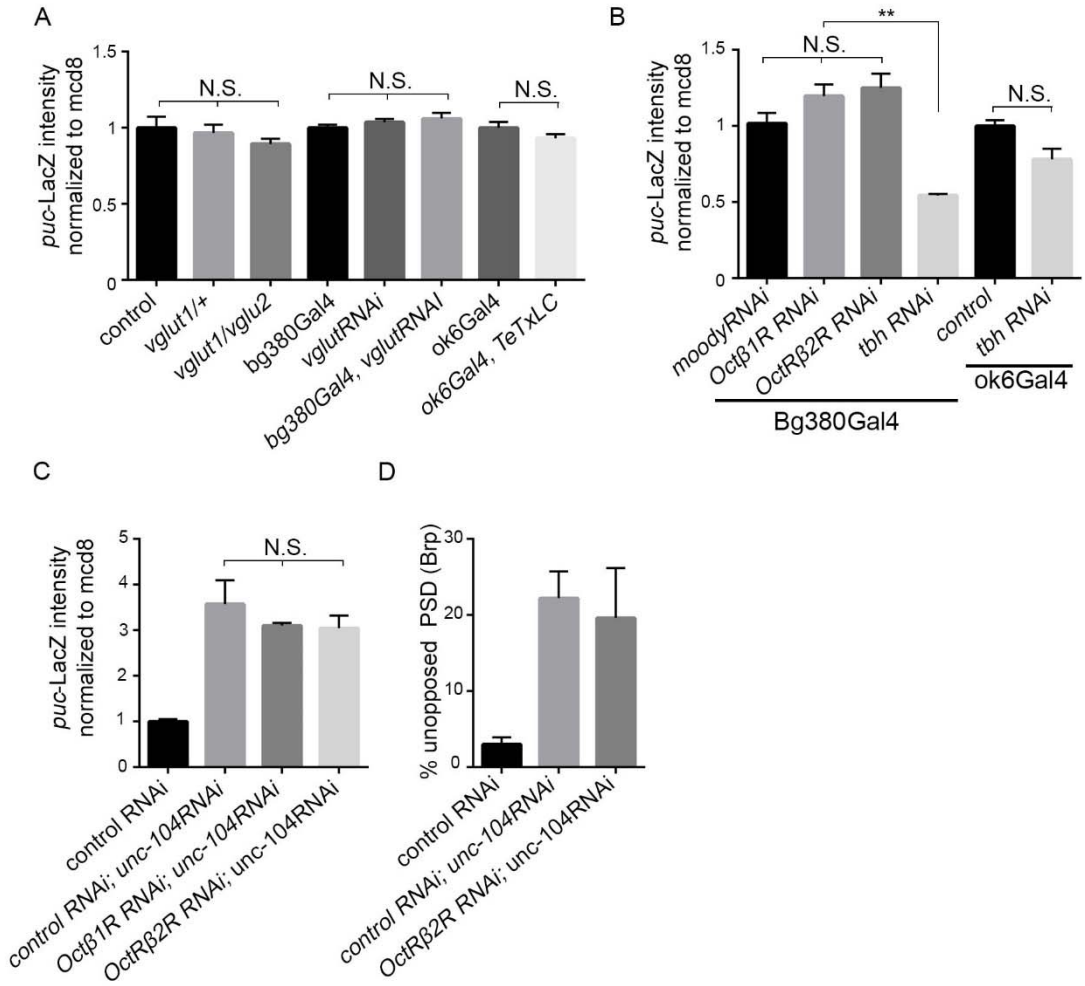
A
puc-LacZ intensity normalized to mcd8
1.5
1
0.5
0
N.S.
N.S.
N.S.
control
vglut1/+
vglut1/vglu2
bg380Gal4
vglutRNAi
bg380Gal4, vglutRNAi
ok6Gal4
ok6Gal4, TeTxLC
B
puc-LacZ intensity normalized to mcd8
**
N.S.
N.S.
moodyRNAi
Octβ1R RNAi
OctRβ2R RNAi
tbh RNAi
control
tbh RNAi
ok6Gal4
Bg380Gal4
C
puc-LacZ intensity normalized to mcd8
5
4
3
2
1
0
N.S.
control RNAi
control RNAi; unc-104RNAi
Octβ1R RNAi; unc-104RNAi
OctRβ2R RNAi; unc-104RNAi
D
% unopposed PSD (Brp)
30
20
10
0
control RNAi
control RNAi; unc-104RNAi
OctRβ2R RNAi; unc-104RNAi
E
control-RNAi
Octβ2R-RNAi;
unc-104-RNAi23465
Brp GluR
Brp
HRP
5um

Figure 4.3 Impaired glutamatergic and octopaminergic release does not mediates Wnd signaling activation and synaptic apposition defects in *unc-104* mutants
(A) Quantification of *puc*-lacZ expression when SV release is impaired by: mutants vglut1/+, vglut1/vglut2, when vglut is knocked down in all neurons (bg380Gal4) and when TeTxLC is expressed in motoneurons (ok6Gal4). No significant difference between these conditions and control.
(B) The *puc*-lacZ expression was not enhanced when Octopaminergic signaling is disrupted by knock-down of Octβ1R, Octβ2R and tbh by RNAi. A reduction was found when tbh was knock-down in all neurons but not only motoneurons.
(C) The elevated *puc*-lacZ expression in *unc-104* mutants was not suppressed when Octopaminergic signaling is disrupted by knock-down of Octβ1R and Octβ2R by RNAi.
(D) The percentage of unopposed GluRIII-labeled PSDs from E. The unopposed PSDs were defined by the GluRIII-labeled PSDs that lacked any trace of the presynaptic AZ protein Brp. Note the apposition defects due to loss of *unc-104* was not suppressed by the knock-down of Octβ2R.
(E) Representative confocal images of third instar larval neuromuscular junctions (NMJ) at muscle 4, when *Unc-104* and Octβ2R are knocked down. Postsynaptic densities (PSDs) identified by GluRIII staining (Green) that lacked apposing AZ components Brp (red) are highlighted by arrowheads.
All data are represented as mean ± SEM; N.S., not significant; ** $P<0.01$, Tukey test for multiple comparison; Scale bar, 5μm.

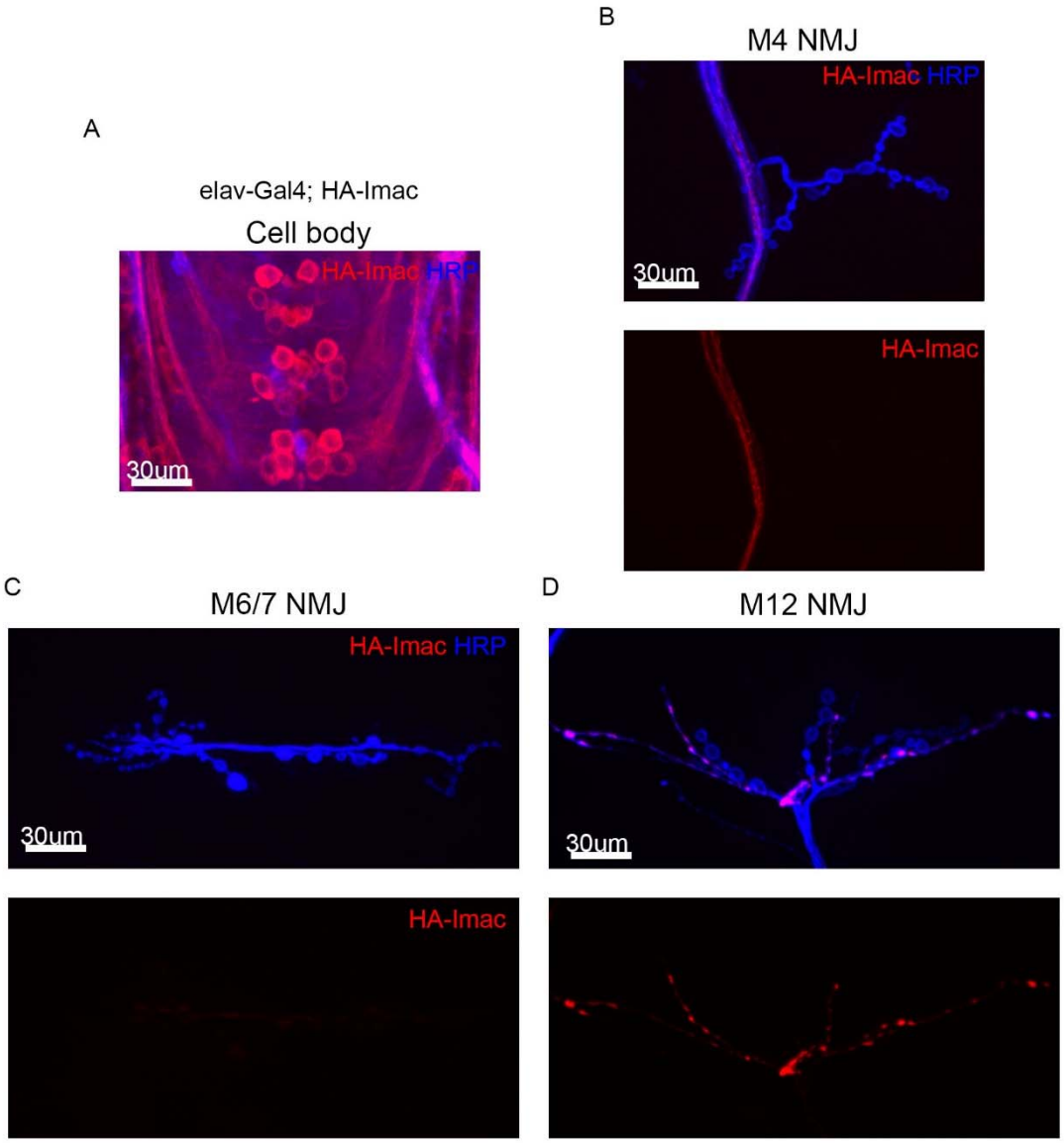

Figure 4.4 The localization of exogenously expressed HA-Unc-104
(A) Representative images showing HA-Unc-104 (red) localized to motoneuron cell body, when driven by elav-Gal4 (pan-neuronal). HRP (blue) labels neuronal membrane.
(B-C) Representative images showing lack of localization of HA-Unc-104 (red) to Type I and Type II NMJ terminals at (B) Muscle 4 and (C) Muscle 6/7. Type I and Type II terminals contains glutamatergic synapses.
(D) HA-Unc-104 (red) preferentially localizes to Type III terminals, which are peptidergic motoneurons. Note the lack of staining in Type I and Type II terminals
Scale bar, 30μm.

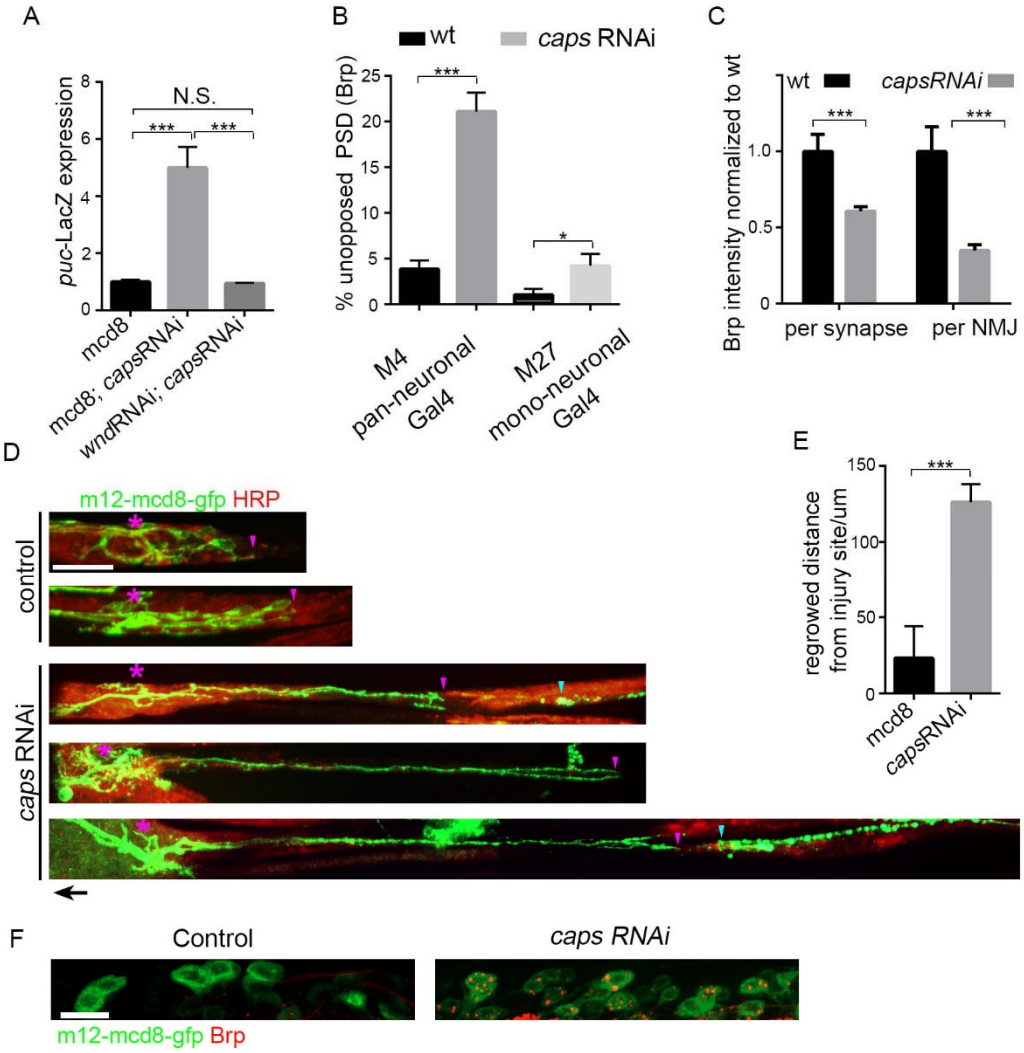
A
puc-LacZ expression
N.S.
***
***
mcd8
mcd8; capsRNAi
wndRNAi; capsRNAi
B
wt
caps RNAi
% unopposed PSD (Brp)
***
*
M4
pan-neuronal
Gal4
M27
mono-neuronal
Gal4
C
wt
capsRNAi
Brp intensity normalized to wt
***
***
per synapse
per NMJ
D
m12-mcd8-gfp HRP
control
caps RNAi
E
regrowed distance
from injury site/um
***
mcd8
capsRNAi
F
Control
caps RNAi
m12-mcd8-gfp Brp

Figure 4.5 knock-down of *caps* leads to synaptic defects and enhanced Wnd signaling, resembling *unc-104* mutants.
(A) Knock-down of *caps* by RNAi led to increase of Wnd-JNK signaling reporter, *puckered*-lacZ, in a Wnd-dependent manner. Pan neuronal Gal4 (*bg380*) was used to drive RNAi expression.
(B) Knockdown of *caps* causes cell autonomous defects in presynaptic assembly. Two different Gal4 drivers were used to express *caps* RNAi, either specifically in SNc neurons, which innervate muscle 26, 27 and 29 (*m12-gal4,* mononeuronal) or all motoneurons (*bg380*-Gal4). Knockdown in all neurons impaired presynaptic assembly on muscle 4 while knock-down in SNc neurons caused mild but significant synaptic assembly defects on muscle 27.
(C) Brp protein intensity at individual synapses and across entire NMJ terminals (at muscle 4) was reduced when *caps* was knocked down in motoneurons (using the *bg380*-Gal4 driver).
(D) Regenerative axonal sprouting of *m12*-Gal4, UAS-*mcd8*-GFP labeled axons 24 hours after nerve crush from wt and *caps knock-down* animals. Asterisk (*) indicates the injury site and arrow indicates the direction of the cell body. Note when *caps* was knocked down, the regenerated neurites (neurite tips are labeled with purple arrowheads) reach passing the injury site, to nearby distal axons (proximal ends are labeled with blue arrowheads).
(E) The axon regeneration was enhanced when *caps* was knocked down, measured by the length of the longest branch per nerve at 24 hours after injury. RNAi was driven by *m12*-Gal4.
(F) Brp (red) accumulated in motoneuron cell bodies cell autonomously when *caps* was knocked down using m12-Gal4. Motoneuron cell bodies were labeled by mcd8-gfp.
All data are represented as mean ± SEM; At least 5 animals and 10 NMJs were examined per genotype; *** $P<0.001$; N.S. not significant. Scale bar, 5μm

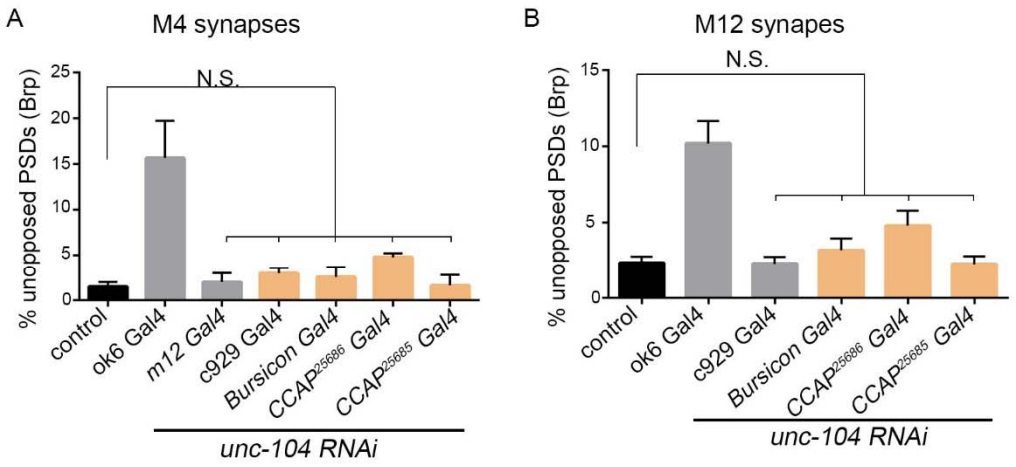

Figure 4.6 the loss of *unc-104* in peptidergic neurons alone is not sufficient to impair presynaptic assembly
The percentage of unopposed GluRIII-labeled PSDs was not altered when *unc-104* was knocked-down in most peptidergic neurons (c929) or a subset of peptidergic neurons (Bursicon-Gal4 and CCAP-Gal4) on (A) muscle 4 or (B) muscle 12. In contrast a significant portion of unopposed PSDs was found on the same muscles when *Unc-104* was knocked down in all motoneurons (ok6-Gal4). The unopposed PSDs were defined by the GluRIII-labeled PSDs that lacked any trace of the presynaptic AZ protein Brp.

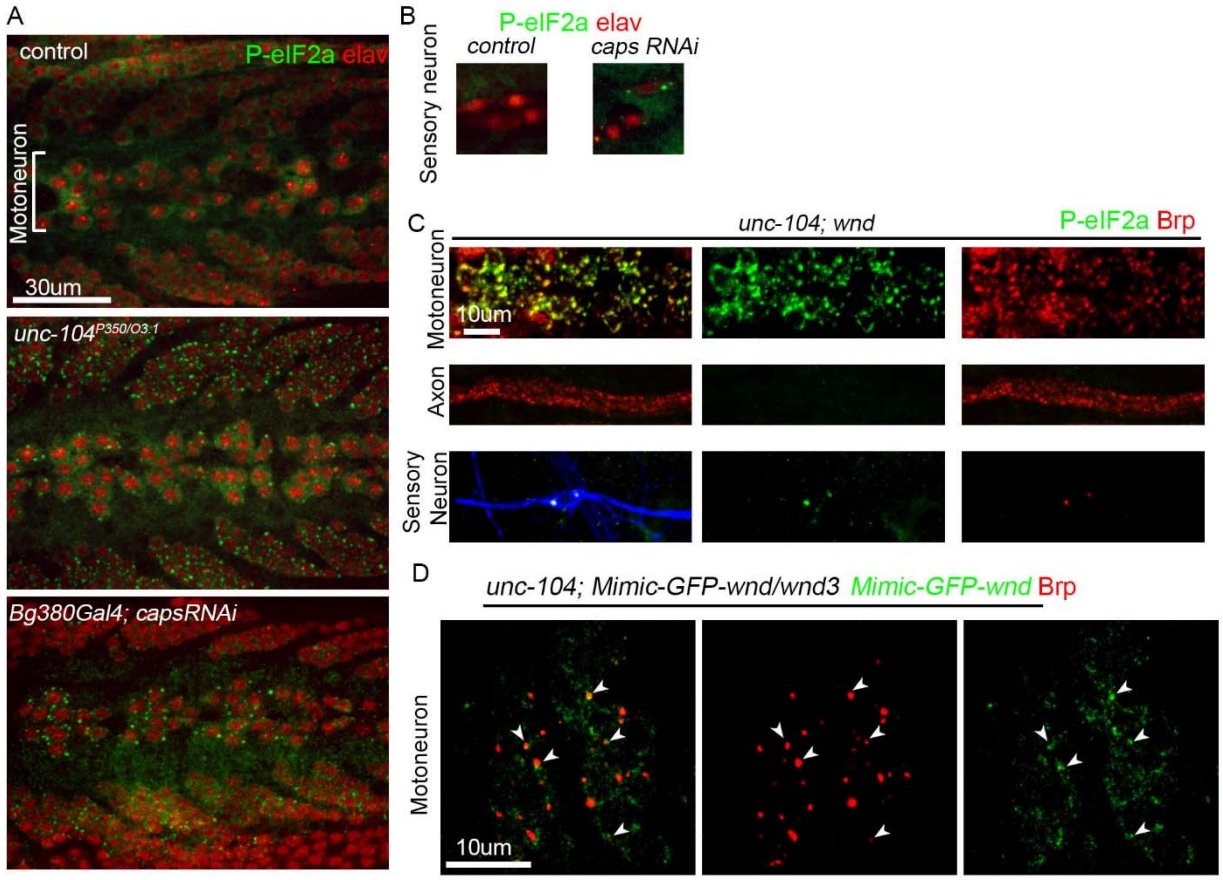

Figure 4.7 P-eIF2α is highly elevated when *unc-104* or *caps* is lost
(A) Representative images of P-eIF2α (green) staining in nerve cord with motoneurons in the middle. Compared to low and diffused P-eIF2α staining in control animal, a formation and elevation of P-eIF2α puncta was observed in *unc-104* mutants and when *caps* was knocked down. Neuronal nuclei is labeled in red.
(B) Representative images of P-eIF2α staining in sensory neuron. A formation of P-eIF2α puncta was observed when *caps* was knocked down. Neuronal nuclei is labeled in red.
(C) P-eIF2α (green) puncta colocalize nicely with Brp (red) puncta in cell bodies of motoneurons and sensory neurons in *unc-104*; wnd mutant animals. No P-eIF2α puncta was found in axons.
(D) Some endogenously tagged Wnd protein (MiMIC-*wnd*-GFP) was found to localize in close proximity to Brp puncta in cell bodies of motoneurons in *unc-104*; MiMIC-GFP-Wnd/wnd animals. The close positions are emphasized by arrowheads.
Scale bar 30um (A) and 10 um (C and D)

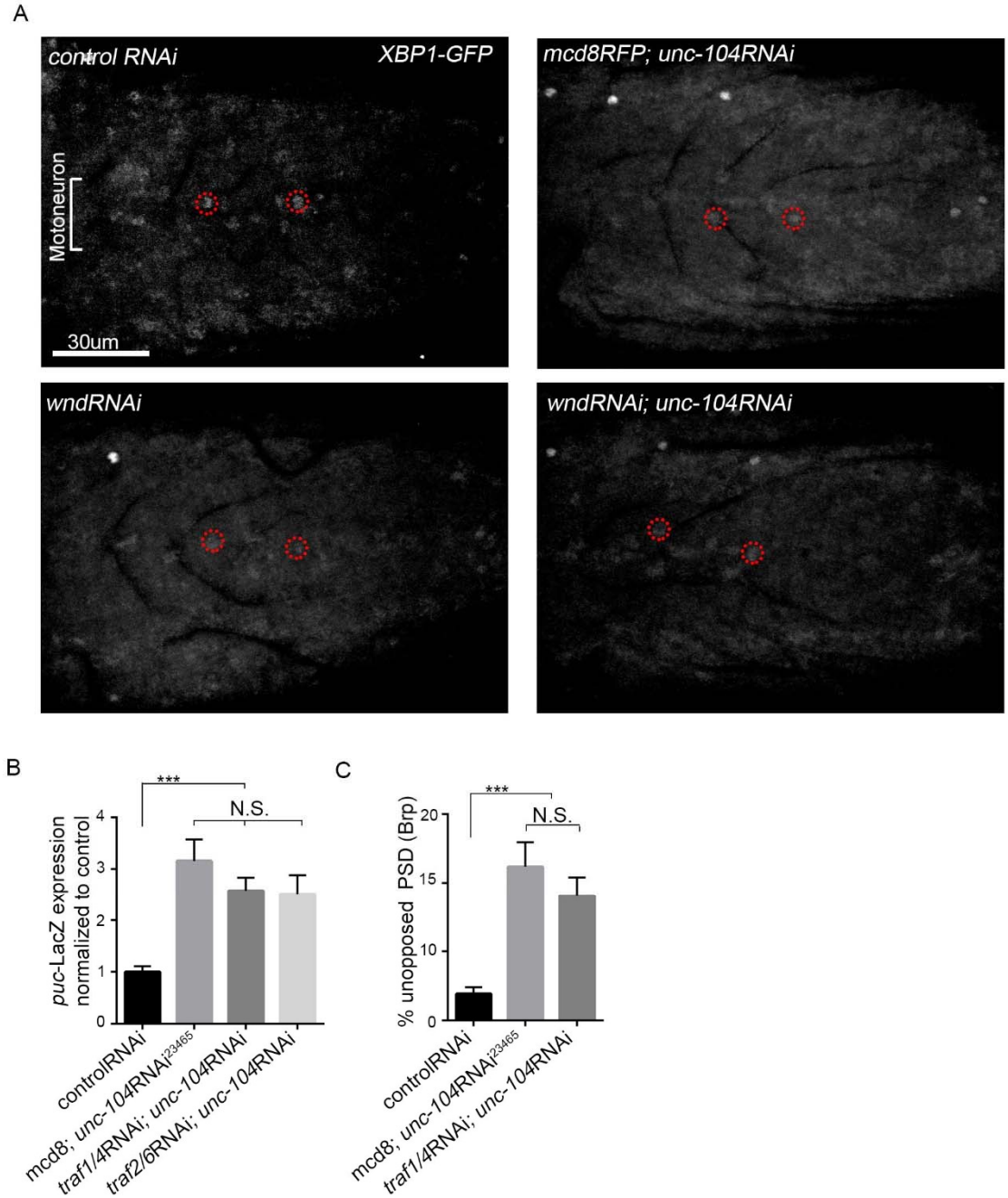
A
control RNAi
XBP1-GFP
Motoneuron
30um
mcd8RFP; unc-104RNAi
wndRNAi
wndRNAi; unc-104RNAi
B
puc-LacZ expression normalized to control
***
N.S.
0
1
2
3
4
controlRNAi
mcd8; unc-104RNAi23465
traf1/4RNAi; unc-104RNAi
traf2/6RNAi; unc-104RNAi
C
% unopposed PSD (Brp)
***
N.S.
0
10
15
20
controlRNAi
mcd8; unc-104RNAi23465
traf1/4RNAi; unc-104RNAi

Figure 4.8 IRE branch of UPR is not activated in *unc-104* mutants
(A) Representative images of XBP1-GFP expressed in all neurons, driven by bg380-Gal4. A few examples of motoneuron-localized XBP1-GFP are circled. There is no obvious change of XBP1-GFP level between control and *unc-104* knockdown and *unc-104*; wnd knockdown.
(B) The elevated *puc*-lacZ expression in *unc-104* knock-down was not suppressed by additional knock-down of traf1/4 or traf2/6 in all neurons.
(C) The increased percentage of unopposed GluRIII-labeled PSDs in *unc-104* knock-down was not suppressed by additional knock-down of traf1/4 in all neurons.
All data are represented as mean ± SEM; At least 5 animals were examined per genotype; *** $P<0.001$; N.S. not significant. Scale bar, 30μm

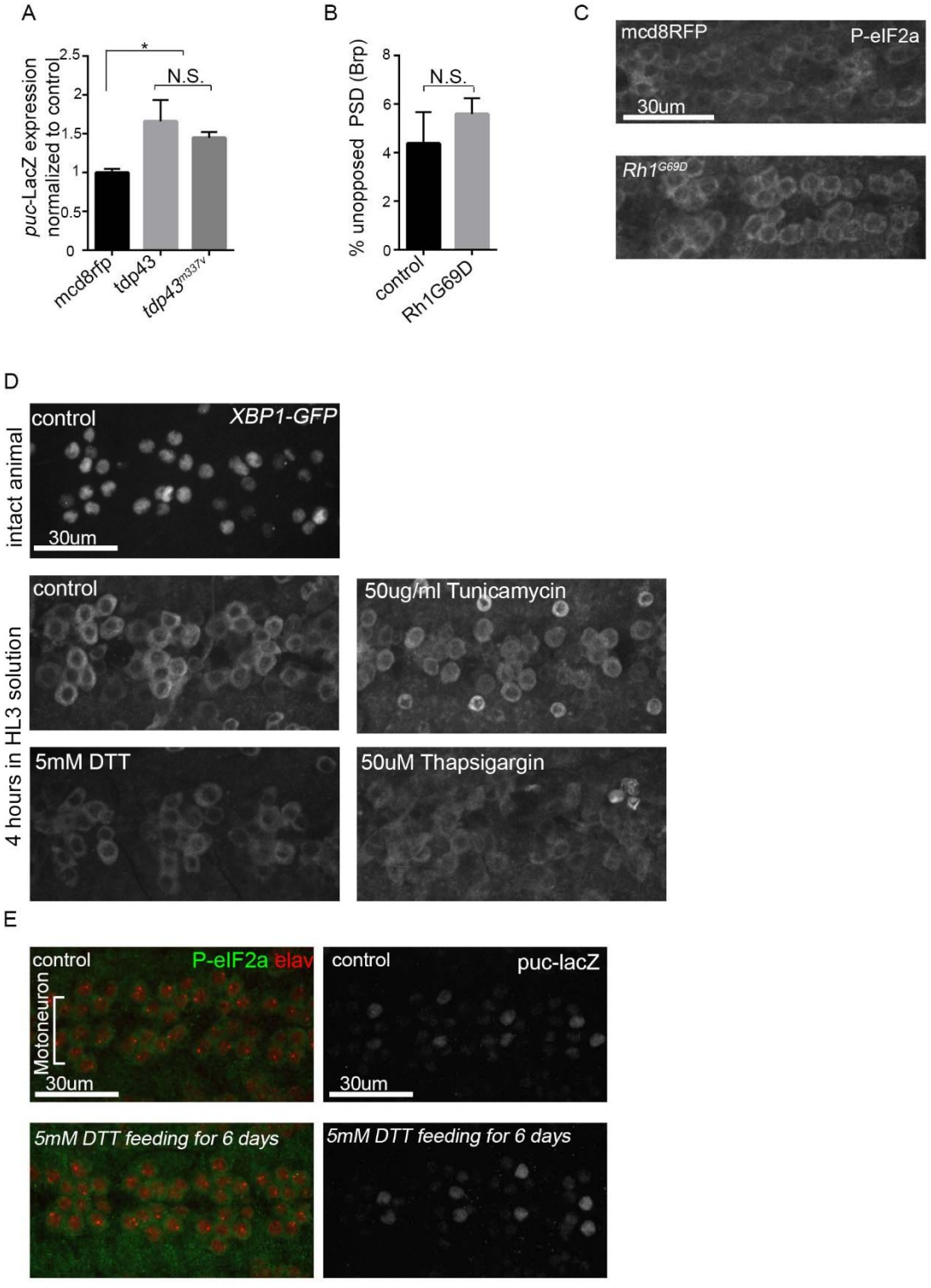
A
puc-LacZ expression normalized to control
2.5
2
1.5
1
0.5
0
*
N.S.
mcd8rfp
tdp43
tdp43m337v
B
% unopposed PSD (Brp)
8
6
4
2
0
N.S.
control
Rh1G69D
C
mcd8RFP
P-eIF2a
30um
Rh1G69D
D
intact animal
control
XBP1-GFP
30um
4 hours in HL3 solution
control
50ug/ml Tunicamycin
5mM DTT
50uM Thapsigargin
E
control
P-eIF2a elav
Motoneuron
30um
control
puc-lacZ
30um
5mM DTT feeding for 6 days
5mM DTT feeding for 6 days

Figure 4.9 The overexpression of TDP43 mildly activates puc-lacZ expression
(A) The overexpression of TDP43 or its mutated form $TDP43^{m337v}$ in all neurons (bg380-gal4) mildly but significantly elevated *puc*-lacZ expression
(B) The percentage of unopposed GluRIII-labeled PSDs remained unchanged when $Rh1^{G69D}$ was overexpressed in all neurons.
(C) Representative images of P-eIF2α (white) staining in motoneurons when mcd8RFP or $Rh1^{G69D}$ is overexpressed.
(D) Representative images of XBP1-GFP expressed in all neurons, driven by bg380-Gal4, when incubated with different UPR inducers for 4 hours. These include: vehicle, 50ug/ml Tunicamycin, 5mMDTT and 50uM Thapsigargin. No elevation of XBP1-GFP was observed.
(E) Representative images of P-eIF2α (green, left panel) and puc-lacZ (white, right panel) staining in nerve cord with motoneurons in the middle. No significant difference was observed between control animals and animals fed with 5mM DTT for a period of 6 days. Neuronal nuclei was labeled in red.
All data are represented as mean ± SEM; At least 5 animals were examined per genotype; * $P<0.05$; N.S. not significant. Scale bar, 30μm

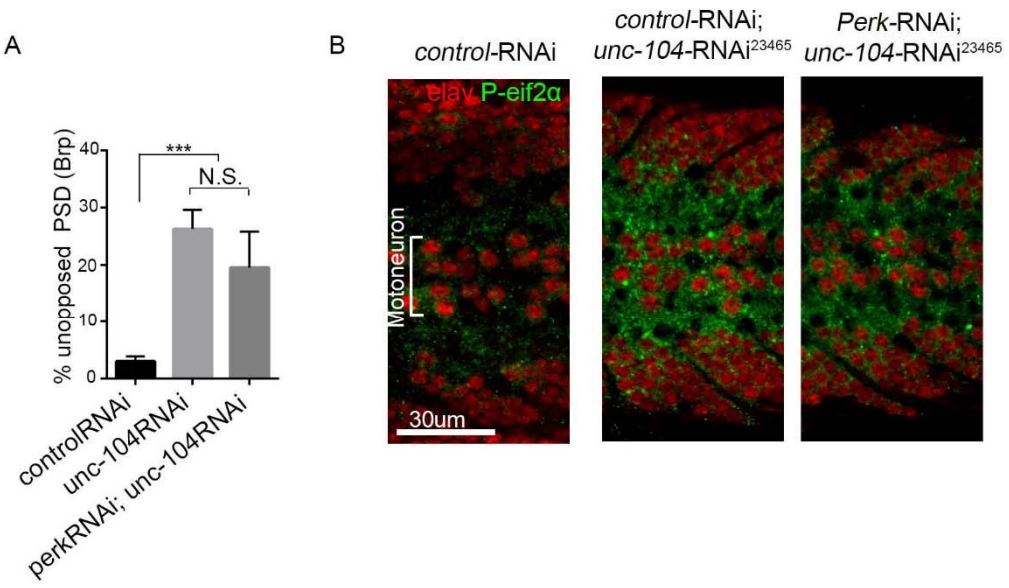

Figure 4.10 PERK does not mediate the P-eIF2α elevation and synaptic defects in *unc-104* mutants
(A) The increased percentage of unopposed GluRIII-labeled PSDs due to loss of *unc-104* was not suppressed when perk was knocked down in motoneurons (D42-Gal4)
(B) Representative images of P-eIF2α (green) staining in nerve cord with motoneurons in the middle. Compared to low and diffused P-eIF2α staining in control animal, a formation and elevation of P-eIF2α puncta was observed when *unc-104* was knocked down, and additional knock-down of perk did not reduce P-eIF2α. Neuronal nuclei is labeled in red.
All data are represented as mean ± SEM; At least 5 animals were examined per genotype; *** $P<0.001$; N.S. not significant. Scale bar, 30μm

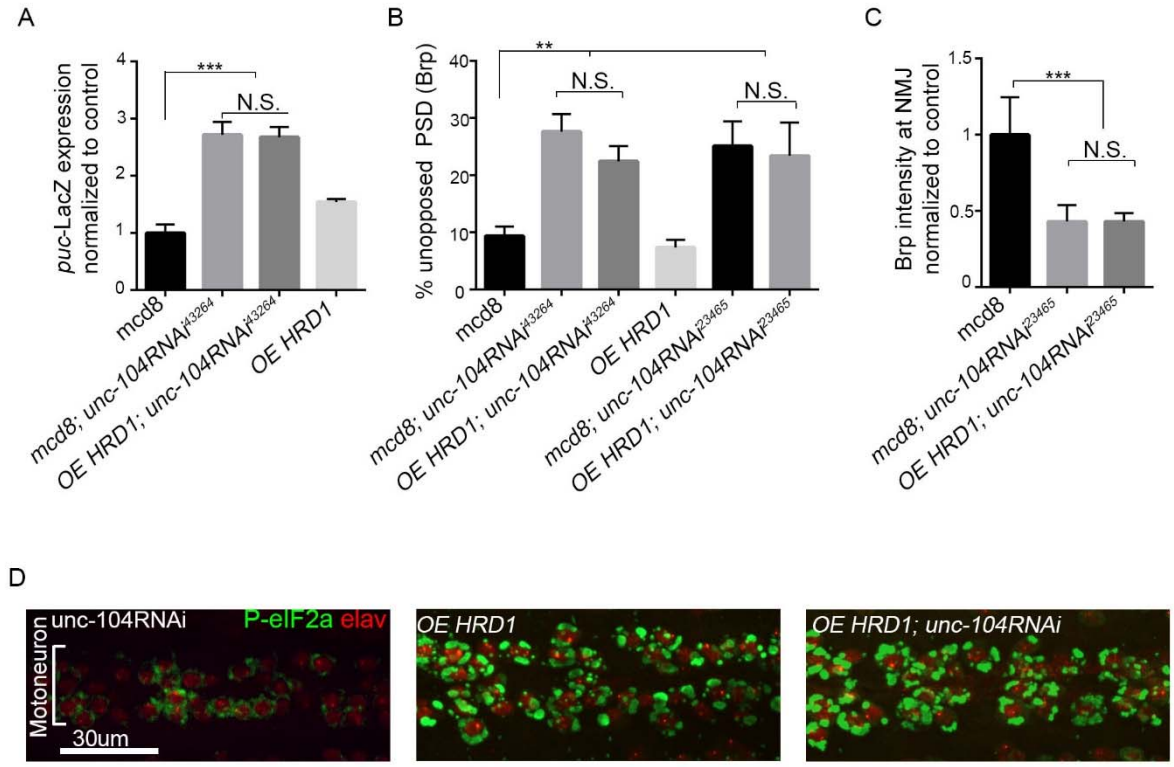

Figure 4.11 Promoting ER protein degradation did not suppress defects in *unc-104* mutants
(A) Knock-down of *unc-104* by RNAi led to an increase of Wnd-JNK signaling reporter, *puckered*-lacZ. This increase was not suppressed by overexpressiong of HRD1 in all neurons (*bg-380*).
(B) RNAi knockdown of *unc-104* caused defects in presynaptic assembly and this was not suppressed by overexpression of HRD1. Two different RNAi lines was tested under bg-380 gal4 driver.
(C) Brp protein intensity across entire NMJ terminals (at muscle 4) was reduced when *unc-104* was knocked down in all neurons (using the *bg380*-Gal4 driver), which was not suppressed by overexpression of HRD-1
(D) Representative images of P-eIF2α (green) staining in motoneurons. The formation and elevation of P-eIF2α puncta when *unc-104* was knocked down, was much further elevated when HRD1 was overexpressed. Note the overexpression of HRD1 itself elevates P-eIF2α level dramatically. Neuronal nuclei is labeled in red.
All data are represented as mean ± SEM; At least 5 animals were examined per genotype; *** P<0.001; ** P<0.01; N.S. not significant. Scale bar, 30μm

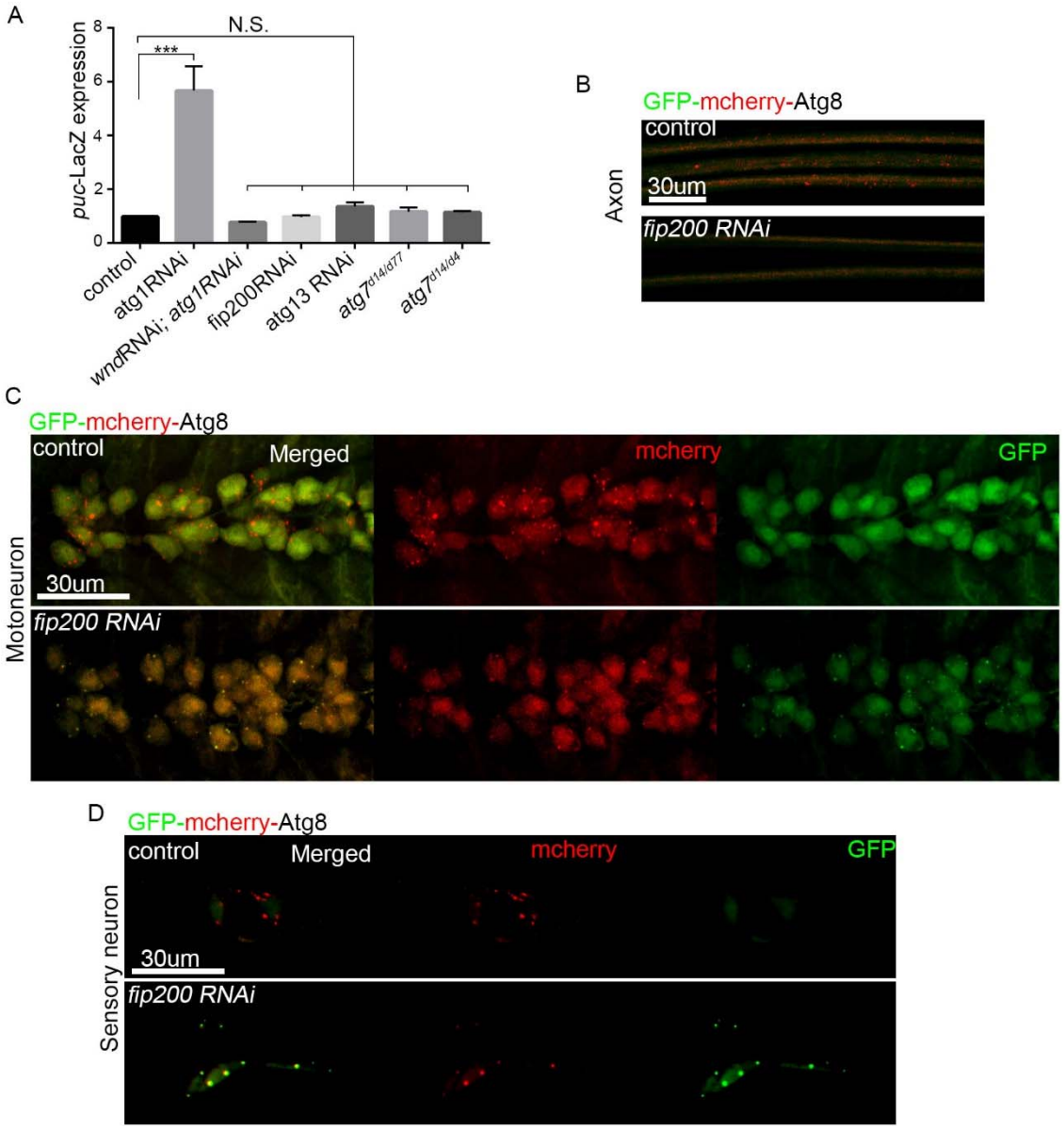
A
puc-LacZ expression
8
6
4
2
0
***
N.S.
control
atg1RNAi
wndRNAi; atg1RNAi
fip200RNAi
atg13 RNAi
atg7d14/d77
atg7d14/d4
B
GFP-mcherry-Atg8
control
30um
fip200 RNAi
Axon
C
GFP-mcherry-Atg8
control
Merged
mcherry
GFP
30um
fip200 RNAi
Motoneuron
D
GFP-mcherry-Atg8
control
Merged
mcherry
GFP
30um
fip200 RNAi
Sensory neuron

Figure 4.12 the loss of Atg1, but not FIP200, Atg13 and atg7, activates Wnd signaling
(A) Knock-down of atg1 by RNAi led to increase of Wnd-JNK signaling reporter, *puckered*-lacZ, in a Wnd-dependent manner. In contrast, knock-down of fip200 and atg13 by RNAI or mutations in atg7 did not induce puc-lacZ expressiong. Pan neuronal Gal4 (*bg380*) was used to drive RNAi expression.
(B-D) Representative images of GFP-mcherry-Atg8 in nervous system of 3rd instar *Drosophila* larvae. In control animals, GFP signal was quenched and Atg8 could be recognized as individual red puncta (presumably autolysosomes) in cell bodies of motoneurons and sensory neurons and axons. When fip200 was knocked down in all neurons, the GFP signal appears in most red-puncta in the cell bodies of neurons and disappear from axons.
All data are represented as mean ± SEM; At least 5 animals were examined per genotype; *** $P<0.001$; N.S. not significant. Scale bar, 30μm

CHAPTER V. DISCUSSION AND FUTURE DIRECTIONS

5.1 *Drosophila* kinesin-3 Unc-104/Imac is critical for transport of several SV associated proteins, but not the AZ components Brp/ELKS

We found that mutations in *unc-104* have two distinct defects: defects in the transport of Unc-104's presumptive cargo and reduced expression levels of presynaptic proteins. Both defects contribute to the defects in synaptic structure and function observed in *unc-104* mutants. Knock-down of *wnd* suppresses the defects in total levels of SV associated proteins, but not the defects in their localization/transport. It is noteworthy than many structural components of AZs, such as Brp/ELKS, can still be delivered to axon terminals in *unc-104;wnd* double. This suggests that Unc-104 does not directly transport or deliver the AZ core material. This finding raises further questions about how AZ components are transported and delivered to nascent synapses.

Previous studies have not identified a direct motor for AZ components. Because dense core vesicle (DCV) transport requires Unc-104 and a type of DCV, the Piccolo-Bassoon transport vesicle (PTV), carries AZ components including Piccolo and Bassoon (Shapira et al., 2003), Unc-104 has been a natural suspect for transporting AZ components. This possibility was also supported by the impaired AZ assembly in *unc-104/imac/kif1a* mutants. However, in both *Drosophila* and *C. elegans unc-104/imac-null* mutants, the initial AZ formation seems normal but the addition of AZs fails as the presynaptic terminals expand, suggesting the existence of alternative motors. Thus despite a number of observations comprising indirect evidence, no

direct evidence has shown Unc-104 as a motor of AZ components and the complex phenotypes in *unc-104* mutants cannot be explained by a simple motor-cargo relationship.

Transport of AZ core components

Despite its delivery to synapses, Brp/ELKS, like SV proteins, accumulates in the cell body in *unc-104*; *wnd* mutants, indicating some degree of defect in transport. This contrasts with the transport defects observed in *kinesin-1* mutants, where Brp accumulates in axons, rather than cell bodies (Siebert et al., 2015). This suggests at least two critical steps for Brp/ELKS transport: entry from cell bodies into axons and localization to synapses from axons. A model based on such notions is that Unc-104 is critical for the movement of Brp or Brp associated vesicles out of cell body compartment while kinesin-1 is important for their transport to axon terminals. An increasing amount of evidence emphasizes a critical role of a 'checkpoint' near the axon hillock region for axon entry and suggests this 'checkpoint' favors certain motors over others (Maeder et al., 2014). This notion of a 'checkpoint' may serve to assign the different transport function for Unc-104 and kinesin-1. While live imaging of Brp/ELKS has been carried out in synapses, live imaging of its entry into axons and its movement in axons have not been well-documented and might shed light on the 'multiple motors' model for Brp/ELKS.

Though our results favor a model that Unc-104 does not directly carry Brp or its associated vesicles in axons, these genetic results could be interpreted differently by a more complex model in which Unc-104 carries Brp and its associated vesicles in axons and its absence makes it possible for a motor switch that is normally inhibited by the Wnd/JNK signaling pathway. Though this model bears several assumptions that are not yet known, it is in accordance with the previously known connections between JNK signaling and kinesin-1(Fu and

Holzbaur, 2013; Horiuchi et al., 2007; Morfini et al., 2006; Stagi et al., 2006; Sun et al., 2011). In order to test this model and distinguish different interpretations from the genetic evidence, the live imaging discussed previously would be useful, when combined with comparisons of transport parameters of Brp between wild type and *unc-104;wnd* double mutants.

A recent study showed that Rim-binding protein moves together with Brp/ELKS (Siebert et al., 2015). This study found that JNK Interacting Protein 1 (JIP1), which was known to interact with Kinesin light chain (KLC) (Verhey et al., 2001), is needed for proper localization of Brp and Rim binding protein to synapses. It raises the possibility that Brp and Rim-binding proteins are both transported by Kinesin-1, at least for its localization to synapses. Besides Brp, *kinesin-1* mutants displayed a similar axonal accumulation phenotype for SV as well (Gindhart et al., 1998; Kurd and Saxton, 1996). These phenotypes suggest a seemingly universal role for Kinesin-1 in delivering presynaptic proteins from axons to synapses. However, since *kinesin-1* mutants result in axon swellings (while *unc-104* mutants do not), the transport defects should be cautiously interpreted to avoid confounding motor-cargo relationship with a general traffic jam. This also raises the question of the nature of the axonal 'accumulation' of presynaptic proteins in *kinesin-1* or *jip1* mutants. Interestingly, a similar 'accumulation' was also observed in *wnd* mutants (Horiuchi et al., 2007). Is Wnd inhibited in *kinesin-1* mutants and mediating the formation of accumulations by saturating the presynaptic protein transport/localization? This alternative model would be an interesting subject of future investigation.

If Brp/ELKS and Rim binding protein are transported by a different kinesin than Unc-104, it raises a further question on how other AZ core components (Rim, Liprin-α and Unc-13) are transported. Characterization of these proteins' transport in *unc-104* mutants and *unc-104; wnd* double mutants could aid in addressing whether Unc-104 is involved. Previous studies suggest

Liprin-α as an adaptor that closely interacts with Unc-104 in transporting cargos (Hsu et al., 2011; Miller et al., 2005; Shin et al., 2003; Wagner et al., 2009). Our data showed the loss of Liprin-α from synapses in *unc-104* mutants. But the results that Liprin-a can be rescued by *wnd* mutations, suggest the possibility that other kinesins also contribute to Liprin-α's transport. Further examination of the rescue in *unc-104* null mutants would help clarify this idea. Previous live imaging studies suggests that Liprin-α arrives at AZ prior to Brp/ELKS (Fouquet et al., 2009). This suggests Liprin-α and Brp is possibly transported by different kinesin motors.

Rim is associated with PTVs, together with Unc-13 (Shapira et al., 2003). Though one biochemical study found association between KIF1A and Rim (Shin et al., 2003), other evidence suggests Kif5b (Kinesin-1) transports PTVs. The loss of either kif5b or syntabulin, a KIF5B binding adaptor, dampens PTV transport in mammals (Cai et al., 2007; Su et al., 2004). No homologue of syntabulin was found in *Drosophila* and *C. elegans*, so either a different adaptor is used or this transport is not conserved in invertebrates.

Local translation of presynaptic proteins

It currently remains possible that besides being transported from cell bodies, AZ proteins could be synthesized locally. In contrast to well-studied local translation in postsynaptic compartments (Bramham, 2008; Buffington et al., 2014; Waung and Huber, 2009), local translation in presynaptic compartment is not well understood. Several studies suggest that mRNA associated proteins localize to the presynaptic compartment, including ribosomal protein S6 kinase (Cheng et al., 2011) and mRNA splicing factor SRPK79D (Graveley, 2000) . These studies also found that these mRNA-associated proteins are important for Brp-containing AZ formation, however it is not clear whether this function involves regulation. If Brp/ELKS is

locally translated, then it remains to be determined how its mRNA is delivered to presynaptic locations.

5.2 Wnd restrains the expression of presynaptic proteins

The restraint on expression of several presynaptic proteins provided insights into the mechanism of how Wnd regulates synaptic structure, function and possibly presynaptic terminal morphology that has been described previously. Our investigation into the unopposed PSDs further suggests a presynaptic-specific regulation by Wnd/DLK, which is distinct from Wnd/DLK's role in regulating postsynaptic receptors localization (Park et al., 2009). In addition, we found that endogenous Wnd/DLK restrains the expression of VGlut and Synaptotagmin I in early development. We showed that several components of synapses, Brp/ELKS, VGluT, Syt I and CSP are susceptible to Wnd's regulation, while Synapsin and Syntaxin are not. A more extensive delineation of all the targets of Wnd's regulation is needed.

Wnd's role in regulating transcription, translation and protein degradation

The restraint on presynaptic proteins by Wnd/DLK signaling likely involves transcriptional and translational mechanisms. The regulation of the VGlut promoter strongly supports a transcriptional regulation mechanism, which is line with the involvement of the Transcription factor Fos. Altered level of transcripts for Cac, Brp were also observed in *unc-104 wnd* double mutants. However, the rab7 promoter driven Liprin-α expression regulated by Wnd suggests a possible regulation at posttranscriptional level because the promoter activity of rab7, which regulates endosome maturation and trafficking, is unlikely affected by the Wnd/DLK pathway. In addition, the expression of several presynaptic proteins was reduced in *unc-104*

mutants in spite of their normal level of transcripts, indicating potential posttranscriptional regulation. The surprising colocalization of accumulated Brp and P-*eIF2α* suggest a possible translation repression mechanism. P-*eIF2α* is found in stress granules, which are known to store mRNAs that are prevented from translation. It remains unclear whether other presynaptic proteins are also accumulated at P-*eIF2α* containing stress granule and the significance of this association.

A translation activation mechanism was proposed previously for the regulation of Dscam by Wnd (Kim et al., 2013). The overexpression of Wnd leads to an increase in Dscam protein levels and Dscam's 3'UTR is required for this regulation. A study in *C. elegans* has also suggested that Wnd/DLK regulates the expression of a downstream transcription factor cebp-1, via its 3'UTR (Yan et al., 2009). Protein turnover is another possible mechanism that could affect the expression of presynaptic proteins, considering the excessive presynaptic proteins accumulated in *unc-104*;*wnd* double mutants; whether Wnd activation can affect the stability of ectopically expressed presynaptic proteins is an important possibility that still needs to be tested.

Wnd/DLK's role in different neuronal cell types

Wnd's role in *unc-104* mutants was largely characterized and analyzed in motor neurons and NMJs. Meanwhile we observed the accumulation of presynaptic proteins broadly in nervous system that include other neuronal types in central nervous system and peripheral sensory neurons. This suggests a more wide ranging effect of *unc-104* defects, but whether and to what extent Wnd restrains presynaptic protein expression in other neurons remains to be addressed. In our experiments, Wnd activation seemed to occur specifically in motoneurons in *unc-104* mutants (data not shown). This is in agreement with no change of total Wnd shown by western

blot of the whole brain while a dramatic increase of Wnd was observed in motoneurons. Whether this is due to unique features of motoneurons (terminal size, glutamatergic transmission or synaptic connectivity to muscle) is currently unknown. One study has shown that the Highwire-Wnd pathway is important in synaptic targeting of photoreceptors (Feoktistov et al., 2016), indicating an important role for Wnd in histaminergic neurons (photoreceptors release histamine). DLK's role revealed in *C. elegans* mostly come from studies in GABAergic motoneurons, and the synapse assembly of cholinergic neurons was less sensitive to DLK signaling activation (Nakata et al., 2005). Thus Wnd's role to restrain presynaptic proteins may be conserved across neuronal types, but the extent may vary depending on the neuronal types. Understanding the roles of Wnd in different neuronal types could reveal uncharacterized cellular components that modulates and respond to Wnd signaling. In our findings, Wnd exerts a strong inhibition on VGlut expression, raising the question whether this regulation occurs for transporters found in other neuronal types, including Vesicular monoamine Transporter (VMAT), Vesicular GABA Transporter (VGAT), and Vesicular Acetylcholine Transporter (VAChT).

Differential regulation of AZ assembly by Wnd/DLK

The 'salt and pepper' pattern of apposition defects when Wnd signaling pathway is activated suggests that some AZs may be more susceptible to Wnd signaling than others. While this could be due to randomness, it is possible that this is caused by a selective mechanism that targets some AZs or synapses versus others. The first step to addressing this possibility would be to characterize the difference between intact synapses and impaired synapses when Wnd signaling is activated. Interestingly, our physiology results have shown strong impairment of mini frequency, compared to mild defect in EJP. This provides a clue that Wnd signaling may

potentially target spontaneous release. The inhibition of VGlut expression by Wnd provides a potential mechanism since *vglut* mutations impair spontaneous release (Daniels et al., 2006). It has been shown that spontaneous release sites and evoked release sites are distinctly separated (Melom et al., 2013; Peled et al., 2014). So maybe AZ assembly at spontaneous release sites are particularly sensitive to Wnd signaling. Thus further characterization of the differences between intact and impaired synapses could reveal important clues on the regulation mechanism by Wnd.

Wnd/DLK's role in regulating presynaptic proteins may affect axonal injury response

The Wnd pathway can be activated by axonal injury, and Wnd activation initiate a series of downstream event to promote axon regeneration (Tedeschi and Bradke, 2013). Based on our findings, the presynaptic proteins are likely also downregulated after injury due to activation of Wnd signaling. It makes sense for neurons at this state to make proteins important for regenerating axons rather than forming and maintaining synapses. This downregulation of presynaptic proteins could avoid premature synapse formation at inappropriate locations, and redistribute resource (such as transport capacity by kinesins) in neurons to promote axon growth. It is also worth noting that among synaptic proteins, VGCC and its regulators has proven to play inhibitory roles in axon growth and they are found to be downregulated after injury (Enes et al., 2010; Tedeschi et al., 2016). Whether this regulation is mediated by the Wnd pathway is currently unclear. It raises the possibility that some presynaptic proteins may inhibit axon growth and downregulation of them after injury via the activation of Wnd signaling is required to release their inhibition on axon growth.

Wnd/DLK's role in regulating presynaptic proteins may be implicated in Wnd/DLK-mediated degeneration

Wnd pathway is also implicated in axonal degeneration. This includes injury-induced degeneration, apoptosis-associated degeneration and developmental axon pruning (Geden and Deshmukh, 2016). In some models for neurodegenerative disease (Glaucoma and Parkinson disease), DLK inhibition delays apoptosis and neurodegeneration (Chen et al., 2008; Ghosh et al., 2011; Watkins et al., 2013). However, it is not known whether the impaired synapse structure and function, which are often found in these disease scenarios, is mediated by Wnd/DLK. Further understanding the role of Wnd/DLK in these models with the emphasis on synapse assembly and disassembly is a relevant and interesting future direction.

REFERENCES

Aberle, H., Haghighi, A.P., Fetter, R.D., McCabe, B.D., Magalhães, T.R., and Goodman, C.S. (2002). Wishful thinking encodes a BMP type II receptor that regulates synaptic growth in Drosophila. Neuron *33*, 545–558.

Ahmari, S.E., Buchanan, J., and Smith, S.J. (2000). Assembly of presynaptic active zones from cytoplasmic transport packets. Nat. Neurosci. *3*, 445–451.

Ainger, K., Avossa, D., Morgan, F., Hill, S.J., Barry, C., Barbarese, E., and Carson, J.H. (1993). Transport and localization of exogenous myelin basic protein mRNA microinjected into oligodendrocytes. J. Cell Biol. *123*, 431–441.

Ali, Y.O., McCormack, R., Darrand, A., and Zhai, R.G. (2011). Nicotinamide Mononucleotide Adenylyltransferase Is a Stress Response Protein Regulated by the Heat Shock Factor/Hypoxia-inducible Factor 1α Pathway. J. Biol. Chem. *286*, 19089–19099.

Ali, Y.O., Ruan, K., and Zhai, R.G. (2012). NMNAT suppresses tau-induced neurodegeneration by promoting clearance of hyperphosphorylated tau oligomers in a Drosophila model of tauopathy. Hum. Mol. Genet. *21*, 237–250.

Ali, Y.O., Li-Kroeger, D., Bellen, H.J., Zhai, R.G., and Lu, H.C. (2013). NMNATs, evolutionarily conserved neuronal maintenance factors. Trends Neurosci. *36*, 632–640.

Ali, Y.O., Allen, H.M., Yu, L., Li-Kroeger, D., Bakhshizadehmahmoudi, D., Hatcher, A., McCabe, C., Xu, J., Bjorklund, N., Taglialatela, G., et al. (2016). NMNAT2:HSP90 Complex Mediates Proteostasis in Proteinopathies. PLoS Biol. *14*, e1002472.

Allison, P., and Benjamin, P.R. (1985). Anatomical Studies of Central Regeneration of an Identified Molluscan Interneuron. Proc. R. Soc. B Biol. Sci. *226*, 135–157.

Ambron, R.T., Schmied, R., Huang, C.C., and Smedman, M. (1992). A signal sequence mediates the retrograde transport of proteins from the axon periphery to the cell body and then into the nucleus. J. Neurosci. *12*, 2813–2818.

Ann, K., Kowalchyk, J.A., Loyet, K.M., and Martin, T.F.J. (1997). Novel Ca2+-binding protein (CAPS) related to UNC-31 required for Ca2+-activated exocytosis. J. Biol. Chem. *272*, 19637–19640.

Araki, T., Sasaki, Y., and Milbrandt, J. (2004). Increased nuclear NAD biosynthesis and SIRT1 activation prevent axonal degeneration. Science *305*, 1010–1013.

Aravamudan, B., Fergestad, T., Davis, W.S., Rodesch, C.K., Broadie, K., Aravamudan, B., Fergestad, T., Davis, W.S., and Rodesch, C.K. (1999). Drosophila UNC-13 is essential for synaptic transmission. Nat. Neurosci. *2*, 965–971.

Ariosa, A.R., and Klionsky, D.J. (2016). Autophagy core machinery: overcoming spatial barriers in neurons. J. Mol. Med. *94*, 1217–1227.

Avery, M.A., Sheehan, A.E., Kerr, K.S., Wang, J., and Freeman, M.R. (2009). Wld S requires

Nmnat1 enzymatic activity and N16-VCP interactions to suppress Wallerian degeneration. J. Cell Biol. *184*, 501–513.

Ayaz, D., Leyssen, M., Koch, M., Yan, J., Sheeba, V., Fogle, K.J., Holmes, T.C., and Hassan, B. a (2008). Axonal injury and regeneration in the adult brain of Drosophila. J. Neurosci. *28*, 6010–6021.

Baas, P.W., and Heidemann, S.R. (1986). Microtubule reassembly from nucleating fragments during the regrowth of amputated neurites. J. Cell Biol. *103*, 917–927.

Babetto, E., Beirowski, B., Russler, E., Milbrandt, J., and DiAntonio, A. (2013). The Phr1 Ubiquitin Ligase Promotes Injury-Induced Axon Self-Destruction. Cell Rep. *3*, 1422–1429.

Bae, H., Chen, S., Roche, J.P., Ai, M., Wu, C., Diantonio, A., and Graf, E.R. (2016). Rab3-GEF Controls Active Zone Development at the Drosophila Neuromuscular Junction. eNeuro *3*.

Baitinger, C., and Willard, M. (1987). Axonal transport of synapsin I-like proteins in rabbit retinal ganglion cells. J. Neurosci. *7*, 3723–3735.

Baker, S.T., Opperman, K.J., Tulgren, E.D., Turgeon, S.M., Bienvenut, W., and Grill, B. (2014). RPM-1 Uses Both Ubiquitin Ligase and Phosphatase-Based Mechanisms to Regulate DLK-1 during Neuronal Development. PLoS Genet. *10*.

Ballinger, M.L., and Bittner, G.D. (1980). Ultrastructural studies of severed medial giant and other CNS axons in crayfish. Cell Tissue Res. *208*, 123–133.

Barkus, R. V, Klyachko, O., Horiuchi, D., Dickson, B.J., and Saxton, W.M. (2008). Identification of an axonal kinesin-3 motor for fast anterograde vesicle transport that facilitates retrograde transport of neuropeptides. Mol. Biol. Cell *19*, 274–283.

Barolo, S., Castro, B., and Posakony, J.W. (2004). New Drosophila transgenic reporters: Insulated P-element vectors expressing fast-maturing RFP. Biotechniques *36*, 436–442.

Beirowski, B., Adalbert, R., Wagner, D., Grumme, D.S., Addicks, K., Ribchester, R.R., and Coleman, M.P. (2005). The progressive nature of Wallerian degeneration in wild-type and slow Wallerian degeneration (WldS) nerves. BMC Neurosci. *6*, 6.

Beirowski, B., Babetto, E., Gilley, J., Mazzola, F., Conforti, L., Janeckova, L., Magni, G., Ribchester, R.R., and Coleman, M.P. (2009). Non-nuclear Wld(S) determines its neuroprotective efficacy for axons and synapses in vivo. J. Neurosci. *29*, 653–668.

Bellato, H.M., and Hajj, G.N.M. (2016). Translational control by eIF2α in neurons: Beyond the stress response. Cytoskeleton *73*, 551–565.

Beneyto, M., Kristiansen, L. V, Oni-Orisan, A., McCullumsmith, R.E., and Meador-Woodruff, J.H. (2007). Abnormal glutamate receptor expression in the medial temporal lobe in schizophrenia and mood disorders. Neuropsychopharmacology *32*, 1888–1902.

Benjamin, P.R., and Allison, P. (1985). Regeneration of Excitatory, Inhibitory and Biphasic Synaptic Connections Made by a Snail Giant Interneuron. Proc. R. Soc. B Biol. Sci. *226*, 159–176.

Ben-Yaakov, K., Dagan, S.Y., Segal-Ruder, Y., Shalem, O., Vuppalanchi, D., Willis, D.E., Yudin, D., Rishal, I., Rother, F., Bader, M., et al. (2012). Axonal transcription factors signal retrogradely in lesioned peripheral nerve. EMBO J. *31*, 1350–1363.

Berwin, B., Floor, E., and Martin, T.F.J. (1998). CAPS (mammalian UNC-31) protein localizes to membranes involved in dense-core vesicle exocytosis. Neuron *21*, 137–145.

Bhatheja, K., and Field, J. (2006). Schwann cells: Origins and role in axonal maintenance and regeneration. Int. J. Biochem. Cell Biol. *38*, 1995–1999.

Binotti, B., Pavlos, N.J., Riedel, D., Wenzel, D., Vorbrüggen, G., Schalk, A.M., Kühnel, K., Boyken, J., Erck, C., Martens, H., et al. (2014). The GTPase RaB26 links synaptic vesicles to the autophagy pathway. Elife *2015*, 1–23.

Birse, S.C., and Bittner, G.D. (1976). Regeneration of giant axons in earthworms. Brain Res. *113*, 575–581.

Bodenstein, D. (1957). Studies on nerve regeneration in Periplaneta americana. J. Exp. Zool. *136*, 89–115.

Böhme, M.A., Beis, C., Reddy-Alla, S., Reynolds, E., Mampell, M.M., Grasskamp, A.T., Lützkendorf, J., Bergeron, D.D., Driller, J.H., Babikir, H., et al. (2016). Active zone scaffolds differentially accumulate Unc13 isoforms to tune Ca(2+) channel-vesicle coupling. Nat. Neurosci.

Bounoutas, A., Kratz, J., Emtage, L., Ma, C., Nguyen, K.C., and Chalfie, M. (2011). Microtubule depolymerization in Caenorhabditis elegans touch receptor neurons reduces gene expression through a p38 MAPK pathway. Proc. Natl. Acad. Sci. U. S. A. *108*, 3982–3987.

Bowman, a B., Kamal, a, Ritchings, B.W., Philp, a V, McGrail, M., Gindhart, J.G., and Goldstein, L.S. (2000). Kinesin-dependent axonal transport is mediated by the sunday driver (SYD) protein. Cell *103*, 583–594.

Brace, E.J., Wu, C., Valakh, V., and DiAntonio, A. (2014). SkpA restrains synaptic terminal growth during development and promotes axonal degeneration following injury. J. Neurosci. *34*, 8398–8410.

Bramham, C.R. (2008). Local protein synthesis, actin dynamics, and LTP consolidation. Curr. Opin. Neurobiol. *18*, 524–531.

Brendza, K.M., Rese, D.J., Gilbert, S.P., and Saxton, W.M. (1999). Lethal kinesin mutations reveal amino acids important for ATPase activation and structural coupling. J. Biol. Chem. *274*, 31506–31514.

Bruckner, J.J., Gratz, S.J., Slind, J.K., Geske, R.R., Cummings, A.M., Galindo, S.E., Donohue, L.K., and O'Connor-Giles, K.M. (2012). Fife, a Drosophila Piccolo-RIM homolog, promotes active zone organization and neurotransmitter release. J. Neurosci. *32*, 17048–17058.

Buchan, J.R., and Parker, R. (2009). Eukaryotic Stress Granules: The Ins and Outs of Translation. Mol. Cell *36*, 932–941.

Budnik, V., Koh, Y.H., Guan, B., Hartmann, B., Hough, C., Woods, D., and Gorczyca, M. (1996). Regulation of synapse structure and function by the Drosophila tumor suppressor gene dlg. Neuron *17*, 627–640.

Buffington, S. a, Huang, W., and Costa-Mattioli, M. (2014). Translational Control in Synaptic Plasticity and Cognitive Dysfunction. Annu. Rev. Neurosci. *37*, 17–38.

Burgoyne, R.D., and Morgan, A. (2011). Chaperoning the SNAREs: a role in preventing neurodegeneration? Nat. Cell Biol. *13*, 8–9.

Byrne, A.B., and Hammarlund, M. (2016). Axon regeneration in C. elegans: Worming our way to mechanisms of axon regeneration. Exp. Neurol.

Cai, Q., Pan, P.-Y.P.-Y., and Sheng, Z.-H. (2007). Syntabulin-kinesin-1 family member 5B-

mediated axonal transport contributes to activity-dependent presynaptic assembly. J. Neurosci. *27*, 7284–7296.

Case, J.F. (1957). The median nerves and cockroach spiracular function. J. Insect Physiol. *1*, 85–94.

Chan, S.S.Y., Zheng, H., Su, M.W., Wilk, R., Killeen, M.T., Hedgecock, E.M., and Culotti, J.G. (1996). UNC-40, a C. elegans homolog of DCC (Deleted in Colorectal Cancer), is required in motile cells responding to UNC-6 netrin cues. Cell *87*, 187–195.

Chen, X., and Ganetzky, B. (2012). A neuropeptide signaling pathway regulates synaptic growth in Drosophila. J. Cell Biol. *196*, 529–543.

Chen, C.-H., Lee, A., Liao, C.-P., Liu, Y.-W., and Pan, C.-L. (2014). RHGF-1/PDZ-RhoGEF and retrograde DLK-1 signaling drive neuronal remodeling on microtubule disassembly. Proc. Natl. Acad. Sci. U. S. A. *111*, 16568–16573.

Chen, C.-Y., Lin, C.-W., Chang, C.-Y., Jiang, S.-T., and Hsueh, Y.-P. (2011). Sarm1, a negative regulator of innate immunity, interacts with syndecan-2 and regulates neuronal morphology. J. Cell Biol. *193*, 769–784.

Chen, L., Stone, M.C., Tao, J., and Rolls, M.M. (2012). Axon injury and stress trigger a microtubule-based neuroprotective pathway. Proc. Natl. Acad. Sci. U. S. A. *109*, 11842–11847.

Chen, X., Rzhetskaya, M., Kareva, T., Bland, R., During, M.J., Tank, A.W., Kholodilov, N., and Burke, R.E. (2008). Antiapoptotic and trophic effects of dominant-negative forms of dual leucine zipper kinase in dopamine neurons of the substantia nigra in vivo. J. Neurosci. *28*, 672–680.

Cheng, L., Locke, C., and Davis, G.W. (2011). S6 kinase localizes to the presynaptic active zone and functions with PDK1 to control synapse development. J. Cell Biol. *194*, 921–935.

Choquet, D., and Triller, A. (2013). The Dynamic Synapse. Neuron *80*, 691–703.

Chuang, C.-F., and Bargmann, C.I. (2005). A Toll-interleukin 1 repeat protein at the synapse specifies asymmetric odorant receptor expression via ASK1 MAPKKK signaling. Genes Dev. *19*, 270–281.

Coleman, M.P., and Freeman, M.R. (2010). Wallerian degeneration, wld(s), and nmnat. Annu. Rev. Neurosci. *33*, 245–267.

Collins, C.A., Wairkar, Y.P., Johnson, S.L., and DiAntonio, A. (2006). Highwire Restrains Synaptic Growth by Attenuating a MAP Kinase Signal. Neuron *51*, 57–69.

Conforti, L., Gilley, J., and Coleman, M.P. (2014). Wallerian degeneration: an emerging axon death pathway linking injury and disease. Nat. Rev. Neurosci. *15*, 394–409.

Couillault, C., Pujol, N., Reboul, J., Sabatier, L., Guichou, J.-F., Kohara, Y., and Ewbank, J.J. (2004). TLR-independent control of innate immunity in Caenorhabditis elegans by the TIR domain adaptor protein TIR-1, an ortholog of human SARM. Nat. Immunol. *5*, 488–494.

Dai, Y., Taru, H., Deken, S.L., Grill, B., Ackley, B., Nonet, M.L., and Jin, Y. (2006). SYD-2 Liprin-alpha organizes presynaptic active zone formation through ELKS. Nat Neurosci *9*, 1479–1487.

Daniels, R.W., Collins, C.A., Chen, K., Gelfand, M. V., Featherstone, D.E., and DiAntonio, A. (2006). A single vesicular glutamate transporter is sufficient to fill a synaptic vesicle. Neuron *49*, 11–16.

Daniels, R.W., Gelfand, M. V., Collins, C.A., and DiAntonio, A. (2008). Visualizing

glutamatergic cell bodies and synapses in Drosophila larval and adult CNS. J. Comp. Neurol. *508*, 131–152.

Davenport, R.W., and Kater, S.B. (1992). Local increases in intracellular calcium elicit local filopodial responses in helisoma neuronal growth cages. Neuron *9*, 405–416.

Debattisti, V., Pendin, D., Ziviani, E., Daga, A., and Scorrano, L. (2014). Reduction of endoplasmic reticulum stress attenuates the defects caused by Drosophila mitofusin depletion. J. Cell Biol. *204*, 303–312.

Deckwerth, T.L., and Johnson, E.M. (1994). Neurites can remain viable after destruction of the neuronal soma by programmed cell death (apoptosis). Dev. Biol. *165*, 63–72.

Devorkin, L., and Gorski, S.M. (2014). Monitoring autophagy in drosophila using fluorescent reporters in the UAS-GAL4 system. Cold Spring Harb. Protoc. *2014*, 967–972.

Dewey, E.M., McNabb, S.L., Ewer, J., Kuo, G.R., Takanishi, C.L., Truman, J.W., and Honegger, H.W. (2004). Identification of the gene encoding bursicon, an insect neuropeptide responsible for cuticle sclerotization and wing spreading. Curr. Biol. *14*, 1208–1213.

Dieni, S., Matsumoto, T., Dekkers, M., Rauskolb, S., Ionescu, M.S., Deogracias, R., Gundelfinger, E.D., Kojima, M., Nestel, S., Frotscher, M., et al. (2012). BDNF and its pro-peptide are stored in presynaptic dense core vesicles in brain neurons. J. Cell Biol. *196*, 775–788.

Easley-Neal, C., Fierro, J., Buchanan, J., and Washbourne, P. (2013). Late Recruitment of Synapsin to Nascent Synapses Is Regulated by Cdk5. Cell Rep. *3*, 1199–1212.

Edwards, J.S., and Sahota, T.S. (1967). Regeneration of a sensory system: the formation of central connections by normal and transplanted cerci of the house cricket Acheta domesticus. J. Exp. Zool. *166*, 387–395.

Enes, J., Langwieser, N., Ruschel, J., Carballosa-Gonzalez, M.M., Klug, A., Traut, M.H., Ylera, B., Tahirovic, S., Hofmann, F., Stein, V., et al. (2010). Electrical activity suppresses axon growth through Cav1.2 channels in adult primary sensory neurons. Curr. Biol. *20*, 1154–1164.

Eresh, S., Riese, J., Jackson, D.B., Bohmann, D., and Bienz, M. (1997). A CREB-binding site as a target for decapentaplegic signalling during Drosophila endoderm induction. EMBO J. *16*, 2014–2022.

Ertürk, A., Hellal, F., Enes, J., and Bradke, F. (2007). Disorganized microtubules underlie the formation of retraction bulbs and the failure of axonal regeneration. J. Neurosci. *27*, 9169–9180.

Eto, K., Kawauchi, T., Osawa, M., Tabata, H., and Nakajima, K. (2010). Role of dual leucine zipper-bearing kinase (DLK/MUK/ZPK) in axonal growth. Neurosci. Res. *66*, 37–45.

Fang, Y., and Bonini, N.M. (2012). Axon Degeneration and Regeneration: Insights from Drosophila Models of Nerve Injury. Annu. Rev. Cell Dev. Biol. *28*, 575–597.

Featherstone, D.E., Chen, K., and Broadie, K. (2009). Harvesting and preparing Drosophila embryos for electrophysiological recording and other procedures. J. Vis. Exp. 3–5.

Feltrin, D., Fusco, L., Witte, H., Moretti, F., Martin, K., Letzelter, M., Fluri, E., Scheiffele, P., and Pertz, O. (2012). Growth Cone MKK7 mRNA Targeting Regulates MAP1b-Dependent Microtubule Bundling to Control Neurite Elongation. PLoS Biol. *10*.

Feoktistov, A.I., Herman, T.G., Baker, S.T., Opperman, K.J., Tulgren, E.D., Turgeon, S.M., Bienvenut, W., Grill, B., Bearce, E.A., Erdogan, B., et al. (2016). Wallenda/DLK protein levels are temporally downregulated by Tramtrack69 to allow R7 growth cones to become stationary

boutons. Development *143*, 2983–2993.

Fernandes, K.A., Harder, J.M., John, S.W., Shrager, P., and Libby, R.T. (2014). DLK-dependent signaling is important for somal but not axonal degeneration of retinal ganglion cells following axonal injury. Neurobiol. Dis. *69*, 108–116.

Fernández-Chacón, R., Wölfel, M., Nishimune, H., Tabares, L., Schmitz, F., Castellano-Muñoz, M., Rosenmund, C., Montesinos, M.L., Sanes, J.R., Schneggenburger, R., et al. (2004). The synaptic vesicle protein CSPα prevents presynaptic degeneration. Neuron *42*, 237–251.

Fink, J.K. (2013). Hereditary spastic paraplegia: clinico-pathologic features and emerging molecular mechanisms. Acta Neuropathol. *126*, 307–328.

Finn, J.T., Weil, M., Archer, F., Siman, R., Srinivasan, A., and Raff, M.C. (2000). Evidence that Wallerian degeneration and localized axon degeneration induced by local neurotrophin deprivation do not involve caspases. J. Neurosci. *20*, 1333–1341.

Fischer, L.R., Culver, D.G., Tennant, P., Davis, A.A., Wang, M., Castellano-Sanchez, A., Khan, J., Polak, M.A., and Glass, J.D. (2004). Amyotrophic lateral sclerosis is a distal axonopathy: Evidence in mice and man. Exp. Neurol. *185*, 232–240.

Fischer von Mollard, G., Mignery, G.A., Baumert, M., Perin, M.S., Hanson, T.J., Burger, P.M., Jahn, R., and Südhof, T.C. (1990). rab3 is a small GTP-binding protein exclusively localized to synaptic vesicles. Proc. Natl. Acad. Sci. U. S. A. *87*, 1988–1992.

Fouquet, W., Owald, D., Wichmann, C., Mertel, S., Depner, H., Dyba, M., Hallermann, S., Kittel, R.J., Eimer, S., and Sigrist, S.J. (2009). Maturation of active zone assembly by Drosophila Bruchpilot. J. Cell Biol. *186*, 129–145.

Frank, E., Jansen, J.K., and Rinvik, E. (1975). A multisomatic axon in the central nervous system of the leech. J. Comp. Neurol. *159*, 1–13.

Fu, M.M., and Holzbaur, E.L.F. (2013). JIP1 regulates the directionality of APP axonal transport by coordinating kinesin and dynein motors. J. Cell Biol. *202*, 495–508.

Füger, P., Sreekumar, V., Schüle, R., Kern, J. V., Stanchev, D.T., Schneider, C.D., Karle, K.N., Daub, K.J., Siegert, V.K., Flötenmeyer, M., et al. (2012). Spastic paraplegia mutation N256S in the neuronal microtubule motor KIF5A disrupts axonal transport in a Drosophila HSP model. PLoS Genet. *8*, e1003066.

Gabel, C. V, Antonie, F., Chuang, C.F., Samuel, A.D.T., and Chang, C. (2008). Distinct cellular and molecular mechanisms mediate initial axon development and adult-stage axon regeneration in C. elegans. Development *135*, 1129–1136.

Gardner, B.M., Pincus, D., Gotthardt, K., Gallagher, C.M., and Walter, P. (2013). Endoplasmic reticulum stress sensing in the unfolded protein response. Cold Spring Harb. Perspect. Biol. *5*.

Gasparini, S., Kasyanov, a M., Pietrobon, D., Voronin, L.L., and Cherubini, E. (2001). Presynaptic R-type calcium channels contribute to fast excitatory synaptic transmission in the rat hippocampus. J. Neurosci. *21*, 8715–8721.

Geden, M.J., and Deshmukh, M. (2016). Axon degeneration: Context defines distinct pathways. Curr. Opin. Neurobiol. *39*, 108–115.

Gerdts, J., Brace, E.J., Sasaki, Y., DiAntonio, A., and Milbrandt, J. (2015). SARM1 activation triggers axon degeneration locally via NAD^+ destruction. Science *348*, 453–457.

Gerdts, J., Summers, D.W., Milbrandt, J., and DiAntonio, A. (2016). Axon Self-Destruction:

New Links among SARM1, MAPKs, and NAD+ Metabolism. Neuron *89*, 449–460.

Ghannad-Rezaie, M., Wang, X., Mishra, B., Collins, C., and Chronis, N. (2012). Microfluidic chips for in vivo imaging of cellular responses to neural injury in Drosophila larvae. PLoS One *7*, e29869.

Ghosh, A.S., Wang, B., Pozniak, C.D., Chen, M., Watts, R.J., and Lewcock, J.W. (2011). DLK induces developmental neuronal degeneration via selective regulation of proapoptotic JNK activity. J. Cell Biol. *194*, 751–764.

Gilley, J., and Coleman, M.P. (2010). Endogenous Nmnat2 Is an Essential Survival Factor for Maintenance of Healthy Axons. PLoS Biol. *8*.

Gindhart, J.G., Desai, C.J., Beushausen, S., Zinn, K., and Goldstein, L.S.B. (1998). Kinesin light chains are essential for axonal transport in Drosophila. J. Cell Biol. *141*, 443–454.

Gitler, D., and Spira, M.E. (1998). Real time imaging of calcium-induced localized proteolytic activity after axotomy and its relation to growth cone formation. Neuron *20*, 1123–1135.

Gitler, D., and Spira, M.E. (2002). Short window of opportunity for calpain induced growth cone formation after axotomy of Aplysia neurons. J. Neurobiol. *52*, 267–279.

Goldstein, A.Y.N., Wang, X., and Schwarz, T.L. (2008). Axonal transport and the delivery of pre-synaptic components. Curr. Opin. Neurobiol. *18*, 495–503.

Gong, T.W., Winnicki, R.S., Kohrman, D.C., and Lomax, M.I. (1999). A novel mouse kinesin of the UNC-104/KIF1 subfamily encoded by the Kif1b gene. Gene *239*, 117–127.

Górska-Andrzejak, J., Makuch, R., Stefan, J., Görlich, A., Semik, D., and Pyza, E. (2013). Circadian expression of the presynaptic active zone protein bruchpilot in the lamina of Drosophila melanogaster. Dev. Neurobiol. *73*, 14–26.

Graf, E.R., Daniels, R.W., Burgess, R.W., Schwarz, T.L., and DiAntonio, A. (2009). Rab3 dynamically controls protein composition at active zones. Neuron *64*, 663–677.

Graf, E.R., Valakh, V., Wright, C.M., Wu, C., Liu, Z., Zhang, Y.Q., and DiAntonio, A. (2012). RIM promotes calcium channel accumulation at active zones of the Drosophila neuromuscular junction. J. Neurosci. *32*, 16586–16596.

Graveley, B.R., Brooks, A.N., Carlson, J.W., Duff, M.O., Landolin, J.M., Yang, L., Artieri, C.G., van Baren, M.J., Boley, N., Booth, B.W., et al. (2011). The developmental transcriptome of Drosophila melanogaster. Nature *471*, 473–479.

Grishanin, R.N., Kowalchyk, J.A., Klenchin, V.A., Ann, K., Earles, C.A., Chapman, E.R., Gerona, R.R.L., and Martin, T.F.J. (2004). CAPS acts at a prefusion step in dense-core vesicle exocytosis as a PIP2 binding protein. Neuron *43*, 551–562.

Grygoruk, A., Fei, H., Daniels, R.W., Miller, B.R., DiAntonio, A., and Krantz, D.E. (2010). A tyrosine-based motif localizes a Drosophila vesicular transporter to synaptic vesicles in vivo. J. Biol. Chem. *285*, 6867–6878.

Hall, A.R. (1921). Regeneration in the annelid nerve cord. J. Comp. Neurol. *33*, 163–191.

Hall, D.H., and Hedgecock, E.M. (1991). Kinesin-related gene unc-104 is required for axonal transport of synaptic vesicles in C. elegans. Cell *65*, 837–847.

Hallam, S.J., Goncharov, A., McEwen, J., Baran, R., and Jin, Y. (2002). SYD-1, a presynaptic protein with PDZ, C2 and rhoGAP-like domains, specifies axon identity in C. elegans. Nat. Neurosci. *5*, 1137–1146.

Hammarlund, M., and Jin, Y. (2014). Axon regeneration in C. elegans. Curr. Opin. Neurobiol. *27*, 199–207.

Hammarlund, M., Jorgensen, E.M., and Bastiani, M.J. (2007). Axons break in animals lacking ??-spectrin. J. Cell Biol. *176*, 269–275.

Hammarlund, M., Nix, P., Hauth, L., Jorgensen, E.M., and Bastiani, M. (2009). Axon regeneration requires a conserved MAP kinase pathway. Science *323*, 802–806.

Hanz, S., and Fainzilber, M. (2006). Retrograde signaling in injured nerve--the axon reaction revisited. J. Neurochem. *99*, 13–19.

Hao, Y., Frey, E., Yoon, C., Wong, H., Nestorovski, D., Holzman, L.B., Giger, R.J., DiAntonio, A., and Collins, C. (2016). An evolutionarily conserved mechanism for cAMP elicited axonal regeneration involves direct activation of the dual leucine zipper kinase DLK. Elife *5*.

Hartenstein, V. (1993). Atlas of Drosophila Development. Atlas Drosoph. Dev. 1–57.

Hellal, F., Hurtado, A., Ruschel, J., Flynn, K.C., Laskowski, C.J., Umlauf, M., Kapitein, L.C., Strikis, D., Lemmon, V., Bixby, J., et al. (2011). Microtubule stabilization reduces scarring and causes axon regeneration after spinal cord injury. Science (80-.). *331*, 928–931.

Hendricks, M., and Jesuthasan, S. (2009). PHR regulates growth cone pausing at intermediate targets through microtubule disassembly. J. Neurosci. *29*, 6593–6598.

Henstridge, C.M., Pickett, E., and Spires-Jones, T.L. (2016). Synaptic pathology: A shared mechanism in neurological disease. Ageing Res. Rev. *28*, 72–84.

Hernandez, D., Torres, C.A., Setlik, W., Cebrián, C., Mosharov, E. V., Tang, G., Cheng, H.C., Kholodilov, N., Yarygina, O., Burke, R.E., et al. (2012). Regulation of Presynaptic Neurotransmission by Macroautophagy. Neuron *74*, 277–284.

Hewes, R.S., Park, D., Gauthier, S. a, Schaefer, A.M., and Taghert, P.H. (2003). The bHLH protein Dimmed controls neuroendocrine cell differentiation in Drosophila. Development *130*, 1771–1781.

Hicks, A.N., Lorenzetti, D., Gilley, J., Lu, B., Andersson, K.E., Miligan, C., Overbeek, P.A., Oppenheim, R., and Bishop, C.E. (2012). Nicotinamide Mononucleotide Adenylyltransferase 2 (Nmnat2) Regulates Axon Integrity in the Mouse Embryo. PLoS One *7*.

Hirai, S., Banba, Y., Satake, T., and Ohno, S. (2011). Axon formation in neocortical neurons depends on stage-specific regulation of microtubule stability by the dual leucine zipper kinase-c-Jun N-terminal kinase pathway. J. Neurosci. *31*, 6468–6480.

Hirokawa, N., Noda, Y., Tanaka, Y., and Niwa, S. (2009). Kinesin superfamily motor proteins and intracellular transport. Nat. Rev. Mol. Cell Biol. *10*, 682–696.

Holland, S.M., Collura, K.M., Ketschek, A., Noma, K., Ferguson, T.A., Jin, Y., Gallo, G., and Thomas, G.M. (2015). Palmitoylation controls DLK localization, interactions and activity to ensure effective axonal injury signaling. Proc. Natl. Acad. Sci. 201514123.

Horiuchi, D., Barkus, R. V, Pilling, A.D., Gassman, A., and Saxton, W.M. (2005). APLIP1, a kinesin binding JIP-1/JNK scaffold protein, influences the axonal transport of both vesicles and mitochondria in Drosophila. Curr. Biol. *15*, 2137–2141.

Horiuchi, D., Collins, C.A., Bhat, P., Barkus, R. V., Diantonio, A., and Saxton, W.M. (2007). Control of a kinesin-cargo linkage mechanism by JNK pathway kinases. Curr. Biol. *17*, 1313–1317.

Hoy, R.R., Bittner, G.D., and Kennedy, D. (1967). Regeneration in Crustacean Motoneurons: Evidence for Axonal Fusion. Science (80-.). *156*, 251–252.

Hsu, C.C., Moncaleano, J.D., and Wagner, O.I. (2011). Sub-cellular distribution of UNC-104(KIF1A) upon binding to adaptors as UNC-16(JIP3), DNC-1(DCTN1/Glued) and SYD-2(Liprin-alpha) in C. elegans neurons. Neuroscience *176*, 39–52.

Hu, Y., Sopko, R., Foos, M., Kelley, C., Flockhart, I., Ammeux, N., Wang, X., Perkins, L., Perrimon, N., and Mohr, S.E. (2013). FlyPrimerBank: an online database for Drosophila melanogaster gene expression analysis and knockdown evaluation of RNAi reagents. G3 (Bethesda). *3*, 1607–1616.

Hung, C.O.Y., and Coleman, M.P. (2016). KIF1A mediates axonal transport of BACE1 and identification of independently moving cargoes in living SCG neurons. Traffic *17*, 1155–1167.

Huntwork-Rodriguez, S., Wang, B., Watkins, T., Ghosh, A.S., Pozniak, C.D., Bustos, D., Newton, K., Kirkpatrick, D.S., and Lewcock, J.W. (2013). JNK-mediated phosphorylation of DLK suppresses its ubiquitination to promote neuronal apoptosis. J. Cell Biol. *202*, 747–763.

Inoue, A., and Okabe, S. (2003). The dynamic organization of postsynaptic proteins: Translocating molecules regulate synaptic function. Curr. Opin. Neurobiol. *13*, 332–340.

Jang, B.G., In, S., Choi, B., and Kim, M.-J. (2014). Beta-amyloid oligomers induce early loss of presynaptic proteins in primary neurons by caspase-dependent and proteasome-dependent mechanisms. Neuroreport *25*, 1281–1288.

Jia, H., Yan, T., Feng, Y., Zeng, C., Shi, X., and Zhai, Q. (2007). Identification of a critical site in Wlds: Essential for Nmnat enzyme activity and axon-protective function. Neurosci. Lett. *413*, 46–51.

Johansen, J., Halpern, M.E., and Keshishian, H. (1989). Axonal guidance and the development of muscle fiber-specific innervation in Drosophila embryos. J. Neurosci. *9*, 4318–4332.

Johnson, E.L., Fetter, R.D., and Davis, G.W. (2009). Negative regulation of active zone assembly by a newly identified SR protein kinase. PLoS Biol. *7*.

Joo, J.H., Wang, B., Frankel, E., Ge, L., Xu, L., Iyengar, R., Li-Harms, X., Wright, C., Shaw, T.I., Lindsten, T., et al. (2016). The Noncanonical Role of ULK/ATG1 in ER-to-Golgi Trafficking Is Essential for Cellular Homeostasis. Mol. Cell *62*, 491–506.

Jung, S., Oshima-Takago, T., Chakrabarti, R., Wong, A.B., Jing, Z., Yamanbaeva, G., Picher, M.M., Wojcik, S.M., Göttfert, F., Predoehl, F., et al. (2015). Rab3-interacting molecules 2α and 2β promote the abundance of voltage-gated Ca v 1.3 Ca^{2+} channels at hair cell active zones. Proc. Natl. Acad. Sci. *112*, 201417207.

Kanai, Y., Dohmae, N., and Hirokawa, N. (2004). Kinesin transports RNA: Isolation and characterization of an RNA-transporting granule. Neuron *43*, 513–525.

Kasai, H., Takahashi, N., and Tokumaru, H. (2012). Distinct Initial SNARE Configurations Underlying the Diversity of Exocytosis. Physiol. Rev. *92*, 1915–1964.

Kaufmann, N., DeProto, J., Ranjan, R., Wan, H., and Van Vactor, D. (2002). Drosophila liprin-α and the receptor phosphatase Dlar control synapse morphogenesis. Neuron *34*, 27–38.

Kawasaki, F., Zou, B., Xu, X., and Ordway, R.W. (2004). Active zone localization of presynaptic calcium channels encoded by the cacophony locus of Drosophila. J. Neurosci. *24*, 282–285.

Keino-Masu, K., Masu, M., Hinck, L., Leonardo, E.D., Chan, S.S.Y., Culotti, J.G., and Tessier-Lavigne, M. (1996). Deleted in Colorectal Cancer (DCC) encodes a netrin receptor. Cell *87*, 175–185.

Kern, J. V, Zhang, Y. V, Kramer, S., Brenman, J.E., and Rasse, T.M. (2013). The kinesin-3, unc-104 regulates dendrite morphogenesis and synaptic development in Drosophila. Genetics *195*, 59–72.

Kiebler, M.A., and Bassell, G.J. (2006). Neuronal RNA Granules: Movers and Makers. Neuron *51*, 685–690.

Kim, H.-J., Raphael, A.R., LaDow, E.S., McGurk, L., Weber, R.A., Trojanowski, J.Q., Lee, V.M.-Y., Finkbeiner, S., Gitler, A.D., and Bonini, N.M. (2013a). Therapeutic modulation of eIF2α phosphorylation rescues TDP-43 toxicity in amyotrophic lateral sclerosis disease models. Nat. Genet. *46*, 152–160.

Kim, J.H., Wang, X., Coolon, R., and Ye, B. (2013b). Dscam Expression Levels Determine Presynaptic Arbor Sizes in Drosophila Sensory Neurons. Neuron *78*, 827–838.

Kim, S.M., Kumar, V., Lin, Y.-Q., Karunanithi, S., and Ramaswami, M. (2009). Fos and Jun potentiate individual release sites and mobilize the reserve synaptic vesicle pool at the Drosophila larval motor synapse. Proc. Natl. Acad. Sci. U. S. A. *106*, 4000–4005.

Klinedinst, S., Wang, X., Xiong, X., Haenfler, J.M., and Collins, C.A. (2013). Independent pathways downstream of the Wnd/DLK MAPKKK regulate synaptic structure, axonal transport, and injury signaling. J. Neurosci. *33*, 12764–12778.

Klopfenstein, D.R., and Vale, R.D. (2004). The lipid binding pleckstrin homology domain in UNC-104 kinesin is necessary for synaptic vesicle transport in Caenorhabditis elegans. Mol. Biol. Cell *15*, 3729–3739.

Kondo, M., Takei, Y., and Hirokawa, N. (2012). Motor protein KIF1A is essential for hippocampal synaptogenesis and learning enhancement in an enriched environment. Neuron *73*, 743–757.

Koon, A.C., Ashley, J., Barria, R., DasGupta, S., Brain, R., Waddell, S., Alkema, M.J., and Budnik, V. (2011). Autoregulatory and paracrine control of synaptic and behavioral plasticity by octopaminergic signaling. Nat. Neurosci. *14*, 190–199.

Koushika, S.P., Richmond, J.E., Hadwiger, G., Weimer, R.M., Jorgensen, E.M., and Nonet, M.L. (2001). A post-docking role for active zone protein Rim. Nat Neurosci *4*, 997–1005.

Kuijpers, M., van de Willige, D., Freal, A., Chazeau, A., Franker, M.A., Hofenk, J., Rodrigues, R.J.C., Kapitein, L.C., Akhmanova, A., Jaarsma, D., et al. (2016). Dynein Regulator NDEL1 Controls Polarized Cargo Transport at the Axon Initial Segment. Neuron *89*, 461–471.

Kurd, D.D., and Saxton, W.M. (1996). Kinesin mutations cause motor neuron disease phenotypes by disrupting fast axonal transport in Drosophila. Genetics *144*, 1075–1085.

Kurup, N., Yan, D., Goncharov, A., and Jin, Y. (2015). Dynamic microtubules drive circuit rewiring in the absence of neurite remodeling. Curr. Biol. *25*, 1594–1605.

Lai, T., and Garriga, G. (2004). The conserved kinase UNC-51 acts with VAB-8 and UNC-14 to regulate axon outgrowth in C. elegans. Development *131*, 5991–6000.

Lee, G.G., Kikuno, K., Nair, S., and Park, J.H. (2013). Mechanisms of postecdysis-associated programmed cell death of peptidergic neurons in drosophila melanogaster. J. Comp. Neurol. *521*,

3972–3991.

Lee, H.-K.P., Wright, A.P., and Zinn, K. (2009). Live dissection of Drosophila embryos: streamlined methods for screening mutant collections by antibody staining. J. Vis. Exp. e1647.

Lee, J.R., Shin, H., Ko, J., Choi, J., Lee, H., and Kim, E. (2003). Characterization of the movement of the kinesin motor KIF1A in living cultured neurons. J. Biol. Chem. *278*, 2624–2629.

Levy-Strumpf, N., and Culotti, J.G. (2007). VAB-8, UNC-73 and MIG-2 regulate axon polarity and cell migration functions of UNC-40 in C. elegans. Nat. Neurosci. *10*, 161–168.

Lewcock, J.W., Genoud, N., Lettieri, K., and Pfaff, S.L. (2007). The Ubiquitin Ligase Phr1 Regulates Axon Outgrowth through Modulation of Microtubule Dynamics. Neuron *56*, 604–620.

Li, L., Bischofberger, J., and Jonas, P. (2007). Differential gating and recruitment of P/Q-, N-, and R-type Ca2+ channels in hippocampal mossy fiber boutons. J. Neurosci. *27*, 13420–13429.

Li, L., Tian, X., Zhu, M., Bulgari, D., Böhme, M.A., Goettfert, F., Wichmann, C., Sigrist, S.J., Levitan, E.S., and Wu, C. (2014). Drosophila Syd-1, liprin-α, and protein phosphatase 2A B' subunit Wrd function in a linear pathway to prevent ectopic accumulation of synaptic materials in distal axons. J. Neurosci. *34*, 8474–8487.

Li, L.B., Lei, H., Arey, R.N., Li, P., Liu, J., Murphy, C.T., Xu, X.Z.S., and Shen, K. (2016). The Neuronal Kinesin UNC-104/KIF1A is a Key Regulator of Synaptic Aging and Insulin Signaling-Regulated Memory. Curr. Biol. *26*, 605–615.

Liao, E.H., Hung, W., Abrams, B., and Zhen, M. (2004). An SCF-like ubiquitin ligase complex that controls presynaptic differentiation. Nature *430*, 345–350.

Liberati, N.T., Fitzgerald, K. a, Kim, D.H., Feinbaum, R., Golenbock, D.T., and Ausubel, F.M. (2004). Requirement for a conserved Toll/interleukin-1 resistance domain protein in the Caenorhabditis elegans immune response. Proc. Natl. Acad. Sci. U. S. A. *101*, 6593–6598.

Lin, D.M., and Goodman, C.S. (1994). Ectopic and increased expression of Fasciclin II alters motoneuron growth cone guidance. Neuron *13*, 507–523.

Lindwall, C., and Kanje, M. (2005). Retrograde axonal transport of JNK signaling molecules influence injury induced nuclear changes in p-c-Jun and ATF3 in adult rat sensory neurons. Mol. Cell. Neurosci. *29*, 269–282.

Liu, K.S.Y., Siebert, M., Mertel, S., Knoche, E., Wegener, S., Wichmann, C., Matkovic, T., Muhammad, K., Depner, H., Mettke, C., et al. (2011). RIM-binding protein, a central part of the active zone, is essential for neurotransmitter release. Science (80-.). *334*, 1565–1569.

Liu, Y., Schirra, C., Stevens, D.R., Matti, U., Speidel, D., Hof, D., Bruns, D., Brose, N., and Rettig, J. (2008). CAPS facilitates filling of the rapidly releasable pool of large dense-core vesicles. J. Neurosci. *28*, 5594–5601.

Loveall, B.J., and Deitcher, D.L. (2010). The essential role of bursicon during Drosophila development. BMC Dev. Biol. *10*, 92.

Lubińska, L. (1977). Early course of wallerian degeneration in myelinated fibres of the rat phrenic nerve. Brain Res. *130*, 47–63.

Lyons, D. a, Naylor, S.G., Scholze, A., and Talbot, W.S. (2009). Kif1b is essential for mRNA localization in oligodendrocytes and development of myelinated axons. Nat. Genet. *41*, 854–858.

Ma, Q.-L., Zuo, X., Yang, F., Ubeda, O.J., Gant, D.J., Alaverdyan, M., Kiosea, N.C., Nazari, S.,

Chen, P.P., Nothias, F., et al. (2014). Loss of MAP function leads to hippocampal synapse loss and deficits in the Morris Water Maze with aging. J. Neurosci. *34*, 7124–7136.

Maas, C., Torres, V.I., Altrock, W.D., Leal-Ortiz, S., Wagh, D., Terry-Lorenzo, R.T., Fejtova, A., Gundelfinger, E.D., Ziv, N.E., and Garner, C.C. (2012). Formation of Golgi-Derived Active Zone Precursor Vesicles. J. Neurosci. *32*, 11095–11108.

MacDonald, J.M., Beach, M.G., Porpiglia, E., Sheehan, A.E., Watts, R.J., and Freeman, M.R. (2006). The Drosophila cell corpse engulfment receptor Draper mediates glial clearance of severed axons. Neuron *50*, 869–881.

Mackler, J.M., Drummond, J. a, Loewen, C. a, Robinson, I.M., and Reist, N.E. (2002). The C(2)B Ca(2+)-binding motif of synaptotagmin is required for synaptic transmission in vivo. Nature *418*, 340–344.

Maeder, C.I., Shen, K., and Hoogenraad, C.C. (2014). Axon and dendritic trafficking. Curr. Opin. Neurobiol. *27*, 165–170.

Mahr, A., and Aberle, H. (2006). The expression pattern of the Drosophila vesicular glutamate transporter: a marker protein for motoneurons and glutamatergic centers in the brain. Gene Expr. Patterns *6*, 299–309.

Marcette, J.D., Chen, J.J., and Nonet, M.L. (2014). The Caenorhabditis elegans microtubule minus-end binding homolog PTRN-1 stabilizes synapses and neurites. Elife *3*, e01637.

Marmor-Kollet, N., and Schuldiner, O. (2016). Contrasting developmental axon regrowth and neurite sprouting of Drosophila mushroom body neurons reveals shared and unique molecular mechanisms. Dev. Neurobiol. *76*, 262–276.

Martin, M., Iyadurai, S.J., Gassman, A., Gindhart, J.G., Hays, T.S., and Saxton, W.M. (1999). Cytoplasmic dynein, the dynactin complex, and kinesin are interdependent and essential for fast axonal transport. Mol. Biol. Cell *10*, 3717–3728.

Martín-Blanco, E., Gampel, A., Ring, J., Virdee, K., Kirov, N., Tolkovsky, A.M., and Martinez-Arias, A. (1998). puckered encodes a phosphatase that mediates a feedback loop regulating JNK activity during dorsal closure in Drosophila. Genes Dev. *12*, 557–670.

Massaro, C.M., Pielage, J., and Davis, G.W. (2009). Molecular mechanisms that enhance synapse stability despite persistent disruption of the spectrin/ankyrin/microtubule cytoskeleton. J. Cell Biol. *187*, 101–117.

Matta, J.A., Ashby, M.C., Sanz-Clemente, A., Roche, K.W., and Isaac, J.T.R. (2011). MGluR5 and NMDA Receptors Drive the Experience- and Activity-Dependent NMDA Receptor NR2B to NR2A Subunit Switch. Neuron *70*, 339–351.

McMahon, S.A., and Díaz, E. (2011). Mechanisms of excitatory synapse maturation by trans-synaptic organizing complexes. Curr. Opin. Neurobiol. *21*, 221–227.

Medina, P.M.B., Swick, L.L., Andersen, R., Blalock, Z., and Brenman, J.E. (2006). A novel forward genetic screen for identifying mutations affecting larval neuronal dendrite development in Drosophila melanogaster. Genetics *172*, 2325–2335.

Menon, K.P., Carrillo, R.A., and Zinn, K. (2013). Development and plasticity of the Drosophila larval neuromuscular junction. Wiley Interdiscip. Rev. Dev. Biol. *2*, 647–670.

Milde, S., Gilley, J., and Coleman, M.P. (2013). Subcellular Localization Determines the Stability and Axon Protective Capacity of Axon Survival Factor Nmnat2. PLoS Biol. *11*.

Millecamps, S., and Julien, J.-P. (2013). Axonal transport deficits and neurodegenerative diseases. Nat. Rev. Neurosci. *14*, 161–176.

Miller, B.R., Press, C., Daniels, R.W., Sasaki, Y., Milbrandt, J., and DiAntonio, A. (2009). A dual leucine kinase-dependent axon self-destruction program promotes Wallerian degeneration. Nat. Neurosci. *12*, 387–389.

Miller, K.E., DeProto, J., Kaufmann, N., Patel, B.N., Duckworth, A., and Van Vactor, D. (2005). Direct observation demonstrates that Liprin-alpha is required for trafficking of synaptic vesicles. Curr. Biol. *15*, 684–689.

Moechars, D., Weston, M.C., Leo, S., Callaerts-Végh, Z., Goris, I., Daneels, G., Buist, A., Cik, M., van der Spek, P., Kass, S., et al. (2006). Vesicular glutamate transporter VGLUT2 expression levels control quantal size and neuropathic pain. J. Neurosci. *26*, 12055–12066.

Morfini, G., Pigino, G., Szebenyi, G., You, Y., Pollema, S., and Brady, S.T. (2006). JNK mediates pathogenic effects of polyglutamine-expanded androgen receptor on fast axonal transport. Nat. Neurosci. *9*, 907–916.

Morgan, J.I., and Curran, T. (1991). Stimulus-transcription coupling in the nervous system: involvement of the inducible proto-oncogenes fos and jun. Annu. Rev. Neurosci. *14*, 421–451.

Muller, K.J., and Carbonetto, S. (1979). The morphological and physiological properties of a regenerating synapse in the C.N.S. of the leech. J. Comp. Neurol. *185*, 485–516.

Nadeau, S., Hein, P., Fernandes, K.J.L., Peterson, A.C., and Miller, F.D. (2005). A transcriptional role for C/EBP β in the neuronal response to axonal injury. Mol. Cell. Neurosci. *29*, 525–535.

Nakata, K., Abrams, B., Grill, B., Goncharov, A., Huang, X., Chisholm, A.D., and Jin, Y. (2005). Regulation of a DLK-1 and p38 MAP kinase pathway by the ubiquitin ligase RPM-1 is required for presynaptic development. Cell *120*, 407–420.

Nässel, D.R., and Winther, Å.M.E. (2010). Drosophila neuropeptides in regulation of physiology and behavior. Prog. Neurobiol. *92*, 42–104.

Neumann, B., Nguyen, K.C.Q., Hall, D.H., Ben-Yakar, A., and Hilliard, M.A. (2011). Axonal regeneration proceeds through specific axonal fusion in transected C. elegans neurons. Dev. Dyn. *240*, 1365–1372.

Nguyen, Q.T., Sanes, J.R., and Lichtman, J.W. (2002). Pre-existing pathways promote precise projection patterns. Nat. Neurosci. *5*, 861–867.

Nichols, A.L.A., Meelkop, E., Linton, C., Giordano-Santini, R., Sullivan, R.K., Donato, A., Nolan, C., Hall, D.H., Xue, D., Neumann, B., et al. (2016). The Apoptotic Engulfment Machinery Regulates Axonal Degeneration in C. elegans Neurons. Cell Rep. *14*, 1673–1683.

Niwa, S., Tanaka, Y., and Hirokawa, N. (2008). KIF1Bbeta- and KIF1A-mediated axonal transport of presynaptic regulator Rab3 occurs in a GTP-dependent manner through DENN/MADD. Nat. Cell Biol. *10*, 1269–1279.

Niwa, S., Lipton, D.M.M., Morikawa, M., Zhao, C., Hirokawa, N., Lu, H., and Shen, K. (2015). Autoinhibition of a Neuronal Kinesin UNC-104/KIF1A Regulates the Size and Density of Synapses. Cell Rep.

Okada, Y., Yamazaki, H., Sekine-Aizawa, Y., and Hirokawa, N. (1995). The neuron-specific kinesin superfamily protein KIF1A is a unique monomeric motor for anterograde axonal

transport of synaptic vesicle precursors. Cell *81*, 769–780.

Oslowski, C.M., and Urano, F. (2011). Measuring ER stress and the unfolded protein response using mammalian tissue culture system. Methods Enzymol. *490*, 71–92.

Osterloh, J.M., Yang, J., Rooney, T.M., Fox, a. N., Adalbert, R., Powell, E.H., Sheehan, a. E., Avery, M. a., Hackett, R., Logan, M. a., et al. (2012). dSarm/Sarm1 Is Required for Activation of an Injury-Induced Axon Death Pathway. Science (80-.). *337*, 481–484.

Otsuka, A.J., Jeyaprakash, A., Garcia-Anoveros, J., Tang, L.Z., Fisk, G., Hartshorne, T., Franco, R., and Born, T. (1991). The C. elegans unc-104 gene encodes a putative kinesin heavy chain-like protein. Neuron *6*, 113–122.

Owald, D., Fouquet, W., Schmidt, M., Wichmann, C., Mertel, S., Depner, H., Christiansen, F., Zube, C., Quentin, C., Körner, J., et al. (2010). A Syd-1 homologue regulates pre- and postsynaptic maturation in Drosophila. J. Cell Biol. *188*, 565–579.

Owald, D., Khorramshahi, O., Gupta, V.K., Banovic, D., Depner, H., Fouquet, W., Wichmann, C., Mertel, S., Eimer, S., Reynolds, E., et al. (2012). Cooperation of Syd-1 with Neurexin synchronizes pre- with postsynaptic assembly. Nat. Neurosci. *15*, 1219–1226.

Owlarn, S., and Bartscherer, K. (2016). Go ahead, grow a head! A planarian's guide to anterior regeneration. Regeneration *3*, 139–155.

Pack-Chung, E., Kurshan, P.T., Dickman, D.K., and Schwarz, T.L. (2007). A Drosophila kinesin required for synaptic bouton formation and synaptic vesicle transport. Nat. Neurosci. *10*, 980–989.

Pakos-Zebrucka, K., Koryga, I., Mnich, K., Ljujic, M., Samali, A., Gorman, A.M., Ron, D., Harding, H., Zhang, Y., Zeng, H., et al. (2016). The integrated stress response. EMBO Rep. *17*, 1374–1395.

Park, E.C., Glodowski, D.R., and Rongo, C. (2009). The ubiquitin ligase RPM-1 and the p38 MAPK PMK-3 regulate AMPA receptor trafficking. PLoS One *4*.

Park, M., Watanabe, S., Poon, V.Y.N., Ou, C.-Y., Jorgensen, E.M., and Shen, K. (2011). CYY-1/cyclin Y and CDK-5 differentially regulate synapse elimination and formation for rewiring neural circuits. Neuron *70*, 742–757.

Peabody, N.C., Diao, F., Luan, H., Wang, H., Dewey, E.M., Honegger, H.-W., and White, B.H. (2008). Bursicon functions within the Drosophila CNS to modulate wing expansion behavior, hormone secretion, and cell death. J. Neurosci. *28*, 14379–14391.

Perlson, E., Hanz, S., Ben-Yaakov, K., Segal-Ruder, Y., Seger, R., and Fainzilber, M. (2005). Vimentin-dependent spatial translocation of an activated MAP kinase in injured nerve. Neuron *45*, 715–726.

Petralia, R.S., Sans, N., Wang, Y.X., and Wenthold, R.J. (2005). Ontogeny of postsynaptic density proteins at glutamatergic synapses. Mol. Cell. Neurosci. *29*, 436–452.

Petzoldt, A.G., and Sigrist, S.J. (2014a). Synaptogenesis. Curr. Biol. *24*, R1076–R1080.

Petzoldt, A.G., and Sigrist, S.J. (2014b). Synaptogenesis. Curr. Biol. *24*, R1076–R1080.

Pielage, J., Fetter, R.D., and Davis, G.W. (2005). Presynaptic spectrin is essential for synapse stabilization. Curr. Biol. *15*, 918–928.

Pierre, S.C., Häusler, J., Birod, K., Geisslinger, G., and Scholich, K. (2004). PAM mediates sustained inhibition of cAMP signaling by sphingosine-1-phosphate. EMBO J. *23*, 3031–3040.

Pinan-Lucarre, B., Gabel, C. V., Reina, C.P., Hulme, S.E., Shevkoplyas, S.S., Slone, R.D., Xue, J., Qiao, Y., Weisberg, S., Roodhouse, K., et al. (2012). The core apoptotic executioner proteins CED-3 and CED-4 promote initiation of neuronal regeneration in caenorhabditis elegans. PLoS Biol. *10*.

Pozniak, C.D., Sengupta Ghosh, A., Gogineni, A., Hanson, J.E., Lee, S.-H., Larson, J.L., Solanoy, H., Bustos, D., Li, H., Ngu, H., et al. (2013). Dual leucine zipper kinase is required for excitotoxicity-induced neuronal degeneration. J. Exp. Med. *210*, 2553–2567.

Rallis, A., Lu, B., and Ng, J. (2013). Molecular chaperones protect against JNK- and Nmnat-regulated axon degeneration in Drosophila. J. Cell Sci. *126*, 838–849.

Renden, R., Berwin, B., Davis, W., Ann, K., Chin, C.T., Kreber, R., Ganetzky, B., Martin, T.F.J., and Broadie, K. (2001). Drosophila CAPS is an essential gene that regulates dense-core vesicle release and synaptic vesicle fusion. Neuron *31*, 421–437.

Richardson, C.E., Spilker, K.A., Cueva, J.G., Perrino, J., Goodman, M.B., and Shen, K. (2014). PTRN-1, a microtubule minus end-binding CAMSAP homolog, promotes microtubule function in Caenorhabditis elegans neurons. Elife *3*, e01498.

Richmond, J.E., Davis, W.S., and Jorgensen, E.M. (1999). UNC-13 is required for synaptic vesicle fusion in C. elegans. Nat. Neurosci. *2*, 959–964.

Rishal, I., and Fainzilber, M. (2014). Axon-soma communication in neuronal injury. Nat Rev Neurosci *15*, 32–42.

Ritzenthaler, S., Suzuki, E., and Chiba, A. (2000). Postsynaptic filopodia in muscle cells interact with innervating motoneuron axons. Nat. Neurosci. *3*, 1012–1017.

Rivire, J.B., Ramalingam, S., Lavastre, V., Shekarabi, M., Holbert, S., Lafontaine, J., Srour, M., Merner, N., Rochefort, D., Hince, P., et al. (2011). KIF1A, an axonal transporter of synaptic vesicles, is mutated in hereditary sensory and autonomic neuropathy type 2. Am. J. Hum. Genet. *89*, 219–301.

Rizo, J., and Xu, J. (2015). The Synaptic Vesicle Release Machinery. Annu. Rev. Biophys. *44*, 339–367.

Rosenberg, T., Gal-Ben-Ari, S., Dieterich, D.C., Kreutz, M.R., Ziv, N.E., Gundelfinger, E.D., and Rosenblum, K. (2014). The roles of protein expression in synaptic plasticity and memory consolidation. Front. Mol. Neurosci. *7*, 86.

Ruan, K., Zhu, Y., Li, C., Brazill, J.M., and Zhai, R.G. (2015). Alternative splicing of Drosophila Nmnat functions as a switch to enhance neuroprotection under stress. Nat. Commun. *6*, 10057.

Ruggiano, A., Foresti, O., and Carvalho, P. (2014). Quality control: ER-associated degradation: protein quality control and beyond. J. Cell Biol. *204*, 869–879.

Ryoo, H.D. (2015). Drosophila as a model for unfolded protein response research. BMB Rep. *48*, 445–453.

Ryoo, H.D., Domingos, P.M., Kang, M.-J., and Steller, H. (2007). Unfolded protein response in a Drosophila model for retinal degeneration. EMBO J. *26*, 242–252.

Sadakata, T., Shinoda, Y., Sekine, Y., Saruta, C., Itakura, M., Takahashi, M., and Furuichi, T. (2010). Interaction of Calcium-dependent Activator Protein for Secretion 1 (CAPS1) with the class II ADP-ribosylation factor small GTPases is required for dense-core vesicle trafficking in the trans-Golgi network. J. Biol. Chem. *285*, 38710–38719.

Sadakata, T., Kakegawa, W., Shinoda, Y., Hosono, M., Katoh-Semba, R., Sekine, Y., Sato, Y., Tanaka, M., Iwasato, T., Itohara, S., et al. (2013). CAPS1 Deficiency Perturbs Dense-Core Vesicle Trafficking and Golgi Structure and Reduces Presynaptic Release Probability in the Mouse Brain. J. Neurosci. *33*, 17326–17334.

Saiga, T., Fukuda, T., Matsumoto, M., Tada, H., Okano, H.J., Okano, H., and Nakayama, K.I. (2009). Fbxo45 forms a novel ubiquitin ligase complex and is required for neuronal development. Mol. Cell. Biol. *29*, 3529–3543.

Sans, N., Petralia, R.S., Wang, Y.X., Blahos, J., Hell, J.W., and Wenthold, R.J. (2000). A developmental change in NMDA receptor-associated proteins at hippocampal synapses. J. Neurosci. *20*, 1260–1271.

Sasaki, Y., Vohra, B.P.S., Baloh, R.H., and Milbrandt, J. (2009a). Transgenic mice expressing the Nmnat1 protein manifest robust delay in axonal degeneration in vivo. J. Neurosci. *29*, 6526–6534.

Sasaki, Y., Vohra, B.P.S., Lund, F.E., and Milbrandt, J. (2009b). Nicotinamide mononucleotide adenylyl transferase-mediated axonal protection requires enzymatic activity but not increased levels of neuronal nicotinamide adenine dinucleotide. J. Neurosci. *29*, 5525–5535.

Sasaki, Y., Margolin, Z., Borgo, B., Havranek, J.J., and Milbrandt, J. (2015). Characterization of Leber congenital amaurosis-associated NMNAT1 mutants. J. Biol. Chem. *290*, 17228–17238.

Saxena, S., and Caroni, P. (2007). Mechanisms of axon degeneration: From development to disease. Prog. Neurobiol. *83*, 174–191.

Schaefer, A.M., Hadwiger, G.D., and Nonet, M.L. (2000). rpm-1, A Conserved Neuronal Gene that Regulates Targeting and Synaptogenesis in C. elegans. Neuron *26*, 345–356.

Schaefer, A.W., Schoonderwoert, V.T.G., Ji, L., Mederios, N., Danuser, G., and Forscher, P. (2008). Coordination of Actin Filament and Microtubule Dynamics during Neurite Outgrowth. Dev. Cell *15*, 146–162.

Schaefer, M.K.E., Schmalbruch, H., Buhler, E., Lopez, C., Martin, N., Guénet, J.-L., and Haase, G. (2007). Progressive motor neuronopathy: a critical role of the tubulin chaperone TBCE in axonal tubulin routing from the Golgi apparatus. J. Neurosci. *27*, 8779–8789.

Scheib, J., and Höke, A. (2013). Advances in peripheral nerve regeneration. Nat. Rev. Neurol. *9*, 668–676.

Schmied, R., and Ambron, R.T. (1997). A nuclear localization signal targets proteins to the retrograde transport system, thereby evading uptake into organelles in aplysia axons. J. Neurobiol. *33*, 151–160.

Schmied, R., Huang, C.C., Zhang, X.P., Ambron, D. a, and Ambron, R.T. (1993). Endogenous axoplasmic proteins and proteins containing nuclear localization signal sequences use the retrograde axonal transport/nuclear import pathway in Aplysia neurons. J. Neurosci. *13*, 4064–4071.

Scholich, K., Pierre, S., and Patel, T.B. (2001). Protein Associated with Myc (PAM) Is a Potent Inhibitor of Adenylyl Cyclases. J. Biol. Chem. *276*, 47583–47589.

Sclip, A., Tozzi, A., Abaza, A., Cardinetti, D., Colombo, I., Calabresi, P., Salmona, M., Welker, E., and Borsello, T. (2014). c-Jun N-terminal kinase has a key role in Alzheimer disease synaptic dysfunction in vivo. Cell Death Dis. *5*, e1019.

Shapira, M., Zhai, R.G., Dresbach, T., Bresler, T., Torres, V.I., Gundelfinger, E.D., Ziv, N.E., and Garner, C.C. (2003). Unitary assembly of presynaptic active zones from Piccolo-Bassoon transport vesicles. Neuron *38*, 237–252.

Shen, W., and Ganetzky, B. (2009). Autophagy promotes synapse development in Drosophila. J. Cell Biol. *187*, 71–79.

Sheng, M., and Kim, E. (2011). The postsynaptic organization of synapses. Cold Spring Harb. Perspect. Biol. *3*.

Shepherd, J.D., and Huganir, R.L. (2007). The cell biology of synaptic plasticity: AMPA receptor trafficking. Annu. Rev. Cell Dev. Biol. *23*, 613–643.

Shin, H., Wyszynski, M., Huh, K.-H.H., Valtschanoff, J.G., Lee, J.-R.R., Ko, J., Streuli, M., Weinberg, R.J., Sheng, M., and Kim, E. (2003). Association of the kinesin motor KIF1A with the multimodular protein liprin-?? J. Biol. Chem. *278*, 11393–11401.

Shin, J.E., Cho, Y., Beirowski, B., Milbrandt, J., Cavalli, V., and DiAntonio, A. (2012). Dual Leucine Zipper Kinase Is Required for Retrograde Injury Signaling and Axonal Regeneration. Neuron *74*, 1015–1022.

Siebert, M., Bohme, M.A., Driller, J.H., Babikir, H., Mampell, M.M., Rey, U., Ramesh, N., Matkovic, T., Holton, N., Reddy-Alla, S., et al. (2015). A high affinity RIM-binding protein/Aplip1 interaction prevents the formation of ectopic axonal active zones. Elife *4*.

Skouras, E., Ozsoy, U., Sarikcioglu, L., and Angelov, D.N. (2011). Intrinsic and therapeutic factors determining the recovery of motor function after peripheral nerve transection. Ann. Anat. *193*, 286–303.

Sone, M., Zeng, X., Larese, J., and Ryoo, H.D. (2013). A modified UPR stress sensing system reveals a novel tissue distribution of IRE1/XBP1 activity during normal Drosophila development. Cell Stress Chaperones *18*, 307–319.

Song, Y., Ori-McKenney, K.M., Zheng, Y., Han, C., Jan, L.Y., and Jan, Y.N. (2012). Regeneration of Drosophila sensory neuron axons and dendrites is regulated by the Akt pathway involving Pten and microRNA bantam. Genes Dev. *26*, 1612–1625.

Spangler, S.A., Schmitz, S.K., Kevenaar, J.T., De Graaff, E., De Wit, H., Demmers, J., Toonen, R.F., and Hoogenraad, C.C. (2013). Liprin-??2 promotes the presynaptic recruitment and turnover of RIM1/CASK to facilitate synaptic transmission. J. Cell Biol. *201*, 915–928.

Speese, S.D., Trotta, N., Rodesch, C.K., Aravamudan, B., and Broadie, K. (2003). The ubiquitin proteasome system acutely regulates presynaptic protein turnover and synaptic efficacy. Curr. Biol. *13*, 899–910.

Spira, M.E., Benbassat, D., and Dormann, a (1993). Resealing of the proximal and distal cut ends of transected axons: electrophysiological and ultrastructural analysis. J. Neurobiol. *24*, 300–316.

Spira, M.E., Oren, R., Dormann, A., and Gitler, D. (2003). Critical calpain-dependent ultrastructural alterations underlie the transformation of an axonal segment into a growth cone after axotomy of cultured Aplysia neurons. J. Comp. Neurol. *457*, 293–312.

Spradling, A.C., Stern, D., Beaton, A., Rhem, E.J., Laverty, T., Mozden, N., Misra, S., and Rubin, G.M. (1999). The Berkeley Drosophila Genome Project gene disruption project: Single P-element insertions mutating 25% of vital Drosophila genes. Genetics *153*, 135–177.

Stagi, M., Gorlovoy, P., Larionov, S., Takahashi, K., and Neumann, H. (2006). Unloading kinesin transported cargoes from the tubulin track via the inflammatory c-Jun N-terminal kinase pathway. FASEB J. *20*, 2573–2575.

Stanley, R.E., Ragusa, M.J., and Hurley, J.H. (2014). The beginning of the end: how scaffolds nucleate autophagosome biogenesis. Trends Cell Biol. *24*, 73–81.

Stavoe, A.K.H., Hill, S.E., Hall, D.H., and Colón-Ramos, D.A. (2016). KIF1A/UNC-104 Transports ATG-9 to Regulate Neurodevelopment and Autophagy at Synapses. Dev. Cell *38*, 171–185.

Stewart, B.A., Atwood, H.L., Renger, J.J., Wang, J., and Wu, C.-F. (1994). Improved stability of Drosophila larval neuromuscular preparations in haemolymph-like physiological solutions. J. Comp. Physiol. A *175*, 179–191.

Strautman, A.F., Cork, R.J., and Robinson, K.R. (1990). The distribution of free calcium in transected spinal axons and its modulation by applied electrical fields. J. Neurosci. *10*, 3564–3575.

Su, Q., Cai, Q., Gerwin, C., Smith, C.L., and Sheng, Z.-H. (2004). Syntabulin is a microtubule-associated protein implicated in syntaxin transport in neurons. Nat. Cell Biol. *6*, 941–953.

Südhof, T.C. (2012). The presynaptic active zone. Neuron *75*, 11–25.

Südhof, T.C., and Rothman, J.E. (2009). Membrane fusion: grappling with SNARE and SM proteins. Science *323*, 474–477.

Sugie, A., Hakeda-Suzuki, S., Suzuki, E., Silies, M., Shimozono, M., Möhl, C., Suzuki, T., and Tavosanis, G. (2015). Molecular Remodeling of the Presynaptic Active Zone of Drosophila Photoreceptors via Activity-Dependent Feedback. Neuron *86*, 711–726.

Summers, D.W., Gibson, D.A., DiAntonio, A., and Milbrandt, J. (2016). SARM1-specific motifs in the TIR domain enable NAD+ loss and regulate injury-induced SARM1 activation. Proc. Natl. Acad. Sci. U. S. A. 201601506.

Sun, F., Zhu, C., Dixit, R., and Cavalli, V. (2011). Sunday Driver/JIP3 binds kinesin heavy chain directly and enhances its motility. EMBO J. *30*, 3416–3429.

Sung, Y.J., Povelones, M., and Ambron, R.T. (2001). Risk-1: A novel MAPK homologue in axoplasm that is activated and retrogradely transported after nerve injury. J. Neurobiol. *47*, 67–79.

Sung, Y.-J., Walters, E.T., and Ambron, R.T. (2004). A neuronal isoform of protein kinase G couples mitogen-activated protein kinase nuclear import to axotomy-induced long-term hyperexcitability in Aplysia sensory neurons. J. Neurosci. *24*, 7583–7595.

Tandon, A., Bannykh, S., Kowalchyk, J.A., Banerjee, A., Martin, T.F.J., and Balch, W.E. (1998). Differential regulation of exocytosis by calcium and CAPS in semi- intact synaptosomes. Neuron *21*, 147–154.

Tao-Cheng, J.H. (2007). Ultrastructural localization of active zone and synaptic vesicle proteins in a preassembled multi-vesicle transport aggregate. Neuroscience *150*, 575–584.

Tedeschi, A., and Bradke, F. (2013). The DLK signalling pathway--a double-edged sword in neural development and regeneration. EMBO Rep. *14*, 605–614.

Tedeschi, A., Dupraz, S., Laskowski, C.J., Xue, J., Ulas, T., Beyer, M., Schultze, J.L., and Bradke, F. (2016). The Calcium Channel Subunit Alpha2delta2 Suppresses Axon Regeneration

in the Adult CNS. Neuron *92*, 419–434.

Tessier-Lavigne, M., and Goodman, C.S. (1996). The Molecular Biology of Axon Guidance. Science (80-.). *274*, 1123–1133.

Thibault, S.T., Singer, M.A., Miyazaki, W.Y., Milash, B., Dompe, N.A., Singh, C.M., Buchholz, R., Demsky, M., Fawcett, R., Francis-Lang, H.L., et al. (2004). A complementary transposon tool kit for Drosophila melanogaster using P and piggyBac. Nat. Genet. *36*, 283–287.

Thummel, C.S., Boulet, A.M., and Lipshitz, H.D. (1988). Vectors for Drosophila P-element-mediated transformation and tissue culture transfection. Gene *74*, 445–456.

Toda, H., Mochizuki, H., Flores, R., Josowitz, R., Krasieva, T.B., LaMorte, V.J., Suzuki, E., Gindhart, J.G., Furukubo-Tokunaga, K., and Tomoda, T. (2008). UNC-51/ATG1 kinase regulates axonal transport by mediating motor-cargo assembly. Genes Dev. *22*, 3292–3307.

Tom, V.J., Steinmetz, M.P., Miller, J.H., Doller, C.M., and Silver, J. (2004). Studies on the development and behavior of the dystrophic growth cone, the hallmark of regeneration failure, in an in vitro model of the glial scar and after spinal cord injury. J. Neurosci. *24*, 6531–6539.

Torres, C.A., and Sulzer, D. (2012). Macroautophagy can press a brake on presynaptic neurotransmission. Autophagy *8*, 1540–1541.

Urano, F. (2000). Coupling of Stress in the ER to Activation of JNK Protein Kinases by Transmembrane Protein Kinase IRE1. Science (80-.). *287*, 664–666.

Valakh, V., Walker, L.J., Skeath, J.B., and DiAntonio, A. (2013). Loss of the spectraplakin short stop activates the DLK injury response pathway in Drosophila. J. Neurosci. *33*, 17863–17873.

Valakh, V., Frey, E., Babetto, E., Walker, L.J., and DiAntonio, A. (2015). Cytoskeletal disruption activates the DLK/JNK pathway, which promotes axonal regeneration and mimics a preconditioning injury. Neurobiol. Dis. *77*, 13–25.

Venken, K.J.T., Schulze, K.L., Haelterman, N.A., Pan, H., He, Y., Evans-Holm, M., Carlson, J.W., Levis, R.W., Spradling, A.C., Hoskins, R.A., et al. (2011). MiMIC: a highly versatile transposon insertion resource for engineering Drosophila melanogaster genes. Nat. Methods *8*, 737–743.

Verhage, M., Maia, A.S., Plomp, J.J., Brussaard, A.B., Heeroma, J.H., Vermeer, H., Toonen, R.F., Hammer, R.E., van den Berg, T.K., Missler, M., et al. (2000). Synaptic assembly of the brain in the absence of neurotransmitter secretion. Science (80-.). *287*, 864–869.

Verhey, K.J., and Hammond, J.W. (2009). Traffic control: regulation of kinesin motors. Nat. Rev. Mol. Cell Biol. *10*, 765–777.

Verhey, K.J., Meyer, D., Deehan, R., Blenis, J., Schnapp, B.J., Rapoport, T.A., and Margolis, B. (2001). Cargo of kinesin identified as JIP scaffolding proteins and associated signaling molecules. J. Cell Biol. *152*, 959–970.

Vérièpe, J., Fossouo, L., and Parker, J.A. (2015). Neurodegeneration in C. elegans models of ALS requires TIR-1/Sarm1 immune pathway activation in neurons. Nat. Commun. *6*, 7319.

Voelzmann, A., Okenve-Ramos, P., Qu, Y., Chojnowska-Monga, M., Del Caño-Espinel, M., Prokop, A., and Sanchez-Soriano, N. (2016). Tau and spectraplakins promote synapse formation and maintenance through Jun kinase and neuronal trafficking. Elife *5*.

Volk, L., Chiu, S.-L., Sharma, K., and Huganir, R.L. (2015). Glutamate Synapses in Human Cognitive Disorders. Annu. Rev. Neurosci. *38*, 127–149.

Vömel, M., and Wegener, C. (2007). Neurotransmitter-induced changes in the intracellular calcium concentration suggest a differential central modulation of CCAP neuron subsets in Drosophila. Dev. Neurobiol. *67*, 792–808.

Vömel, M., and Wegener, C. (2008). Neuroarchitecture of aminergic systems in the larval ventral ganglion of Drosophila melanogaster. PLoS One *3*.

Wagner, O.I., Esposito, A., Köhler, B., Chen, C.-W.W., Shen, C.-P.P., Wu, G.-H.H., Butkevich, E., Mandalapu, S., Wenzel, D., Wouters, F.S., et al. (2009). Synaptic scaffolding protein SYD-2 clusters and activates kinesin-3 UNC-104 in C. elegans. Proc. Natl. Acad. Sci. U. S. A. *106*, 19605–19610.

Wairkar, Y.P., Toda, H., Mochizuki, H., Furukubo-Tokunaga, K., Tomoda, T., and Diantonio, A. (2009). Unc-51 controls active zone density and protein composition by downregulating ERK signaling. J. Neurosci. *29*, 517–528.

Waites, C.L., Leal-Ortiz, S. a, Okerlund, N., Dalke, H., Fejtova, A., Altrock, W.D., Gundelfinger, E.D., and Garner, C.C. (2013). Bassoon and Piccolo maintain synapse integrity by regulating protein ubiquitination and degradation. EMBO J. *32*, 954–969.

Wan, H.I., DiAntonio, A., Fetter, R.D., Bergstrom, K., Strauss, R., and Goodman, C.S. (2000). Highwire Regulates Synaptic Growth in Drosophila. Neuron *26*, 313–329.

Wang, X., Kim, J.H., Bazzi, M., Robinson, S., Collins, C.A., and Ye, B. (2013). Bimodal Control of Dendritic and Axonal Growth by the Dual Leucine Zipper Kinase Pathway. PLoS Biol. *11*.

Wang, Y., Okamoto, M., Schmitz, F., Hofmann, K., and Südhof, T.C. (1997). Rim is a putative Rab3 effector in regulating synaptic-vesicle fusion. Nature *388*, 593–598.

Watari-Goshima, N., Ogura, K.-I., Wolf, F.W., Goshima, Y., and Garriga, G. (2007). C. elegans VAB-8 and UNC-73 regulate the SAX-3 receptor to direct cell and growth-cone migrations. Nat. Neurosci. *10*, 169–176.

Watkins, T.A., Wang, B., Huntwork-Rodriguez, S., Yang, J., Jiang, Z., Eastham-Anderson, J., Modrusan, Z., Kaminker, J.S., Tessier-Lavigne, M., and Lewcock, J.W. (2013). DLK initiates a transcriptional program that couples apoptotic and regenerative responses to axonal injury. Proc. Natl. Acad. Sci. U. S. A. *110*, 4039–4044.

Waung, M.W., and Huber, K.M. (2009). Protein translation in synaptic plasticity: mGluR-LTD, Fragile X. Curr. Opin. Neurobiol. *19*, 319–326.

Weber, U., Paricio, N., and Mlodzik, M. (2000). Jun mediates Frizzled-induced R3/R4 cell fate distinction and planar polarity determination in the Drosophila eye. Development *127*, 3619–3629.

Welsbie, D.S., Yang, Z., Ge, Y., Mitchell, K.L., Zhou, X., Martin, S.E., Berlinicke, C.A., Hackler, L., Fuller, J., Fu, J., et al. (2013). Functional genomic screening identifies dual leucine zipper kinase as a key mediator of retinal ganglion cell death. Proc. Natl. Acad. Sci. U. S. A. *110*, 4045–4050.

Wen, Y., Parrish, J.Z., He, R., Zhai, R.G., and Kim, M.D. (2011). Nmnat exerts neuroprotective effects in dendrites and axons. Mol. Cell. Neurosci. *48*, 1–8.

White, J.G., Southgate, E., Thomson, J.N., and Brenner, S. (1986). The structure of the nervous system of the nematode Caenorhabditis elegans. Philos. Trans. R. Soc. London *314*, 1–340.

Wishart, T.M., Rooney, T.M., Lamont, D.J., Wright, A.K., Morton, A.J., Jackson, M., Freeman, M.R., and Gillingwater, T.H. (2012). Combining Comparative Proteomics and Molecular Genetics Uncovers Regulators of Synaptic and Axonal Stability and Degeneration In Vivo. PLoS Genet. *8*.

Wu, C., Wairkar, Y.P., Collins, C.A., and DiAntonio, A. (2005). Highwire function at the Drosophila neuromuscular junction: spatial, structural, and temporal requirements. J. Neurosci. *25*, 9557–9566.

Wu, C., Daniels, R.W., and DiAntonio, A. (2007a). DFsn collaborates with Highwire to down-regulate the Wallenda/DLK kinase and restrain synaptic terminal growth. Neural Dev. *2*, 16.

Wu, Y., Huo, L., Maeder, C., Feng, W., and Shen, K. (2013). The Balance between Capture and Dissociation of Presynaptic Proteins Controls the Spatial Distribution of Synapses. Neuron *78*, 994–1011.

Wu, Z., Ghosh-Roy, A., Yanik, M.F., Zhang, J.Z., Jin, Y., and Chisholm, A.D. (2007b). Caenorhabditis elegans neuronal regeneration is influenced by life stage, ephrin signaling, and synaptic branching. Proc. Natl. Acad. Sci. U. S. A. *104*, 15132–15137.

Xiong, X., and Collins, C.A. (2012). A Conditioning Lesion Protects Axons from Degeneration via the Wallenda/DLK MAP Kinase Signaling Cascade. J. Neurosci. *32*, 610–615.

Xiong, X., Wang, X., Ewanek, R., Bhat, P., DiAntonio, A., and Collins, C.A. (2010). Protein turnover of the Wallenda/DLK kinase regulates a retrograde response to axonal injury. J. Cell Biol. *191*, 211–223.

Xiong, X., Hao, Y., Sun, K., Li, J., Li, X., Mishra, B., Soppina, P., Wu, C., Hume, R.I., and Collins, C. a. (2012). The Highwire Ubiquitin Ligase Promotes Axonal Degeneration by Tuning Levels of Nmnat Protein. PLoS Biol. *10*, 1–18.

Yan, D., and Jin, Y. (2012). Regulation of DLK-1 Kinase Activity by Calcium-Mediated Dissociation from an Inhibitory Isoform. Neuron *76*, 534–548.

Yan, D., Wu, Z., Chisholm, A.D., and Jin, Y. (2009). The DLK-1 Kinase Promotes mRNA Stability and Local Translation in C. elegans Synapses and Axon Regeneration. Cell *138*, 1005–1018.

Yao, I., Takagi, H., Ageta, H., Kahyo, T., Sato, S., Hatanaka, K., Fukuda, Y., Chiba, T., Morone, N., Yuasa, S., et al. (2007). SCRAPPER-Dependent Ubiquitination of Active Zone Protein RIM1 Regulates Synaptic Vesicle Release. Cell *130*, 943–957.

Yaron, A., and Schuldiner, O. (2016). Common and Divergent Mechanisms in Developmental Neuronal Remodeling and Dying Back Neurodegeneration. Curr. Biol. *26*, R628–R639.

Yawo, H., and Kuno, M. (1985). Calcium dependence of membrane sealing at the cut end of the cockroach giant axon. J. Neurosci. *5*, 1626–1632.

Yonekawa, Y. (1998). Defect in Synaptic Vesicle Precursor Transport and Neuronal Cell Death in KIF1A Motor Protein-deficient Mice. J. Cell Biol. *141*, 431–441.

Yoshii, A., Sheng, M.H., and Constantine-Paton, M. (2003). Eye opening induces a rapid dendritic localization of PSD-95 in central visual neurons. Proc. Natl. Acad. Sci. U. S. A. *100*, 1334–1339.

Zhai, R.G., Vardinon-Friedman, H., Cases-Langhoff, C., Becker, B., Gundelfinger, E.D., Ziv, N.E., and Garner, C.C. (2001). Assembling the presynaptic active zone: A characterization of an

active zone precursor vesicle. Neuron *29*, 131–143.

Zhai, R.G., Cao, Y., Hiesinger, P.R., Zhou, Y., Mehta, S.Q., Schulze, K.L., Verstreken, P., and Bellen, H.J. (2006). Drosophila NMNAT maintains neural integrity independent of its NAD synthesis activity. PLoS Biol. *4*, e416.

Zhai, R.G., Zhang, F., Hiesinger, P.R., Cao, Y., Haueter, C.M., and Bellen, H.J. (2008). NAD synthase NMNAT acts as a chaperone to protect against neurodegeneration. Nature *452*, 887–891.

Zhang, J., Schulze, K.L., Robin Hiesinger, P., Suyama, K., Wang, S., Fish, M., Acar, M., Hoskins, R.A., Bellen, H.J., and Scott, M.P. (2007). Thirty-one flavors of Drosophila Rab proteins. Genetics *176*, 1307–1322.

Zhang, K.X., Tan, L., Pellegrini, M., Zipursky, S.L., and McEwen, J.M. (2016a). Rapid Changes in the Translatome during the Conversion of Growth Cones to Synaptic Terminals. Cell Rep. *14*, 1258–1271.

Zhang, X.P., Ambron, R.T., Mason, C., and Erskine, L. (2000). Positive injury signals induce growth and prolong survival in Aplysia neurons. J. Neurobiol. *45*, 84–94.

Zhang, Y. V., Hannan, S.B., Stapper, Z.A., Kern, J. V., Jahn, T.R., and Rasse, T.M. (2016b). The Drosophila KIF1A Homolog unc-104 Is Important for Site-Specific Synapse Maturation. Front. Cell. Neurosci. *10*, 207.

Zhen, M., and Jin, Y. (1999). The liprin protein SYD-2 regulates the differentiation of presynaptic termini in C. elegans. Nature *401*, 371–375.

Zhen, M., Huang, X., Bamber, B., and Jin, Y. (2000). Regulation of presynaptic terminal organization by C. elegans RPM-1, a putative guanine nucleotide exchanger with a RING-H2 finger domain. Neuron *26*, 331–343.

Zheng, Q., Ahlawat, S., Schaefer, A., Mahoney, T., Koushika, S.P., and Nonet, M.L. (2014). The Vesicle Protein SAM-4 Regulates the Processivity of Synaptic Vesicle Transport. PLoS Genet. *10*.

Zhou, H.M., Brust-Mascher, I., and Scholey, J.M. (2001). Direct visualization of the movement of the monomeric axonal transport motor UNC-104 along neuronal processes in living Caenorhabditis elegans. J. Neurosci. *21*, 3749–3755.

Ziv, N.E., and Spira, M.E. (1995). Axotomy induces a transient and localized elevation of the free intracellular calcium concentration to the millimolar range. J. Neurophysiol. *74*, 2625–2637.